INVESTIGATING THE PATHWAY AND FATE OF INORGANIC IMPURITIES IN A BISULFITE DISSOLVING PULP PRODUCTION PROCESS

By

JOSEPH NYINGI KAMAU

Submitted in fulfillment of the academic requirements for the degree of

Doctor of Philosophy

School of Chemistry

Faculty of Science and Agriculture

University of KwaZulu-Natal

Durban, South Africa

November 2011

INVESTIGATING THE PATHWAY AND FATE OF INORGANIC IMPURITIES IN A BISULFITE DISSOLVING PULP PRODUCTION PROCESS

JOSEPH NYINGI KAMAU

November 2011

A thesis submitted to the School of Chemistry, Faculty of Science and Agriculture University of KwaZulu Natal, Westville, for the degree of Doctor of Philosophy

This thesis has been prepared according to Format 4 as outlined in the guidelines from the Faculty of Science and Agriculture which states:

> This is a thesis in which the chapters are written as a set of discrete research papers with an overall introduction and final conclusion.
>
> As the candidate's supervisor I have approved the final printing of the Thesis.

Supervisor:

Name…**Prof JC Ngila**……

Signed……  …….

Date…….**8th November 2011**…….

PREFACE

The research work described in this dissertation was carried out in the School of Chemistry, University of KwaZulu Natal, from September 2008 to May 2011, under the supervision of Dr (Prof) Jane Catherine Ngila, Professor Andrew Kindness and Dr Tammy Bush.

These studies represent original work by the author and have not been submitted in any form for any degree or diploma to any tertiary institution. Where use has been made of the work of others it is duly acknowledged in the text

DECLARATION 1- PLAGIARISM

I, ……..... declare that

1. The research reported in this thesis except where otherwise indicated, is my original work.
2. This thesis has not been submitted for any degree or examination at any university.
3. This thesis does not contain other persons' data, pictures, graphs, or other information, unless specifically acknowledged as been sourced from other persons.
4. This thesis does not contain other persons' writing, unless specifically acknowledged as been sourced from other researchers. Where other written sources have been quoted, then:
    a. Their words have been rewritten but the general information attributed to them has been referenced
    b. Where there exact words have been used, then their writing has been placed in italics and inside quotation marks, and referenced.
5. This thesis does not contain text, graphics or tables copied and pasted from the internet, unless specifically acknowledged, and the source been detailed in the thesis and in the reference sections.

Signed ……

DECLARATION 2- PUBLICATIONS

DETAILS OF CONTRIBUTION TO PUBLICATION that form part and/or include research presented in this thesis (include publications in preparation, submitted, in press and published and give details of the contributions of each author).

Publication 1

- Joseph Nyingi Kamau, Jane Catherine Ngila, Andrew Kindness, and Tammy Bush. 2011. PCA modeling of eucalyptus forest soil geochemical parameters, labile metals and tree species variability. *Journal of Wood Chemistry and Technology* (*Submitted*).

Contributions: I performed the research, data analysis and write-up; all my Supervisors provided guidance and ideas as well as editing the manuscript.

Publication 2

- Joseph Nyingi Kamau, Jane Catherine Ngila, Andrew Kindness, and Tammy Bush. 2011. The dynamics of metal extraction in a pulp bleaching process. *Manuscript*

Contributions: I performed the research, data analysis and write-up; all my Supervisors provided guidance and ideas as well as editing the manuscript.

Publication 3

- Joseph Nyingi Kamau, Jane Catherine Ngila, Andrew Kindness, and Tammy Bush. 2011. Investigating the influence of organic ligands in pulp filtrate on metal mobility. Submitted *Journal of Wood Chemistry and Technology*.

Contributions: I performed the research, data analysis and write-up; all my Supervisors provided guidance and ideas as well as editing the manuscript.

Publication 4

- Joseph Nyingi Kamau, Jane Catherine Ngila, Andrew Kindness, and Tammy Bush. 2011. Development of a novel environmentally friendly method for the extraction of residual metals in dissolving pulp. (*In preparation-awaiting patent process*)

Contributions: I performed the research, data analysis and write-up; all my Supervisors provided guidance and ideas as well as editing the manuscript.

Publication 5

- Joseph Nyingi Kamau, Jane Catherine Ngila, Andrew Kindness, and Tammy Bush. 2011. Equilibrium and Kinetic Studies for Extracting Cu, Mn and Fe from Pulp Wastewater onto a C-18 Column with Acetylacetone Complexing Ligand. *Analytical letter*s, 44:1891–1906.

- Contributions: I performed the research, data analysis and write-up; all my Supervisors provided guidance and ideas as well as editing the manuscript.

Conferences attended

- Joseph Nyingi Kamau, Jane Catherine Ngila, Andrew Kindness, and Tammy Bush. Equilibrium Studies for the Sorption of Cu, Mn, and Fe from complex liquid matrices using C-18 Solid Phase Material and Acetylacetone as the Complexing Ligand. The International Council for the Exploration of the Sea (ICES) 2010 Annual Science Conference in Nantes, France, 20–24 September 2011 (*Poster*).

- Joseph Nyingi Kamau, Jane Catherine Ngila, Andrew Kindness, and Tammy Bush. Equilibrium Studies for the Sorption of Cu, Mn, and Fe from complex seawater matrices using C-18 Solid Phase Material and Acetylacetone as the Complexing Ligand. International Conference on Aquatic resources of Kenya (ARK-II) 16th -19th November, 2010 Naivasha Kenya (*Oral*).

ABSTRACT

This study sought to investigate the pathway and fate of metals and Si in a bisulfite pulp production process, at the same time providing a means to mitigate on the residual metals bound in the final pulp. The metals pathway and fate was traced from the *Eucalyptus* plantation, through the pulp production process. Principal component analysis was employed to determine the correlation between the observations and the variable of interest. It was established that Fe is a limiting factor in the growth of the *Eucalyptus* trees in the forest under study. The main pathway for the metals and silicon was found to be the exchangeable soil fraction. The residual metals in the pulp material during pulping and bleaching process are influenced by the media pH, the accessibility of the active sites, the affinity of the metal towards the active sites and the degree of delignification and hemicelluloses extraction. Metal desorption under the influence of acetylacetone at both pH 6 and 8 were best described by Langmuir desorption model. Pulp metal desorption under the influence of EDTA was also best described by the Langmuir model except for Al (R^2) 0.572 and 0.004, at pH 6 and 8 respectively. This implies that most of the metals in the dissolving pulp sample were chemically adsorbed on the surface of the pulp. However, aluminum was poorly described by the Langmuir isotherm model. This is because polyvalent metals like Al are hard Lewis acids, capable of strong and specific bonding to hard Lewis base functional groups on organic molecules. The Freundlich model described Mg, Al and Cu desorption suggesting some fraction of these metals to have been physically adsorbed onto the pulp material. It is possible that the metal fraction being physically desorbed was introduced onto the pulp during the pulp bleaching process. Voltammetry was employed to investigate the effect of organic ligands on metal mobility in bleaching filtrates. It was observed that filtrate samples obtained from the alkaline-oxygen bleaching stage produced higher current peak suppression at pH 2 as compared to the filtrate samples obtained from alkaline bleaching stage; this indicates the presence of stronger none-labile metal ligands. At a higher pH of 3.6 the voltammograms of the filtrates obtained from the alkaline-oxygen delignification produced higher cathodic peak shifts. The extent to which the peak potential shifts cathodically is indicative of the magnitude of the stability constant. This may imply that the samples obtained from the alkaline-oxygen delignification comprise of ligands that form strong metal-ligand complexes

ACKNOWLEDGEMENT

I wish to convey my gratitude and sincere appreciation to my supervisors for their support and guidance throughout the research study. Each of my supervisors uniquely contributed towards the fulfillment of my research study. Professor Catherine Ngila played an instrumental role in shaping my research work. She is my mentor; it has been a learning process from MSc now to PhD. She has always been there to encourage me and was always available when I required consulting. I wish to reemphasis my gratitude to Professor Andrew Kindness, despite his busy work schedule as the head of school of chemistry and now as the deputy dean he has always found time whenever I knocked on his door for advice. He played an instrumental role in the shaping of my thesis this involved some frequent visits to his office yet the door stayed open. I am short of words to express my gratitude to Dr Tammy Bush she excellently managed my study. I was kept on my toes to make sure I had results to present every fortnight, the comments from these presentation shaped and fast tracked my research.

The weekly research group meetings formed a forum for group peers to constructively criticize my work and were fundamental towards keeping me on track. I wish to appreciate the input of the Analytical Research group members Mr. Richard, Mr. Banele, Miss. Philiswa, Mr. Waweru, Miss. Dukhi, Mr. Musyoka, Mr. Hamza and Mr. Mbugwa.

Without the financial support of the Council for Scientific Industrial Research-Forestry and Forest Products (CSIR-FFP), this research study would not have been possible. They were the necessary fuel in the whole process.

I wish also to appreciate the role played by the occasional meetings at the SAPPI SAICCOR factory the comments from these meetings gave me impedance to forge on with the work and also assured me that I was on the right track.

I wish to also appreciate and aknowledege the role played by Kenya Marine and Fisheries Research Institute (KMFRI), they faciliteded in my PhD study by granting me a study leave for the duration of the study.

My heart goes out to my family, my wife Alice, daughters Wambui and Wanjiru and my son Kamau, they beared the sacrifice of the 4,000 Km separation over several long months.

All would not have been accomplished if it were not for the grace of God He gave me the ability and the opportunity to do what entailed in the study.

DEDICATION

This work is dedicated to my beloved wife, Mrs. Alice Nyingi, my son Ian Kamau Nyingi and my two daughters Cynthia Wanjiru Nyingi and Sheila Wambui Nyingi

TABLE OF CONTENTS

PREFACE ii

DECLARATION 1- PLAGIARISM iii

DECLARATION 2- PUBLICATIONS iv

ABSTRACT vi

ACKNOWLEDGEMENT vii

DEDICATION ix

TABLE OF CONTENTS x

LIST OF FIGURES xvii

LIST OF TABLES xxi

CHAPTER 1 1

1.1 INTRODUCTION 1

1.1.1 Problem statement 3

1.1.2 Hypothesis 3

1.1.3 Aims and Objective of the study 4

1.1.3.1 Specific Objectives 4

1.2 LITERATURE REVIEW 5

1.2.1 Structural Components of Wood 5

1.2.1.1 Cellulose 6

1.2.1.2 Lignin 7

1.2.1.3 Hemicelluloses 8

1.2.2 Soils Types 9

1.2.2.1 Sandy soils 10

1.2.2.3 Clay soils 10

1.3 MATERIAL AND METHODS 10

1.3.1 Instrumental Techniques 10

1.3.2 Sampling: Pulp Samples 11

1.3.3 Dissolving Pulp Production. 11

1.3.2.2 Pulping process 12

i) Sulfite Chemical Pulping 12

ii) Alkaline Oxygen delignification (O-Stage) 13

iii) Chlorine dioxide bleaching (D_1-stage) 13

iv) Alkaline extraction (E-stage) 14

v) Hypochlorite bleaching 14

1.3.4 Sampling of Soils 15

1.4 THESIS OVERVIEW 15

1.4.1 Overview 15

1.4.1.1 An overview of the research design entailing forest research component and pulp research component 16

1.4.2.1 Sampling of soils, wood and pulping design 17

1.4.3 Experimental procedures: sample pretreatment 17

1.4.3.1 Soil grain size classification 17

1.4.3.2 Extraction of labile soil metals 18

1.4.3.3 Microwave Digestion 18

1.4.4 Data analysis 18

1.4.4.1 Principle component analysis 19

(i) Theory of principal component analysis 20

1.5 THESIS HIGHLIGHTS: RESEARCH FINDINGS 25

1.5.1 PCA modeling of *Eucalyptus* forest soil geochemical parameters, labile metals and tree species variability. 25

1.5.2 The dynamics of metal extraction in a pulp bleaching process 26

1.5.3 Investigating the influence of organic ligands in pulp filtrate on metal mobility 28

1.5.4 Development of a novel environmentally friendly method for the extraction of residual metals in dissolving pulp 29

1.5.5 Equilibrium and Kinetic Studies for Extracting Cu, Mn and Fe from Pulp Wastewater onto a C-18 Column with Acetylacetone Complexing Ligand 30

REFERENCES 31

CHAPTER 2: PAPER I 37

PCA MODELING OF SOIL GEOCHEMICAL PARAMETERS, LABILE METALS AND TREE SPECIES VARIABILITY OF *EUCALYPTUS* FOREST PLANTATION 37

ABSTRACT 37

INTRODUCTION 38

METHODOLOGY 39

Sampling sites 39

Analytical protocol 41

Soil samples 41

Wood samples 42

Quality check 42

Statistical analysis 43
RESULTS AND DISCUSSION 44
Data quality 44
Interpretation of PCA results 47
CONCLUSIONS 61
REFERENCES 61
CHAPTER 3: PAPER II 65
THE DYNAMICS OF METAL EXTRACTION IN A PULP BLEACHING PROCESS 65
ABSTRACT 65
INTRODUCTION 66
EXPERIMENTAL 67
Laboratory scale acid bi-sulfite pulping 67
Pulp bleaching 68
Determination of hemicelluloses content 69
Lignin determination by Kappa (K) number 69
RESULTS AND DISCUSSION 70
CONCLUSIONS 83
REFERENCES 83
CHAPTER 4: PAPER III 85
INVESTIGATING THE METAL COMPLEXING CAPACITIES OF ORGANIC LIGANDS IN PULP BLEACHING FILTRATE 85
ABSTRACT 85
INTRODUCTION 86

Theory 87

METHODOLOGY 88

Background 88

Experimental 90

Apparatus 90

Sample preparation 90

Procedure 90

RESULTS AND DISCUSSION 91

CONCLUSIONS 102

REFERENCES 103

CHAPTER 5: PAPER IV 107

DEVELOPMENT OF A NOVEL ENVIRONMENTALLY FRIENDLY METHOD FOR THE EXTRACTION OF RESIDUAL METALS IN DISSOLVING PULP 107

ABSTRACT 107

INTRODUCTION 108

EXPERIMENT 109

Material and method 109

Reagents 109

Influence of pH on metal desorption 110

Batch desorption 111

Determining the optimum volume of acetylacetone 112

Determining the optimum desorption temperature and time 112

Desorption isotherm models 112

Desorption kinetics 114

RESULTS AND DISCUSSION 116

pH influence 116

Determining volume of acetylacetone, extraction time and temperature 119

Desorption isotherms 124

Desorption kinetics 128

Activation energy 130

Quality control 132

CONCLUSIONS 134

REFERENCES 134

CHAPTER 6: PAPER V 139

EQULIBRIUM AND KINETIC STUDIES FOR EXTRACTING Cu, Mn AND Fe FROM PULP WASTEWATER ONTO A C-18 COLUMN WITH ACETYLACETONE 139

ABSTRACT 139

INTRODUCTION 140

EXPERIMENT 140

Reagents 140

Preconcentration Procedure 141

Influences of pH on Sorption 141

Influence of Acetylacetone on Metal Recovery 142

Effect of Sample Volume 142

Effect of Sample Matrix 143

Procedure for Standard Reference Material....143
Application of Proposed Method on Pulp Filtrate....143
Equilibrium Isotherm Models....143
Background theory....143
Procedure for adsorption studies....144
RESULTS AND DISCUSSION....145
pH influence on acetylacetone metal complex formation....145
Influence of Acetylacetone on Recovery....148
Effect of sample volume....149
Effect of sample matrix....151
Detection limit and standard reference material....151
Application of proposed method on dissolving pulp wastewater....154
Adsorption isotherms....155
CONCLUSIONS....157
ACKNOWLEDGEMENT....157
REFERENCES....157
CHAPTER 7....162
7.0 GENERAL CONCLUSIONs....162
7.1 RECOMMENDATIONS....163

LIST OF FIGURES

Figure 1.1. Cellulose structure 7

Figure 1.2. Lignin precursors 8

Figure 1.3. The structure of xylan 9

Figure 1.4. Oval-shaped data set with two main components; extract from Agilent Technologies (2005). 20

Figure 1.5. *Eucalyptus* forest data analysed by PCA, presented on the score plot (A) and related to the site quality loading plot (B) 26

Figure 1.6. Surface plot of Eucalyptus species E. smithii on the effect of lignin extraction during the alkaline oxygen delignification on the residual metal composition. 27

Figure 1.7. Observed peak potential in the presence of Cu^{2+} ions of O-Stage and E-Stage bleaching filtrates for different *Eucalyptus* species and clone at a pH of 3.6; and fixed Cu concentration (47 μM)and fixed pulp filtrate volume(20 μL). 28

CHAPTER 2: PAPER I

Figure 1. Map of the South African *Eucalyptus* forest sampling zones 40

Figure 2. *Eucalyptus* forest data analysed by PCA, presented on the score plot (A) and related to the site quality loading plot (B) 48

Figure 3. Relationship between soil pH and site quality of the *Eucalyptus* forest under study; pH (S) is soil surface pH and pH (B) is soil bottom pH. 49

Figure 4. Relationship between surface (Ex; S) and bottom (Ex; B) soil exchangeable Fe fraction and site quality of the *Eucalyptus* forest under study 51

Figure 5. Iron concentrations in *Eucalyptus* wood of different species/clones sampled in two size classes (small and large). 52

Figure 6. *Eucalyptus* forest data analysed by PCA presented on the score plot (A) and related to the concentration of Fe in the *Eucalyptus* wood loading plot (B). 54

Figure 7. Relationship between surface (Ex; S) and bottom (Ex; B) soil exchangeable Cu fraction and site quality of the *Eucalyptus* forest under study.....55

Figure 8. *Eucalyptus* forest data analysed by PCA as presented on the score plot (A) and related to the concentration of Si in the *Eucalyptus* wood loading plot (B).....57

Figure 9. Scatter plots relating surface (Exch; S) and bottom (Exch; B) soil exchangeable fraction of Si and Mn.....59

Figure 10. Scatter plots relating surface (Redu; S) and bottom (Redu; B) soil Reducible fraction of Si and Fe.....60

CHAPTER 3: PAPER II

Figure 1. Surface plots of *Eucalyptus* tree species and clones after the O-stage alkaline-oxygen delignification showing the effect of lignin loss on pulp metal composition; GC and GU are *Eucalyptus* clones.....71

Figure 2 Surface plots of *Eucalyptus* tree species and clones after the alkaline E-stage bleaching process showing the effect of lignin loss on pulp metal composition; GC and GU are *Eucalyptus* clones.....73

Figure 3 Surface plots of *Eucalyptus* tree species and clones after the alkaline oxygen delignification process (O-stage) showing the effect of hemicelluloses loss on pulp metal composition; GC and GU are *Eucalyptus* clones.....75

Figure 4 Surface plots of *Eucalyptus* tree species and clones after the alkaline bleaching stage (E-stage) process showing the effect of hemicelluloses loss on pulp metal composition; GC and GU are *Eucalyptus* clones.....76

Figure 5. Box plots of *Eucalyptus* species comparing the residual metals after the alkaline oxygen delignification stage (O-stage) with that of the raw wood material; Si (A) is the silicon obtained after acid digestion and Si (F) is the silicon obtained after fussion.....78

Figure 6. Box plots of *Eucalyptus* clones comparing the residual metals after the alkaline oxygen delignification stage (O-stage) with that of the raw wood material; Si (A) is the silicon obtained after acid digestion and Si (F) is the silicon obtained after fussion.....80

Figure 7. Box plots of *Eucalyptus* species comparing the residual metals after the alkaline bleaching stage (E-stage) with that of the raw wood material; Si (A) is the silicon obtained after acid digestion and Si (F) is the silicon obtained after fussion.. 81

Figure 8. Presents box plots of *Eucalyptus* clones comparing the residual metals after the E-stage bleaching with that of the raw wood material; Si (A) is the silicon obtained after acid digestion and Si (F) is the silicon obtained after fussion.. 82

CHAPTER 4: PAPER III

Figure 1. The effect of pH on titrating fixed Cu metal (MT) and fixed model lignin (LT) with 0.5 M NaOH.....92

Figure 2 The effect of titrating 47 μM Cu with aliquots of sample filtrate at a fixed pH of 2. 93

Figure 3. Observed peak currents in the presence of Cu^{2+} ions of O-Stage and E-Stage bleaching filtrates for different Eucalyptus tree species and clone at a fixed pH of 2. 95

Figure 4. Observed peak potential in the presence of Cu^{2+} ions of O-Stage and E-Stage bleaching filtrates for different Eucalyptus tree species and clone at a fixed pH of 2. 96

Figure 5. Products of delignification derived from alkali-oxygen treatment of an α-5 lignin diphenylmethane model dimmer.[40] 97

Figure 6. Observed peak potential in the presence of Cu^{2+} ions of O-Stage and E-Stage bleaching filtrates for different *Eucalyptus* species and clone at a pH of 3.6; and fixed Cu concentration (47 μM) and fixed pulp filtrate volume (20 μL). 98

Figure 7. Observed peak currents of O and E-Stage bleaching filtrates for different Eucalyptus tree species and clone at a pH of 3.6; fixed Cu concentration (47 μM) and fixed pulp filtrate volume (20 μL). 99

Figure 8. Titrating 70 μL fixed ligand (sourced from the O and E-stage bleaching filtrates of different *Eucalyptus* tree species and clone) with Cu^{2+} ions; titration conducted at a fixed pH (3.6). 100

Figure 9. Titrating a fixed Cu^{2+} ions (47 μM) with a ligand sample (sourced from the O and E-stage bleaching filtrates of different Eucalyptus tree species and clone); titration conducted at a fixed pH (3.6). 102

CHAPTER 5: PAPER IV

Figure 1. The Keto (I) enol (II) tautomeric structures of acetylacetone and its anion (II) 110

Figure 2. Effect of pH on acetylacetone metal complex formation illustrated by % metal complexed. 117

Figure 3. The intermediate complex in the formation of the copper acetonato complex 118

Figure 4. The optimum acetylacetone volume; this corresponds to the volume that enables highest % recovery of the metal (Cu) in solution. 120

Figure 5. Influence of time and temperature on metal desorption from pulp at pH 6; A, B, C and D = 30, 40, 50 and 60 ºC respectively..... 121

Figure 6. Influence of time and temperature on metal desorption from pulp at pH 8; A, B, C and D = 30, 40, 50 and 60 ºC respectively..... 122

Figure 7. Metal desorption using acetylacetone as the extracting ligand at pH 6 over 30 min under varying temperatures..... 123

Figure 8. Metal desorption using acetylacetone as the extracting ligand at pH 8 over 30 min under varying temperatures..... 123

Figure 9. IR spectra of unextracted pulp (A), pulp extracted with acetylacetone (B) and pulp extracted with EDTA (C)..... 132

Figure 10. ^{13}C NMR spectra of unextracted pulp (pure pulp), pulp extracted with acetylacetone and pulp extracted with EDTA. 133

CHAPTER 6: PAPER V

Figure 1**.** Effect of pH on % recovery of metal (Cd, Cr, Cu, Fe, Mn and Pb) as acetylacetone complexes, adsorbed onto different SPE material (C-18, XAD-1180 and XAD-7)..... 146

Figure 2. The Keto (I) enol (II) tantomeric structures of acetylacetone and its anion (II) 147

Figure 3. The intermediate complex in the formation of the copper acetonato complex 147

Figure 4. The % complexed of 0.2 ppm Cu model solution (pH 6) adsorbed onto C-18 columns under varying volumes (0 to 2 mL) of 1.0 mM acetylacetone. 149

Figure 5**.** The % Recovery under varying volumes (10 to 150 mL) of 0.2 ppm Cu model solution (pH 6). 151

Figure 6. Adsorption isotherm for Cu, Fe and Mn acetylacetone complexes on C-18 SPE column.....155

LIST OF TABLES

CHAPTER 1: INTRODUCTION

Table 1. Contents of the main wood components in % dry wood, adapted from Sjöström (1993). 5

Table 2. Langmuir parameters for the desorption of Al, Cu, Fe, Mg, and Ca from pulp at pH 8 by EDTA and acetylacetone 29

CHAPTER 2: PAPER I

Table 1. CRM BCR-701 stage 1 extraction quality check.....44

Table 2. % Recovery, % extraction efficiency, detection limit and reproducibility expressed in % RSD 45

Table 3 Matrix effect: Comparison of the slopes obtained from the direct calibration and the standard addition graphs. 46

Table 4. Comparing data with standard reference material NCS DC 73348 Bush branches and leaves.....47

CHAPTER 3: PAPER II

Table 1. Pulp bleaching stages and their conditions for the laboratory production of 92α cellulose. 68

Table 2. Percentage lignin and hemicelluloses extraction during the O and E bleaching stage 74

CHAPTER 4: PAPER III

Table 1. Observed complexing capacity C_{obs} in μM; percentage suppression of Cu peak after sample filtrate and model lignin addition at pH 2; calculated complexing capacity C_{cal} in μM; and the R^2 value for the plots of C_{cal} 94

CHAPTER 5: PAPER IV

Table 1. Relating % metal recovery with metal electronegativity and Δ Electronegativity of metal to oxygen atom. 119

Table 2. Langmuir parameters for the desorption of Al, Cu, Fe, Mg, and Ca from pulp at pH 6 by EDTA and acetylacetone 124

Table 3. Langmuir parameters for the desorption of Al, Cu, Fe, Mg, and Ca from pulp at pH 8 by EDTA and acetylacetone 125

Table 4. Freundlich parameters for the desorption of Al, Cu, Fe, Mg, and Ca from pulp at pH 6 by EDTA and acetylaceton 127

Table 5. Freundlich parameters for the desorption of Al, Cu, Fe, Mg, and Ca from pulp at pH 8 by EDTA and acetylaceton 127

Table 6. Pseudo 2^{nd} order Kinetic parameters for the desorption of Al, Cu, Fe, Mg, and Ca from pulp at pH 6 by EDTA and acetylaceton; *K_2 values expressed in $g.\mu mol^{-1}.min^{-1}$ 129

Table 7. Pseudo 2^{nd} order Kinetic parameters for the desorption of Al, Cu, Fe, Mg, and Ca from pulp at pH 8 by EDTA and acetylacetone; *K_2 values expressed in $g.\mu mol^{-1}.min^{-1}$ ... 130

Table 8. Arrhenius parameters for the desorption of Al, Cu, Fe, Mg, and Ca from pulp at pH 6 and 8 by acetylaceton 131

Table 9. Analysed trace elements in IAEA–V-9 cellulose cotton reference material compared to the recommended values. 133

CHAPTER 6: PAPER V

Table 1**.** The metal electronegativities (EN), electronegativity difference (ΔEN) of the metal and oxygen and % recovery; recovery performed at pH 6 (slightly acidic). 148

Table 2. Effect of matrix ions on the recovery of Cu and Fe (pH 8; sample volume: 30ml, n=3) 150

Table 3**.** Detection limits of metal ions (Cd, Cu, Fe, and Pb) at different sample volumes and the analysis of 60 mL NASS-5 Seawater reference material. 152

Table 4. Heavy metal (Cu, Ni, and Pb) analysis in pulp filtrate after acetylacetone complexation and preconcentration on C-18 SPE 153

Table 5**.** Comparative data from literature reports on solid phase extraction. 154

Table 6**.** Langmuir and Freundlich adsorption isotherm parameters for Cu, Fe and Mn acetylacetone complexes on C-18 SPE. Showing regression line characteristics R^2, a_L/k_L, $1/k_L$, b_F and $\ln K_F$ 156

CHAPTER 1

1.1 INTRODUCTION

Pulp is a lignocellulosic fibrous material prepared by chemically or mechanically separating cellulose fibres from mainly wood raw material. During the production process of paper and pulp, multiple chemicals (additives) need to be added and a large number of parameters measured and controlled. The pulping process involves two major stages the cooking and bleaching stages. The cooking stage is the initial pulping stage where most of the lignin and hemicelluloses are extracted. After the cooking stage the residual lignin and hemicelulose are further extracted in the bleaching stages, this leads to the opening up of the pulp material increasing its porosity and wetability, thereby availing more active sites for metal adsorption.

The chemical pulp production process produces mainly paper and dissolving pulps. Dissolving pulps are chemical pulps that are suitable for subsequent chemical conversion into products such as rayon, cellophane, cellulose acetate, cellulose nitrate, carboxymethyl cellulose graft, cross-linked cellulose derivatives and sausage skin (Behin, *et al*. 2008; Christov *et al*. 1998). The viscose-rayon process is the largest user of dissolving pulps. World-wide, the supply of dissolving pulp fluctuates in volume and in quality, yet demand for viscose rayon fibers is growing. World wood pulp production in 2003 amounted to 170 million tons (FAO 2005). The dissolving pulps are low-yeild chemical pulps (30-35%) with a high cellulose (>90%), relatively low hemicelluloses and low lignin (<0.05%) content, this is mainly as a result of extensive pulping and bleaching (Christov *et al*. 1998; Christov et al. 2000). They are mainly produced by acid sulfite and prehydrolysis kraft processes. Unlike in paper grade pulping, acid sulfite process is the dominant production process for dissolving pulps. In each case, the objective is to produce a relatively pure (very low metal levels) and uniform cellulose product with a controlled weight-averaged degree of polymerization (Behin, *et al*. 2008).

The acid sulfite process is characterized by a high recovery rate of inorganic cooking chemicals. Acid magnesium sulfite pulping represents one of the most environmentally benign technologies in the whole pulping industry (Gotzinger *et al.* 2000). The main disadvantages of the acid magnesium sulfite pulping process compared by the prehydrolysis kraft process are the; rather broad molecular weight distribution (MWD) of the resulting pulp, the high specific investment costs, and the low viscosity at a given purity level. In kraft pulping the wood is treated with a solution of sodium hydroxide and sodium sulfide at high

temperature (Schwanninger 2006). This results in wood delignification through the degradation of lignin. Although a major fraction of wood lignin (~95%) can be removed in kraft pulping the remainder of the lignin (residual) is rather resistant under the pulping conditions (Schwanninger 2006). The residual lignin is removed from the pulp by oxidative lignin degradation with bleaching agents such as oxygen, hydrogen peroxide, ozone, and chlorine dioxide (Schwanninger 2006).

Bleaching is usually classified into oxidative and reductive bleaching. Oxidative bleaching destroys the chromophores irreversibly, while reductive bleaching can be reversible (Süss 2000). It can for example, be reversed by atmospheric oxygen. Reduction of transition metal ions chelated by conjugated compounds can increase brightness provided the metals are washed off to prevent reoxidation (Süss 2000). The bleaching effect is measured by the increase in brightness. Remission photometers are used to determine brightness relative to a standard, $BaSO_4$ is the most widely used standard. However, there are several similar methods that may be used to determine brightness (TAPPI 1973; TAPPI 1993). The quality and efficiency of bleaching is also reflected by brightness stability. Light and heat may change the color of bleached materials. Before bleaching can be carried out, pretreatments may be necessary to remove detrimental substances like transition metals, which decompose peroxy compounds (Süss 2000). Chelating agents like the sodium salts of diethylenetriaminepentaacetic acid (DTPA), or ethylenediaminetetraacetic acid (EDTA), are used under mildly acidic conditions to accelerate the elimination of metals (Süss, 2000). This allows the removal of transition metals with conservation of magnesium and calcium ions, which are of benefit as stabilizers (Süss 2000). For chemical pulp produced by alkaline pulping, such a metals-removal stage is necessary if totally chlorine free (TCF) bleaching is to be applied. In conventional or ECF (elemental chlorine free) bleaching, the metals are removed during the acidic chlorine dioxide stages (Süss 2000). The rather poor selectivity of oxygen delignification as compared to chlorine dioxide is further impaired by the presence of transition metal ions (Brelid *et al.* 1998). The wood used in kraft pulping is the primary source of the majority of non-process elements (metals and extractives) (Brelid *et al.* 1998). The content of inorganic ions depends on the wood species and the plantation site (Brelid *et al.* 1998). Metal ions in wood are assumed to be bound onto carboxylate groups in hemicelluloses, pectine, lignin, and extractives (Brelid *et al.* 1998). In oxygen delignification and peroxide bleaching cellulose degradation reactions are promoted by the presence of even trace amounts of transition metal ions, such as copper, cobalt and iron (Ericsson *et al*. 1971).

The presence of cobalt (II) and iron (II) salts during oxygen delignification of cotton linters cause the highest rate and extent of cellulose degradation, while copper has a less damaging behavior and nickel has no visible effect (Gilbert *et al*. 1973). Manganese on the other hand, demonstrates both characteristics, being a degradation catalyst below 10 ppm and a protective agent above 60 ppm (Brelid *et al*. 1997; Gilbert *et al*. 1973). The addition of magnesium carbonate significantly retards cellulose degradation in the presence of iron salts (Brelid *et al*. 1997). However, the catalytic effect of cobalt ions on cellulose degradation and oxidation cannot be offset by the addition of magnesium carbonate (Brelid *et al*. 1997). The transition to a cellulose-preserving agent has also been observed with iron when present at sufficiently excess concentrations. At a concentration level above 0.1% on pulp, the precipitated ferric hydroxide acts as an oxidation inhibitor (Gilbert *et al*. 1973).

Hydrogen peroxide undergoes Fenton-type reactions with metal ions such as iron and manganese, leading to hydroxyl radicals that are then able to oxidatively cleave and /or peel polysaccharide chains (Liden and Ohman 1998; Perng *et al*. 1994). Kishimoto and Nakatsubo (1998) using methyl 4-*O*-ethyl-*β*-D-glucopyranoside as a cellulose model reported that Fe (II) ions were the most harmful species to carbohydrates in the presence of hydrogen peroxide. The extent of glycosidic bond cleavage decreases with increasing initial pH and in the presence of oxygen, presumably due to the preferred formation of less-reactive hydroperoxyl radicals (Kishimoto and Nakatsubo 1998). The Fenton reaction is drastically inhibited under alkaline conditions at room temperature, most likely due to the reduced solubility of Fe (II) and Fe (III) ions (Kishimoto and Nakatsubo 1998).

1.1.1 Problem statement

The impact of transition metals on the pulp production process forms the bases of this research study. The transition metals can either antagonize or synergize the pulp production process, thus impacting on the pulp quality and cost of production.

1.1.2 Hypothesis

1. The residual metals in the pulp originate from the raw material (wood) and reagents introduced during the pulping and bleaching process.
2. The *Eucalyptus* tree obtains metals from the metal soil labile fraction.
3. Metals in the pulp material are adsorbed on lignin and hemicelluloses.

4. The pulping process opens up the pulp structure availing more active sites from metal adsorption.

1.1.3 Aims and Objective of the study

The main aim of this project was to determine the fate and pathway of metals in the *Eucalyptus* plantations taking into consideration the soil geochemistry and tree genetic variability. The study also seeks to determine the pathway and fate of metals through the pulp bleaching process, while considering the role of delignification and hemicelluloses on metal fluxes.

1.1.3.1 Specific Objectives

1. Determine the pathway of metals from the soil to the *Eucalyptus* trees, grown in South African plantations.
2. Determine the fate of metals during dissolving pulp processing
3. Investigate the role of lignin in the extraction of metals in dissolving pulp process
4. To formulate a feasible scheme for the extraction of residual metals from pulp.

1.2 LITERATURE REVIEW

At present more than 90% of the pulp produced worldwide is wood pulp (Sixta 2006b). The first species of trees to be used in great quantities for paper making were pine and spruce from the temperate coniferous forests located in the cool northern climates of Europe and North America (Sixta 2006b). However there has been a gradual shift to the use of hardwood species mainly driven by lower costs and better availability (Sixta 2006b).
For any given type of pulp production, the properties of the unbleached pulp are determined by the structural and chemical composition of the raw material.

1.2.1 Structural Components of Wood

The main components of wood are structural components. The structural components are cellulose, hemicelluloses and lignin, together with smaller amounts of pectic substances (Fengel and Wegener 1989; Timell 1967). For softwood and hardwood in general, the contents of the main components vary in the ranges shown in Table 1. Polysaccharides represent the major component of both wood types.

Table 1. Contents of the main wood components in % dry wood, adapted from Sjöström (1993).

	Cellulose	Glucomannan	Xylan	Other polysaccharides	Lignin
Softwood	33-42	14-20	5-11	3-9	27-32
hardwood	38-51	1-4	14-30	2-4	21-31

There are significant differences between softwoods and hardwoods in relation to the type and content of the various hemicelluloses in the wood cell walls. It is apparent that hardwood has a higher proportion of xylan than soft wood.

1.2.1.1 Cellulose

Cellulose is the most abundant compound in the cell wall of plants and woods, with a degree of polymerization of approximately 10 000 and a relatively high degree of crystallinity averaging 50–70% (Thygesen 2005; Newman 2004). Payen was the first to determine the elemental composition of cellulose, reporting in 1838 that it had the empirical formula $C_6H_{10}O_5$ (Payen 1842; Krässig 1996). It was also found that during hydrolysis it yields cellobiose and finally glucose. The nature of the bonds between the atoms in the glucose units and between the glucose units were recognized by Haworth, (1928) but it was Staudinger, (1932) who reported a proof of the polymeric nature of the cellulose molecule. The chain–like, linear, macromolecular structure proposed by Haworth in the 1920s is today generally accepted, Figure 1.1. The glucose units are linked together by β-1,4-glucosidic bonds between carbon C(1) and C(4) of adjacent glucose units. Cellulose is actually a β-1, 4-polyacetal of cellobiose. The terminal hydroxyl groups at each end of the polymer chain differ in chemical nature. The C(1) hydroxyl is an aldehyde hydrate group with reducing activity and originates from the formation of the pyranose ring through an intramolecular hemiacetal reaction. The hydroxyl on carbon C(4) is an alcoholic hydroxyl and therefore non-reducing. The β-glucosidic bonds are sensitive to hydrolytic attack. At the supermolecular level the cellulose chains are held together by hydrogen bonds. The resulting cellulose aggregates can be ordered as crystalline cellulose or unordered, amorphous cellulose.

Industrially produced cellulose show deviations from the "ideal" natural molecular structure. This is mainly due to the isolation procedure (pulping and bleaching), since cellulose in higher plants is always incorporated into a matrix of hemicelluloses, lignin and low molecular-weight substances (Sixta 2006a). During pulping and bleaching a number of other fucnctionalites, such as carboxyl and carbonyl groups, are introduced (Sixta 2006a).

Cellulose has an inherent ability to form different types of hydrogen bonds, either within the same cellulose chain (intramolecular) or between different chains (intrermolecular). The ability to form intramolecular hydrogen bonds is a major factor that contributes to chain stiffness and conformation (Klemm *et al*. 1998; Klemm *et al.* 2002). Intrermolecular bonds are responsible for the formation of supramolecuar aggregates, such as crystalline domain or fibrils (Klemm *et al*. 1998; Klemm *et al.* 2002).

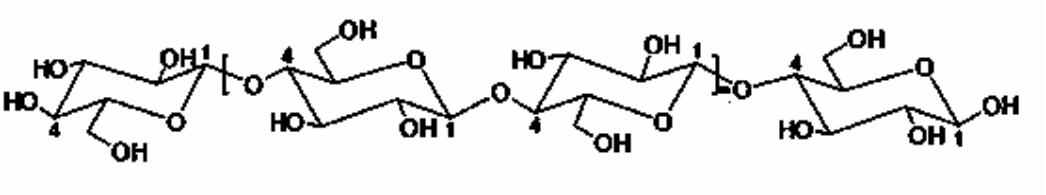

Figure 1.1. Cellulose structure

1.2.1.2 Lignin

Lignin is the second most abundant and important polymeric organic substance in plants after cellulose. It typically occurs in the vascular tissue, specialized for liquid transport and mechanical strength (Fengel and Wegener 1989). The amount of lignin present in different plants is quite variable. In wood species the lignin content ranges from 20 to 40%, aquatic and herbaceous angiosperms as well as many monocotyledons are less lignified (Sarkanen *et al.* 1971). The distribution of lignin within the cell wall and the lignin content of different parts of a tree are not uniform. For example, large amounts of lignin in soft wood are located in the branches and compression wood (Timell 1986).

Lignin is a phenolic biopolymer formed through oxidative radical coupling of monolignols in the cell wall of vascular plants. Lignin macromolecules consist of phenylpropanoid units that are connected by various types of ether and carbon–carbon linkages, mainly including *β–O–*4, *β–*5, *β–β*, *β–*1, 5–5*–O–*4 and 4*–O–*5 types (Adler, 1977; Zhang and Gellerstedt, 2001; Karhunen *et al.* 1995). It is a three-dimensional amorphous polymer of high molecular weight being predominantly aromatic (polyphenolic) in character and is derived from a biosynthetic process in which the main precursors are *p*-courmaryl alcohol, coniferyl alcohol, and sinapyl alcohol (Freudenberg and Neish 1968; Sjöström 1993) (Figure 1.2). These basic units are linked by multitudes of bonds, including ether and carbon-carbon bonds, forming complex structures specific for different plant species (Quintana *et al.* 2008). The structure of kraft lignin is a complex polymer of coniferin, with propane units containing various acidic functions such as phenolic, carboxylic and enolic groups (Marton 1971). The formation of most of these well-recognized structures in lignin polymers can theoretically be explained by the mechanism of lignin biosynthesis, *i.e*. the oxidative radical coupling mechanism (Schwanninger 2006).

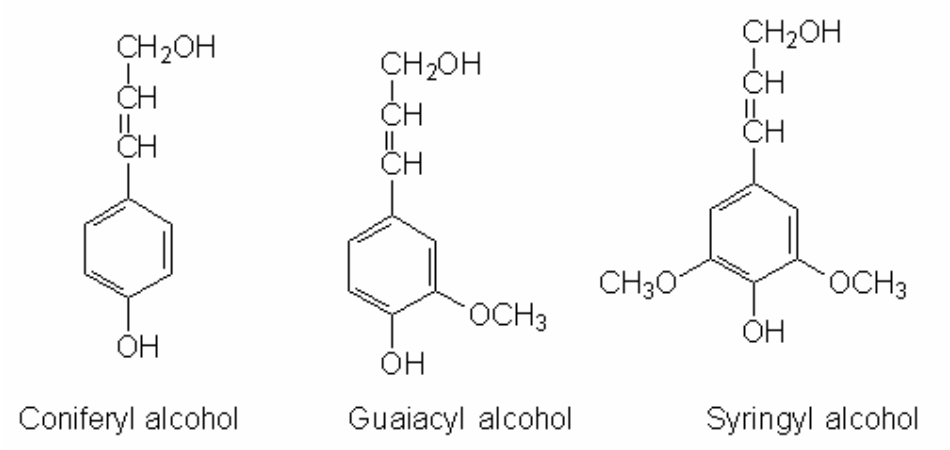

Figure 1.2. Lignin precursors

Lignin mostly contains methoxyl groups, phenolic hydroxyl groups, and few terminal aldehyde groups. Only a small proportion of the phenolic hydroxyl groups are free since most are occupied in linkages to neighbouring phenylpropane linkages (Adler 1977). Carbonyl and alcoholic hydroxyl groups are incorporated into the lignin structure during enzymatic dehydrogenation.

Studies have also suggested that covalent linkages between lignin and hemicelluloses exist in native wood (Erikkson and Lindgren 1977; Björkman 1957). These structures are typically referred to as lignincarbohydrate complexes or simply LCCs. The lignin is covalently bound to the hemicelluloses which, in turn, are bound to cellulose through extensive hydrogen bonding. Lignin-carbohydrate complexes could be very important when considering pulping of wood since lignin is chemically bound to the cellulose.

1.2.1.3 Hemicelluloses

Hemicelluloses are heteropolysaccharides, and differ from cellulose in that they consist of several sugar moieties, are mostly branched, and have lower molecular masses with a degree of polymerization of 50-200 (Sixta 2006a). The sugar units making up the supramolecular structures of hemicelluloses can be subdivided into groups such as pentoses (xylose and arabinose units), hexoses (glucose and mannose units), hexuronic acids (glucuronic acid) and deoxy-hexoses (rhamnose units) (Sixta 2006a).

The main hemicelluloses in hardwood is a *xylan*, more specifically an *O*-acetyl-4-*O*-methylglucurono-*β*-D-xylan (Fengel and Wegener 1989; Sjöström 1993; Shimizu 2001). In softwood xylan, the backbone consists of *β*-(1→4)-linked xylopyranose units (Figure 1.3). Most of the hydroxyl groups at C2 and/or C3 of the xylose units are substituted with acetyl groups. In addition, xylose units are substituted with α-(1→2)-linked 4-*O*-methylglucuronic acid residues, in most hardwood xylans on average at every 10th xylose unit. Unlike softwood xylan, hardwood xylan does not contain arabinose side chains. Hardwood also contains glucomannan with a backbone of *β*-(1→4)-linked D-mannopyranose and D-glucopyranose units (Figure 1.3) (Fengel and Wegener 1989; Sjöström 1993; Shimizu 2001). The ratio of mannose to glucose units is between 1:1 and 3:1.

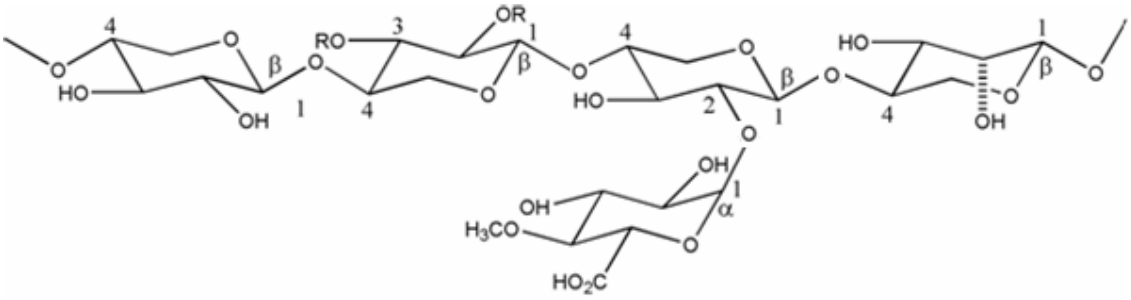

Figure 1.3. The structure of xylan

1.2.2 Soils Types

Soil types are a major factor in determining what types of plants will grow in a certain area. Plants use inorganic elements from the soil, such as nitrogen, phosphorus and essential metallic nutrients. The community of fungi, bacteria, and other microscopic creatures living within the soil complete the nutrients regeneration cycle. These living organisms help with the decomposition of dead plants and animals, breaking them down to release the locked up nutrients as well as provide organic matter necessary for improving the soils water retention capacity. There are different types of soils each unique in its geochemical properties, derived from the geological setup of the locality and the activity of the flora and fauna present in the site. The combination of sand, silt, gravel, and clay gives various soils different textures.
Boundaries between the various soils generally merge into one another. Soils usually display horizontal layers that are identified by their colour, texture (the relative proportions of sand,

silt and clay), structure and consistence (Hodgson and Thompson 1985). The overall colour of the profile reflects how well water drains through it: uniformly brown usually indicate a well aerated soil through which water drains freely, soils that are grey throughout are commonly waterlogged for long periods (Hodgson and Thompson 1985).
Generally sandy and clay soils fall within the two extremes, the ratio in composition of these two soil types give rise to different soil textures.

1.2.2.1 Sandy soils

Sandy soils are relatively "newly" formed compared to other soil types. It is easy for both air and water to move between the large grains of sand, so this soil type stores water very poorly and is susceptible to drought. The composition of sand is highly variable, depending on the local rock sources and conditions. The bright white sands found in tropical and subtropical coastal settings are eroded limestone and may contain coral and shell fragments in addition to other organic or organically derived fragmental material (Scott 2002). Podosols: these are strongly leached sandy soils which are poor in nutrients and acidic to strongly acidic throughout. They are characterized by having variably cemented iron and humus accumulations in the subsoil.

1.2.2.3 Clay soils

Clay soils are composed of very fine particles with few air spaces. They are often waterlogged because the tiny clay particles are packed tightly together, making it hard for air and water to move through. Clay soils can be dense enough to make it difficult for plant roots to spread through them.

1.3 MATERIAL AND METHODS

1.3.1 Instrumental Techniques

The main analytical instruments employed in the study were Inductive Coupled Plasma Optical Emission Spectrometer (ICP-OES; PerkinElmer Optima 5300DV) and Electroanalytica (Metrohm Model 797 VA).

Solid samples were first digested in a Microwave digester (PerkinElmer Paar Physica multiwave) before being run in the ICP-OES. Filtrate samples obtained from the pulp

bleaching stages were digested by a UV digester (Metrohm 705 UV digester) and then run through the ICP-OES.

Voltammetric measurements were carried out with a Metrohm Model 797 VA Computrace Metrodata in conjunction with a model 797 VA stand. A conventional three-electrode arrangement, consisting of a platinum rod as an auxiliary electrode, a Ag/AgCl/KCl (3 M) double-junction electrode as a reference electrode and a Metrohm multi-mode electrode (MME) used in the glassy carbon rotating disc electrode/solid state electrode mode (RDE/SSE), was employed.

1.3.2 Sampling: Pulp Samples

The pulp samples were obtained after the alkaline oxygen delignification process and the alkaline bleaching stage. The alkaline oxygen delignification process occurs just after the cooking stage, and is the stage where most of the residual lignin remaining after the cooking process is extracted. It offers an opportunity to study the effect of delignification and metal extraction from the pulp. The alkaline bleaching stage mostly entails the removal of hemicelluloses from the pulp. This offers an opportunity to study the effect of hemicelluloses extraction and metal removal from the pulp during this bleaching stage.

1.3.3 Dissolving Pulp Production.

Soft and hard woods, containing about one-third each of lignin, cellulose and hemicelluloses (manly xylans, mannans, arabinans, and polyuronic acids), require a severe treatment in pulping and bleaching in order to arrive at a high-quality dissolving pulp, and these steps of isolation and purification are always accompanied by a significant decrease in dissolving pulp (Edwards 1962). A small amount of organo-soluble extractives can exert an undesirable surfactant effect, and some inorganic matter can promote a clogging of spinnerets in artificial fiber spinning. The cations of Ca and Fe, as well as SiO_2, are considered to be especially detrimental in this respect.

Bleached chemical pulps, especially those that are obtained by means of total chlorine free (TCF) sequences involving ozone stages, show an enhanced tendency to heat-induced yellowing because of the carbonyl groups, which are responsible for heat-induced (Edwards 1962) and photochemically induced (Argyropoulos 1995) brightness reversion of pulps. Increased brightness stability is reached when peroxide is used in the last stage of a bleaching sequence because of its ability to remove α-carbonyl groups and quinone structures

(Lachenal *et al.* 1994; Zhang and Gellerstelt 1993). The major concern regarding the use of H_2O_2 is its stability. Metal ions, including Fe^{2+}, Mn^{2+} and Cu^{2+} catalyse the decomposition of H_2O_2.Transition metals such as cobalt, iron and copper have been found to cause increased viscosity reduction in the cause of alkaline –oxygen treatment (Manouchehri and Samuelson 1973). It is assumed that these metals promote free radical generation by catalyzing the decomposition of the peroxides formed during oxygen delignification (Manouchehri and Samuelson 1973).

1.3.2.2 Pulping process

i) Sulfite Chemical Pulping

The sulfite process was developed around the acid calcium bisulfate process; it remained the principal process for wood pulping due to its low cost, until the beginning of the 1950s when the need to recover the waste liquor and pulping chemicals emerged. Calcium sulfite is soluble only below pH 2.3, requiring an excess of SO_2. At high cooking temperatures the calcium hydrogen sulfite decomposes to calcium sulfite and hydrated SO_2. For these reasons calcium has been replaced by more soluble bases. The dominating base being used in sulfite pulping being magnesium (Sixta 2006a). The specification of a typical acid sulfite cooking liquor is total SO_2; 17.5 (% to wood), free SO_2; 10.5 (% to wood), combined SO_2; 7.0 (% to wood) and MgO 2.2 (% to wood). The procedure of acid sulfite cooking typically comprises the steps chip filling, steaming, cooking liquor charging, impregnation, side relief, SO_2 charge, heating to maximum temperature, maintain the digester at this temperature until the desired degree of cooking is achieved, relieving the pressure (degassing), displacement of the cooking liquor, and discharging the digester (Sixta 2006a).

A uniform distribution of pulping chemicals within the wood chip structure is the key step of any pulping process. The impregnation step is carried out immediately after the chips have been immersed in cooking liquor (Sixta 2006a). Due to the decrease in the acid dissociation constant of hydrated sulfur dioxide, with increasing temperature the pH level of acid sulfite cooking liquor is shifted to higher values at higher cooking temperature (Sixta 2006a).

ii) Alkaline Oxygen delignification (O-Stage)

Environmental restrictions for bleach plant effluents and the necessity to reduce the amount of organochlorine compounds in the pulp led the pulp industry to develop new environmentally benign delignification and bleaching technologies (Sixta 2006b). In this context, oxygen delignification emerged as an important delignification technology. One of the major drawbacks of oxygen delignification is its lack of selectivity for delignification (Sixta 2006b). It extracts beyond 50% of lignin resulting in excessive cellulose damage which is reflected in a decrease in viscosity and loss of pulp strength (Sixta 2006b). However addition of a small amount of magnesium carbonate preserves the strength of paper-grade pulp. The initial step of alkaline-oxygen delignification involves the deprotonation of the phenolic hydroxyl group (Gierer 1985) to produce the phenolate anion (Gierer 1982) that furnishes a high electron density needed for a one electron transfer (Sixta 2006b). Oxygen attacks at an electrophilic (δ-) site and abstracts an electron, leaving a phenoxyl radical (Gierer 1997) and/ or a mesomeric cyclohexadienonyl radical, while oxygen itself is reduced to the superoxide anion radical.

The efficiency of delignification depends on structural features such as free phenolic hydroxyl groups, methoxyl groups, carbonyl groups, and on the composition of the residual lignin-carbohydrate complex (Brelid *et al.* 1998; Entwistle *et al*. 1949a; Entwistle *et al*. 1949b). The linkages between phenylpropane units in lignin contribute to a better bleachability of the pulp (Gellerstedt and Al-Dajani 2000),

iii) Chlorine dioxide bleaching (D_1-stage)

The residual lignin from unbleached or semibleached pulps, which could not be removed by pulping, must be removed from pulp through oxidative lignin degradation with bleaching reagents such as chlorine dioxide (Sixta 2006b). The initial step of bleaching with chlorine dioxide involves the oxidation of aromatic substrates with chlorine dioxide initiated by electrophilic addition of the oxidant to the aromatic nuclei. This results in the generation of charge-transfer (= π) complexes (Brage *et al.* 1991). These complexes become protonated in acidic media, thereby enhancing the formation of corresponding resonance-stabilized cation radicals by the elimination of chlorous acid. In the case of phenolic substrates, these cation radical intermediate readily losses a proton, affording phenoxyl radicals in various resonance

forms. In the case of nonphenolic substrates, the intermediary cation radicals exist in various ortho- and para-oxonium ion forms (Brage *et al.* 1991).

iv) Alkaline extraction (E-stage)

Wood pulp obtained from the acid sulfite process still contains considerable amounts of low molecular-weight carbohydrates (hemicelluloses) (Sixta 2006b). These make the pulp less suitable for the production of cellulose acetate, high purity cellulose ethers or high-tenacity regenerated fibers (Sixta 2006b). The pulp is refined with alkali either at temperatures below 50 ºC whereby strong solutions of sodium hydroxide are used (cold caustic extraction), or at higher temperatures using weaker alkaline solutions (hot caustic extraction) (Sixta 2006b). The extraction of wood pulp with strong sodium hydroxide solutions at low temperatures produces higher levels of alpha-cellulose than with dilute solutions at higher temperatures, the yields obtained are also considerably higher. The conditions of cold caustic extraction include the homogeneous distribution of pulp in 5-10% NaOH for at least 10 min at temperatures between 25 and 45 ºC in a down-flow, unpressurized tower. Hot caustic extraction is carried out at low caustic concentrations typically 3-18 g L^{-1} NaOH, with pulp consistencies of 10-15% and temperatures ranging between 70 ºC to 120 ºC (Sixta 2006b). Alkaline hydrolysis reactions reduce the molecular weight of the lignin structures and also remove the methoxyl groups (-O-CH_3) causing the formation of phenolate ions (Behin, *et al.* 2008).

v) Hypochlorite bleaching

In hypochlorite bleaching, pulp is brightened as the chemical destroys and removes the residual lignin and lignin derivatives. Hypochlorite use is quite rare nowadays, but it is still used for adjustment of pulp viscosity. Hypochlorite bleaching stage is quite similar to chlorine dioxide stage. Bleaching with hypochlorite solution, usually in the form of sodium or calcium salts (NaClO, CaClO) is called the H-stage (Laskin 2001). This stage is carried out at 4-8% of pulp consistency, 35-45 C for 1-5 h, at a pH of 10 (Laskin 2001). Hypochlorite is more selective than elemental chlorine and extracts lignin as it is depolymerized (Laskin 2001).

1.3.4 Sampling of Soils

Soil samples were collected using a soil auger around the tree at 20 cm below the surface and at two meters deep. The geochemistry of the sampling site was determined by analyzing soil samples for grain size composition, organic matter, soil pH and exchangeable acidity. Soil metal labile fractions were determined by fractionating the exchangeable and easily reducible metal phases. Organic matter was determined by weight loss after ashing in the furnace at 450 ^{o}C for six hours. Active acidity was determined as H^{+} ions in soil solution as measured with a pH meter.

1.4 THESIS OVERVIEW

1.4.1 Overview

This thesis seeks to investigate the fate and pathway of metals and Si in a bisulfite pulp production process. While providing a means to mitigate on the residual metals bound in the final pulp, the study also appreciates the importance of conserving the environment by limiting the discharge of pollutants. To facilitate the achievement of this goal, a novel analytical tool is outlined involving the preconcentration/extraction of metals in a sample with a complex organic matrix. A metal extraction method (involving acetylacetone as a chelating agent for the extraction of pulp residual metals) is developed that is not only environmentally friendly but is also more efficient than the conventional methods currently being employed.

Viscose-grade pulps require stringent processing to ensure high quality products. A concern to the industry is the inorganic extractives and Si; these affect the purity of viscose-grade pulp. An understanding of the pathway and fate of these inorganic extractives provides vital information necessary to formulate mitigative measures, and enables the prediction of viscose-grade pulp quality, while considering the constituents of the raw material. To accomplish the objectives of the study the research project was conducted in two phases.

The first phase sought to investigate the contributing factors (entailing genetic, climatic and biogeochemical), influencing the amount of metals and Si in the wood of *Eucalyptus* trees, grown in areas with different climatic and geological settings. Labile metal and Si fractions were determined (using atomic spectroscopy; ICP-OES) from the soil collected around the Eucalyptus roots. A wood sample was obtained from the sampled

Eucalyptus tree at its breast height. Principal component analysis statistical approach was employed to determine the correlations within the data.

The second phase was focused on the pulp production process. Labile and residual metals were analyzed in the pulp at the various production stages. The metals in the liquor and filtrate were fractionated into the organic and inorganic phases. The data generated was treated statistically to determine the influencing parameters that affect metal and Si extractability. Lignin synergistic effect on metals extraction during the pulping process was investigated. The complexing capacity of the ligands in the liquor and filtrate was determined by electroanalytical technique.

1.4.1.1 An overview of the research design entailing forest research component and pulp research component

The research design overview is a flowchart of all the stages encompassed in the study. It shows the parameters determined on the samples collected from the *Eucalyptus* forest. It further shows the pulping process entailing the cooking and bleaching stages, indicating the type of samples obtained from the process and the research query being addressed.

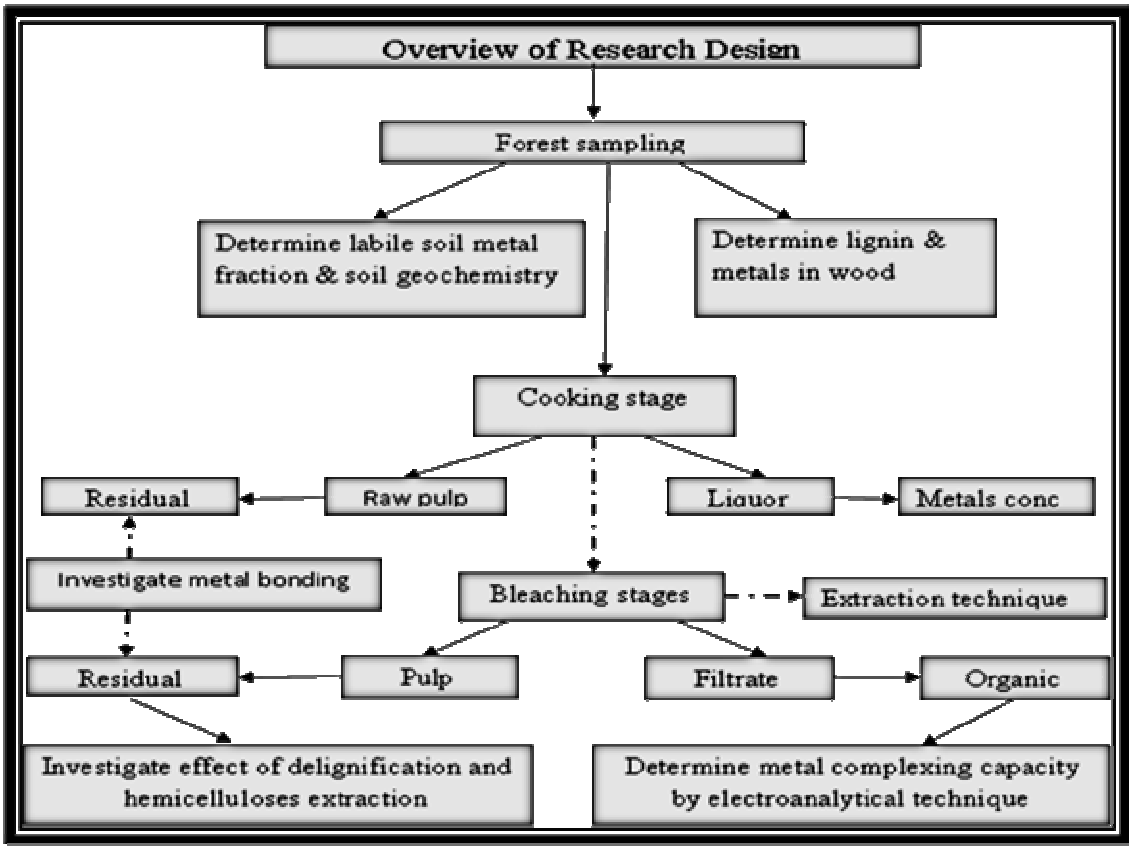

1.4.2 Sampling

1.4.2.1 Sampling of soils, wood and pulping design

The sampling and pulping design gives an in-depth breakdown on the source and type of samples being analysed as well as the type of analysis being performed. It gives a classification of the trees that were sampled and the species/clone sampled. It also indicates where in the vertical soil profile the soil samples were obtained.

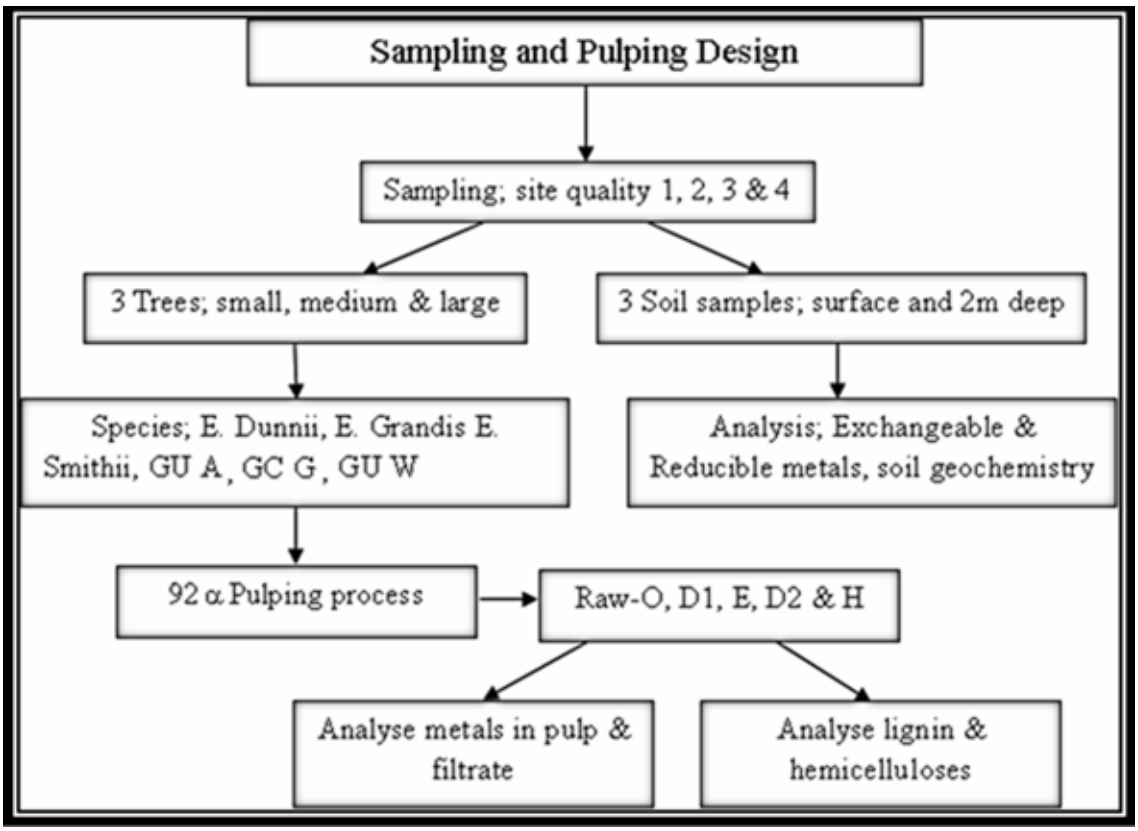

1.4.3 Experimental procedures: sample pretreatment

1.4.3.1 Soil grain size classification

Soil samples were fractionated into different grain sizes by shaking 100 g of soil through vertically arranged sieves of reducing mesh size. The grain size of soil particles and their aggregate structures affect the ability of a soil to transport and retain water, air, and nutrients.

Grain size was classified as clay for particle size <0.002 mm, as silt for particle size between 0.002 mm and 0.06 mm, or as sand for particle size between 0.06 mm and 2 mm.

1.4.3.2 Extraction of labile soil metals

The exchangeable and reducible soil metal fractions represented the soil labile metal pool. The soil exchangeable and reducible metal fractions were determined by a modified BCR extraction protocol according to Rauret *et al*. (1999). The exchangeable metal fraction was obtained by adding 40 mL of 0.11 M acetic acid to 1.00 g of dry soil sample in a 50-mL polypropylene tube. The mixture was then shaken for 16 h at 22 ± 3 °C (overnight). After shaking for 16 h the extract was separated from the solid phase by centrifugation at 3800 rpm for 20 min. The residue was washed by adding 20 mL of Milli-Q water, shaking for 15 min, and then centrifuging. The resulting supernatant liquid was discarded without any loss of residue. Metals bound to iron and manganese oxides were extracted by adding 40 mL of 0.1 M hydroxylammonium chloride (adjusted to pH 2 with 2 M nitric acid) onto the residue from the first step. After shaking the mixture for 16 h, it was centrifuged for 15 min, and then decanted into an ICP vialn for analysis by ICP-OES.

1.4.3.3 Microwave Digestion

About 0.3 g of pulp/sawdust sample was weighed in Teflon tubes and 6 ml of HNO_3 (TraceSelect ICP grade >69% supplied by Fluka) added. The tubes were then sealed with a cap fitted with a pressure regulation valve and placed in a microwave oven (Perkin Elmer Paar Physica multiwave). The microwave digested samples were transferred quantitatively into 50 ml volumetric flasks and made to the mark with milli-Q water of resistivity 18.2 Ω cm^{-1}, thereafter analysis by ICP-OES was performed.

1.4.4 Data analysis

Overall the study was focused on investigating the dynamics of metals in the dissolving pulp production process. A holistic approach was adopted to not only investigate the metal pathway, through the pulping process, but to also mitigate the ensuing problem of residual metals and pollution. In the process of addressing these issues five different thought lines were pursued, that culminated into five manuscripts, each one of them uniquely addressing the objective of the study. The generated data was therefore diverse and required different

data processing approach. Some of the data was specifically generated to fit into the investigative model of interest this includes; adsorption isotherm models, kinetic model and thermodynamic model. In other instances the data generated was so immense and diverse and required a more powerful statistical tool that could unpack the intricate correlations within the data. In this case descriptive statistics was employed, using principle component analysis (PCA).

1.4.4.1 Principle component analysis

Researchers across the disciplines have used Principal Component Analysis (PCA) to determine trends, and for making predictive models. Nilsson (1995) investigated the chemical state of Swedish forest soils using PCA. Li (2008) and co-workers used PCA to estimate forest biomass from light detection and ranging data. Zheng and co-workers (2009) used PCA to determine the significant and contribution of chromatograms of tea extracts to the largest variance in the data and used the information to classify the samples.

Principal Components Analysis is a method that reduces data dimensionality by performing a covariance analysis between factors. To characterize the trends exhibited by this data, PCA extracts directions where the cloud is more extended. For instance, if the cloud is shaped like a football, the main direction of the data would be a midline or axis along the length of the football according to the least squares criterion. This is called the first component, or the principal component (PC or factor). PCA will then look for the next direction, orthogonal to the first one, reducing the multidimensional cloud into a two-dimensional space (Figure 1.4). The second component would be the axis along the football width. Each sample has a score on each Principle component (PC), which represents the sample location along that PC. Each variable has a loading on each PC, reflecting how much the variable contributes to that PC. In geometric terms, a loading is the cosine of the angle between the variable and the current PC. Note that because the goal of PCA is to ‘summarize’ the data, it is not considered a clustering tool.

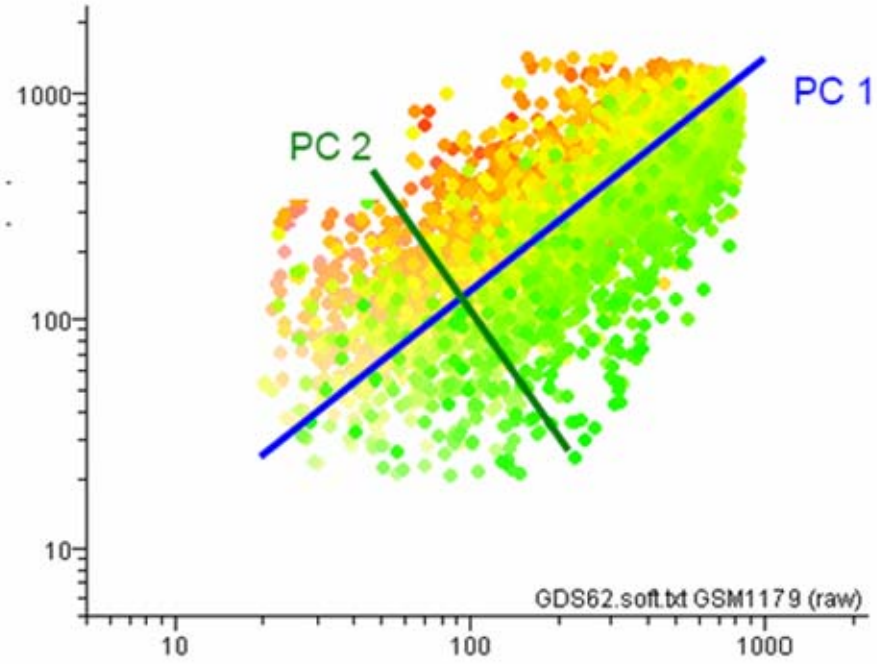

Figure 1.4. Oval-shaped data set with two main components; extract from Agilent Technologies (2005).

(i) Theory of principal component analysis

Advanced computational modeling is applied in processing the data for Principal Components Analysis. A combination of several formulas are applied as stipulated under this theory section (Jambu 1991).

Consider a dataset of p active and k supplementary variables and n active and m supplementary cases. The data pertaining to the active variables and active cases can be arranged in the matrix, X, of n rows and p columns:

$$X = \begin{bmatrix} X_{11}, X_{12}, ..., X_{1p} \\ X_{21}, X_{22}, ..., X_{2p} \\ ....., ..., ... \\ X_{n1}, X_{n2}, ..., X_{np} \end{bmatrix}$$

Where X_{ij} represents the value of the j^{th} variable for the i^{th} case, standardized or centered about their respective means. Similarly, the data pertaining to the supplementary variables can be arranged in the matrix Y of n rows and k columns:

$$Y = \begin{bmatrix} Y_{11}, Y_{12}, \ldots\ldots\ldots, Y_{1k} \\ Y_{21}, Y_{22}, \ldots\ldots\ldots, Y_{2k} \\ \ldots\ldots, \ldots\ldots, \ldots\ldots\ldots\ldots \\ Y_{n1}, Y_{n2}, \ldots\ldots\ldots, Y_{nk} \end{bmatrix}$$

where Y_{it} is the value of the t^{th} supplementary variable for the i^{th} case, standardized or centered about their respective means. The data pertaining to m supplementary cases can be arranged in the matrix Z of m rows and p columns:

$$Z = \begin{bmatrix} Z_{11}, Z_{12}, \ldots\ldots\ldots, Z_{1p} \\ Z_{21}, Z_{22}, \ldots\ldots\ldots, Z_{2p} \\ \ldots\ldots, \ldots\ldots, \ldots\ldots\ldots\ldots \\ Z_{m1}, Z_{m2}, \ldots\ldots\ldots, Z_{mp} \end{bmatrix}$$

where Z_{ls} is the value of the s^{th} variable for the l^{th} case, standardized or centered about their respective means.

Symmetric Matrix to be diagonalized: The orthogonal set of vectors are obtained by diagonalizing the matrix. $X'X$ is the correlation matrix, if the values are standardized. $X'X$ is the covariance matrix, if the values are centered about their means, where X' is the transposed data matrix

$$X = \begin{bmatrix} X_{11}, X_{12}, ..., X_{n1} \\ X_{21}, X_{22}, ..., X_{n2} \\ ....., ..., ... \\ X_{1p}, X_{2p}, ..., X_{np} \end{bmatrix}$$

Eigenvalues and Eigenvectors: Eigenvalues of the correlation matrix, or the covariance matrix of the active variables play an important role in computing the principal components. In addition to determining the factor coordinates of the variables and cases, they give a fairly good idea about the variance that can be explained by the given number of factors. This information can further be utilized for determining the order by which you can afford to reduce the dimensions of the original space of variables or cases, without loosing much information. Based on the eigenvalues, many criteria can be used to decide the ideal number of factors in a given situation. Since the sum of eigenvalues is equal to the number of 'active' variables, the average of the eigenvalues is 1,and the general approach is to first start with the eigenvalues that are greater than 1 (Jambu 1991).

The set of q positive eigenvalues of the matrix $X'X$ (correlation or covariance) is denoted as:

$$\{\lambda_1, \lambda_1, ...\lambda_q\}$$

The set of q eigenvectors corresponding to q eigenvalues is denote as:

$$\{u_1, u_1, ...u_q\}$$

Quality of representation: One of the important questions that has to be answered in PCA is the number of principal components that could ideally represent the whole set of points (variables or cases). As each eigenvalue of the correlation or covariance matrix is representative of the variance explained by a principal component, a percent of cumulative

variance (explained) can be attributed to a given number of factors. This is referred to as the 'quality of representation and is an important measure of the variance accounted for by a given set of principal components (Jambu 1991).

Quality of representation of first *s* principal components is denoted as:

$$= \sum_{\alpha-1}^{q} \lambda_\alpha \Big/ \sum_{\alpha-}^{p} \lambda_\alpha$$

Factor coordinates of active variable: In the terminology of the factor analysis, the factor coordinates are also referred to as 'factor loadings'. Mathematically speaking, a principal component is a linear combination of the variables that are most correlated with it. This further implies that the factor coordinates of a variable are the correlations between the variable and the factor axes. Accordingly, interpretation of the principal components must be done in terms of the correlation. With this fact and the objective of factor interpretation in mind, given a set of variables you should naturally be looking for those variables that have the highest (absolute) values of the factor coordinates for the given factors. Some other statistics that are useful for the purpose of interpretation are: relative contribution of the factor axis to the eccentricity of the variables, and the relative contribution of a variable to the variance of the factor axis. These statistics depend on the magnitudes of the factor coordinates (Jambu 1991).

The α^{th} factor coordinate of the j^{th} active variable is denoted as::

$$(\lambda_\alpha)^{1/2} u_{\alpha j}$$

Factor and variable correlation: The correlation between a th factor and the j th variable is denoted as:

$$(\lambda_\alpha)^{1/2} u_{\alpha j}$$

Contributions of variables: Contribution of a variable is, in fact, the relative contribution of the variable to the variance of a factor axis. The values of this statistic are used for screening the variables, before they are considered on the basis of the factor coordinates, i.e., the correlations, for interpretation of the factor axis. Naturally, those variables should be the candidates for further examination that contribute, relatively, more to the variance of the factor axis (Jambu 1991).

Relative contribution of the j th variable to the variance of the a-factor axis is denoted as:

$$(u_{\alpha j})^2$$

Contributions of cases (active): As in the case of variables, contributions of cases, too, are their relative contributions to the variance of a factor axis. Thus, in a way, the contribution of a case is a measure of the importance of a case as a determiner of the factor axis. The higher the contribution of a case the heavier it weighs on the factor. Accordingly, when it comes to the interpretation of the principal components, the cases with the highest contributions are used first. Genuinely speaking, this statistic for the supplementary cases has no relevance and is, therefore, computed only for the active cases (Jambu 1991).

Contribution of the i th active case for the a th factor is denoted as:

$$= \left(\sum_{j-1}^{p} X_{ij} u_{\alpha j} \right)^2 \Big/ \lambda_i$$

1.5 THESIS HIGHLIGHTS: RESEARCH FINDINGS

The research findings from the study are reported under five topics (Papers I to V) that is 1.5.1 to 1.5.5 as discussed in the sections that follow below.

1.5.1 PCA modeling of *Eucalyptus* forest soil geochemical parameters, labile metals and tree species variability.

The objectives of Paper I of the study were to: (i) investigate the metal and silicon uptake by Eucalyptus trees in reference to the soil geochemistry and metal speciation, (ii) Subject the data to Principle Component Analysis and statistically relate the variables to determine their correlations with Eucalyptus metal uptake, silicon uptake and growth.

The interpretation of the data by PCA was performed by comparing the score plot with the loading plot. The PCA model projects a correlation of the forest plantation site qualities with data on soil geochemistry, labile soil metal content, tree growth and metal and Si wood content. The observed correlations indicated that the high site quality (SQ 1) was favored by a high exchangeable acidity in the bottom soil and was related to the Al in the *Eucalyptus* wood (Figure 1.5). The correlations were well related by the first and second principal component that explained 53.6 % and 14.6 % of the data, respectively. The observation implies that the trees in these high site (sites with high *Eucalyptus* tree productivity) areas obtain their essential mineral nutrients (Fe, Cu, Mn and Zn) from the bottom and not from the surface soil. The acidification of soils results in firstly the dissolution of carbonates and other basic rocks, then the replacement of exchangeable base cations by H^+ and Al, and finally the dissolution of Al and then iron (Fe) bearing minerals.

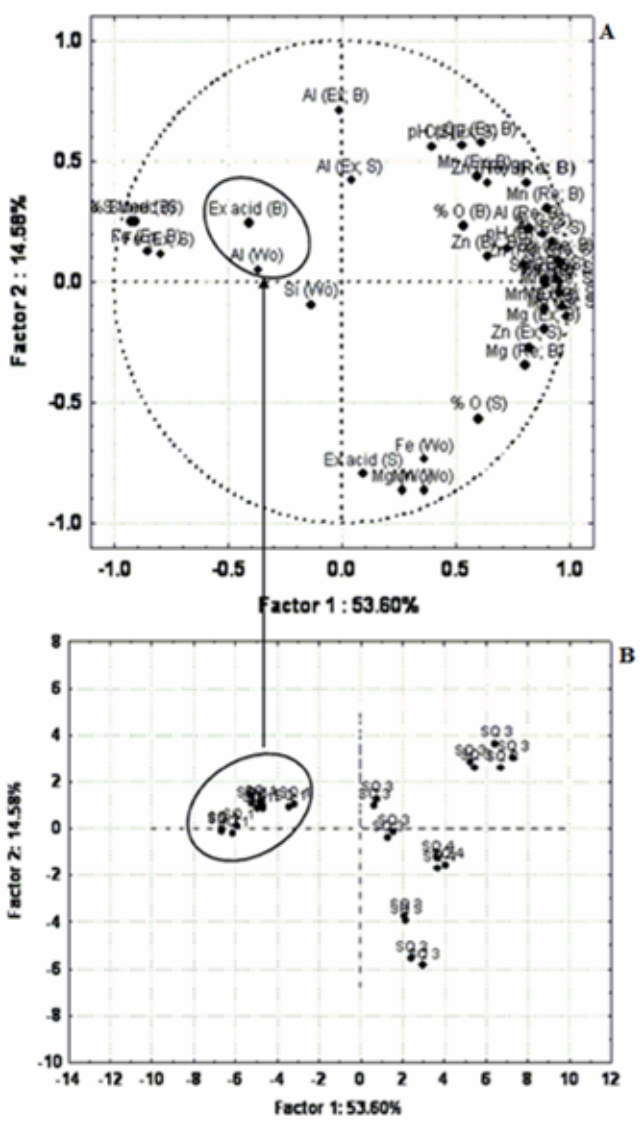

Figure 1.5. *Eucalyptus* forest data analysed by PCA, presented on the score plot (A) and related to the site quality loading plot (B)

1.5.2 The dynamics of metal extraction in a pulp bleaching process

In paper II, the residual metals in the pulp obtained from oxygen delignification (O-stage) and alkaline bleaching stage (E-stage) were investigated to determine the effect of cellulose degradation, delignification and hemicelluloses extraction. A laboratory scale acid bi-sulfite pulping process was employed to pulp the wood obtained from different *Eucalyptus* species and clones, grown in South Africa.

The interpretation of the generated data was conducted with the aid of surface plots. The plots enabled relating three variables on a contour surface. Figure 1.6 is an abstract of the generated data projected on a scatter plot. The figure presents a projection of the variation of lignin (Kappa-Number) during alkaline oxygen delignification, on the Z-axis and relates it to a number of metals and their varying concentration, on the Y and X axis respectively. It can be deduced from the scatter plot that the metals in the pulp are not attached to the lignin, thus the delignification process does not lead to metal loss. On the contrary as the pulp structure opens up due to delignification more metal adsorption sites are availed leading to metal adsorption onto the pulp, thus the inverse metal correlation with lignin.

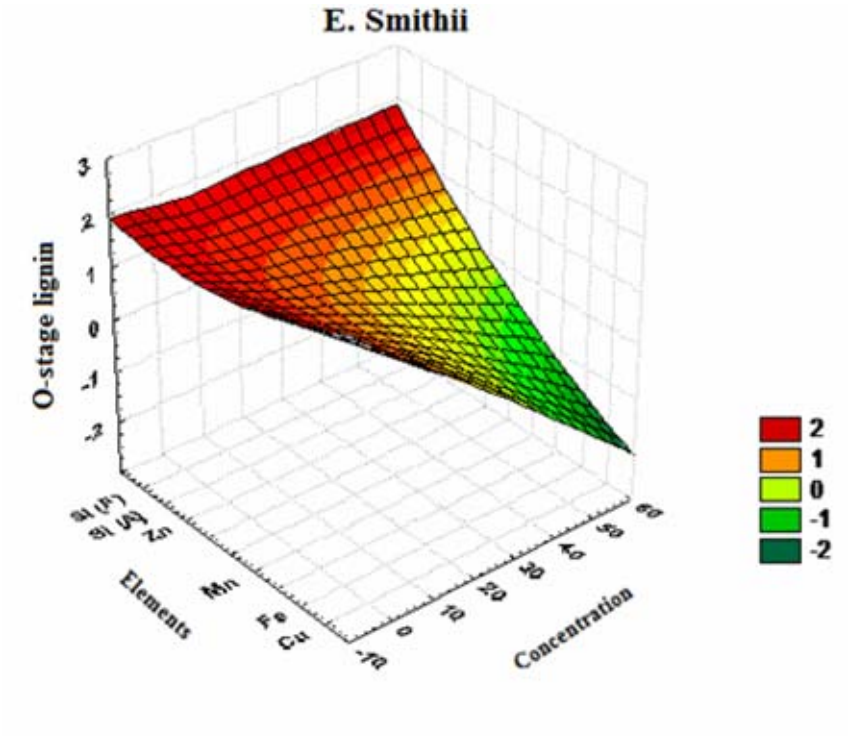

Figure 1.6. Surface plot of Eucalyptus species E. smithii on the effect of lignin extraction during the alkaline oxygen delignification on the residual metal composition.

1.5.3 Investigating the influence of organic ligands in pulp filtrate on metal mobility

Paper III focused on the complexing capacities of filtrates obtained from an alkaline oxygen delignification process and an alkaline bleaching process were determined using electroanalytical technique. A comparison is made between the filtrate samples from the pulp bleaching processes of the different Eucalyptus species/clones. The essence of the study was to obtain an insight of variability in the complexing capacities of the filtrates obtained from the pulp bleaching of the various Eucalyptus species/clones. Filtrates with higher metal complexing capacities provide an environment that reduces the possibility of the metal being adsorbed from the solution onto the pulp. A clear distinction was observed between the peak potentials of O-Stage and E-Stage bleaching filtrates in the presence of Cu^{2+} ions (Figure 5.3.1). A higher shift towards the negative charge is an indication of the stability of the formed Cu^{2+} labile species. The O-Stage bleaching filtrates formed more stable complexes as compared to the E-Stage (Figure 1.7).

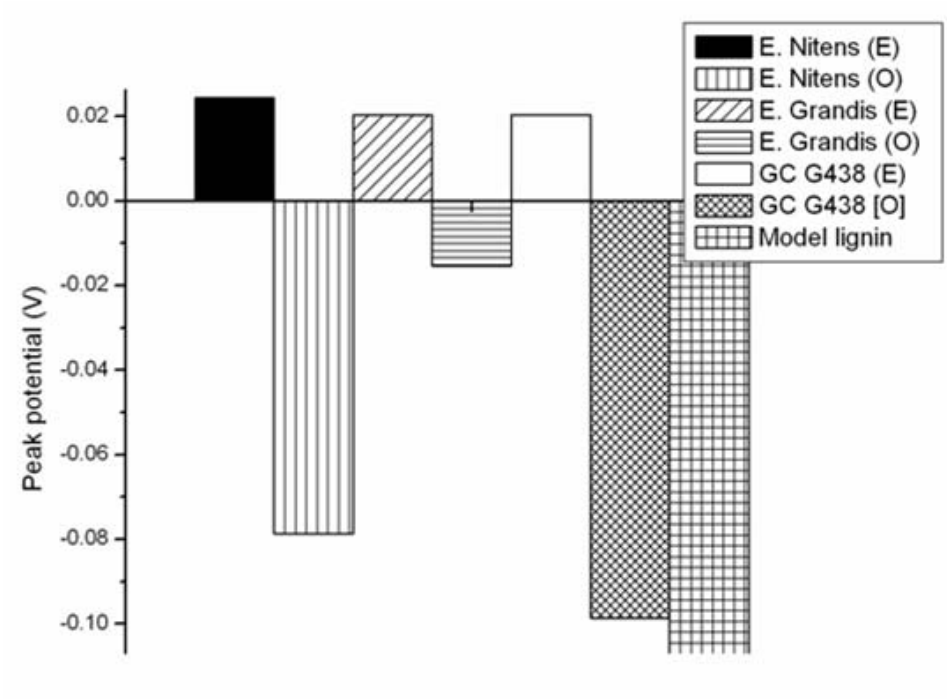

Figure 1.7. Observed peak potential in the presence of Cu^{2+} ions of O-Stage and E-Stage bleaching filtrates for different *Eucalyptus* species and clone at a pH of 3.6; and fixed Cu concentration (47 μM)and fixed pulp filtrate volume(20 μL).

1.5.4 Development of a novel environmentally friendly method for the extraction of residual metals in dissolving pulp

Paper IV reports on a novel method for the extraction of metals adsorbed onto pulp using acetylacetone as a ligand. Environmentally the use of EDTA in the pulp production industries has raised concerns due to its resistance towards biodegradation. Unlike EDTA, acetylacetone is biodegradable and is known to degrade hydrolytically via cleavage at the central C—C bond of the β-diketone moiety.

Table 2 presents an abstract of the results of a comparative study to determine which among acetylacetone or EDTA is a better metal extracting ligand. The pulp was treated with either EDTA or acetylacetone at pH 8. It was observed that acetylacetone was more efficient in extracting residual metals from the pulp material, the metal q_{max} (this quantity represents the amount of metals that remain on the pulp unextracted) quantity with acetylacetone was lower than that with EDTA. The extraction process was well explained by Langmuir isotherm indicating that the metals were chemically adsorbed onto the pulp.

Table 2. Langmuir parameters for the desorption of Al, Cu, Fe, Mg, and Ca from pulp at pH 8 by EDTA and acetylacetone

	EDTA at pH 8			**Acetylacetone pH 8**		
n=15	$\mathbf{R^2}$	***b***	$\boldsymbol{q_{max}}$ **μmole g^{-1}**	$\mathbf{R^2}$	***b***	$\boldsymbol{q_{max}}$ **μmole g^{-1}**
Al	0.004	0.05	1.29	0.951	4.33	0.08
Cu	0.914	3.13	0.06	0.938	5.12	0.06
Fe	0.839	7.68	0.04	0.898	-177.63	0.03
Mg	0.920	2.26	0.29	0.973	-5.88	0.17
Ca	0.870	0.55	0.82	0.838	1.99	0.35

The desorption was performed at a temperature of 30 ºC; for a period of 60 and 50 minutes with EDTA and Acetylacetone respectively

1.5.5 Equilibrium and Kinetic Studies for Extracting Cu, Mn and Fe from Pulp Wastewater onto a C-18 Column with Acetylacetone Complexing Ligand

The last component of the project reports (Part V) on a novel analytical procedure for the solid phase extraction/preconcentration (SPE) of metals in pulp wastewater matrices and saline environmental water samples prior to their determination by inductively coupled plasma-atomic emission spectrometry (ICP-OES).. The extraction/preconcentration is based on the chelation of metals with acetylacetone prior to adsorption onto a C-18 SPE column.

REFERENCES

Adler, E. Lignin - Past, Present and Future. *Wood Sci. and Tech.* 11(3). p. 169-218. (1977).

Agilent Technologies, Inc. 2005. Principle component analysis Main 866.744.7638 http://www.chem.agilent.com/cag/bsp/products/gsgx/Downloads/pdf/pca.pdf. Visited 7th May 2011

Argyropoulos, D. 1995. Fundamental NMR studies in lignins: Emerging answers to issues of concern in relation to pulping TCF bleaching and yellowing. 81st CPPA Annual Meeting Preprints, Tech. Sect., CPPA, Montreal: A209

Behin, J., F. Mikaniki, and Z. Fadaei. 2008. Dissolving pulp (alpha-cellulose) from corn stalk by kraft process. Iranian. *J. Chem. Eng*. 5(3): 14-28

Björkman, A. 1957. Studies on Finley Divided Wood Part 3. Extraction of Lignin-Carbohydrate Complexes with Neutral Solvents. *Svensk Papperstidning* 60(7):243-251.

Brage, C., J. Eriksson, and J. Gierer. 1991. Reactions of chlorine dioxide with lignins in unbleached pulps. Part 1. *Holzfrschung*. 45:1 23-30).

Brelid, H., T. Friberg, and R. Simonson. 1997. TCF bleaching of softwood kraft pulp. Part 3. Ion exchange of softwood kraft pulp prior to oxygen delignification. *Nordic Pulp Paper Res. J.* 12(2): 80-85.

Brelid, H., T. Friberg, and R. Simonson. 1998. TCF bleaching of softwood kraft pulp. Part 4. Removal of manganese from wood shavings prior to cooking. *Nordic Pulp Paper Res. J.* 13(1): 50-56.

Christov, L. P., M. Akhtar, and B. A. Prior. 1998. "Ther potential of bisulfite pulping in dissolving pulp production,' *Enzyme and Microbial Tech*. 23:70.

Christov, L., P. Biely, E. Kalogeris, P. Christakopoulos, B. A. Prior, and M. K. Bhat. 2000. Effects of purified endo-b-1,4-xylanases of family 10 and 11 and acetyl xylan esterases on eucalypt sulphite dissolving pulp *J. of Biotech*. 83:231

Dang, V. Q., N. K. Bhardwaj V. Hoang, and K. L. Nguyen. 2007. "Determination of lignin content in high-yield kraft pulps using photoacoustic rapid scan Fourier transform infrared spectrosco[py," carbohydrate Polymers, 68(3): 489.

Edwards, J. O. 1962. *Peroxide reaction mechanisms*. Edwards Eds.; Interscience, New York.

Entwistle, D., E. H., N .S. Cole. 1949a. Wooding, The autoxidation of alkali cellulose . Part II. *Textile Res. J.* 19(9): 609-624.

Entwistle, D., E. H., N. S. Cole. 1949b. Wooding, The autoxidation of alkali cellulose . Part I: An experimental study of the kinetics of the reaction. *Textile Res. J.* 19(9): 527-546.

Ericsson B, B. O Lindgren, and O. Theander. 1971. Factors influencing the carbohydrate degradation under oxygen-alkali bleaching: *Svensk Papperstidn* 74:757-765

Erikkson, O., and B. O. Lindgren. 1977. About the Linkage Between Lignin and Hemicelluloses in Wood. *Svensk Papperstidning.* 80 (2):59-63.

FAO 2005. Survey of World pulp and paper.www.fao.org/forestry/FOP/FOPW/paper/public-e.stm

Fengel D., and G. Wegener. 1989. *Wood-Chemistry, Ultrastructure reactions*. Walter de Gruyter, Berlin, New York.

Fengel, D., and G. Wegener. 1989. *Wood: chemistry, ultrastructure, reactions*. Walter de Gruyter, Berlin.

Freudenberg, K. and A. C. Neish. 1968. *Constitution and Biosynthesis of Lignin*. Springer, G.F. and Kleinzeller, A. Eds.; Springer-Verlag: New York. 129 pp.

Garrote, G., M. E. Eugenio, M. J. Diaz, J. Ariza, F. Lopez. 2003. "Hydrothermal and pulp processing of Eucalyptus," *Bioresource Techn*., 88:61.

Gellerstedt, G., and W. W. Al-Dajani. 2000. bleachability of alkaline pulps. Part 1. The importance of b-aryl ether linkages in lignin. *Holzforschung*. 54(6):609-617.

Gierer, J. 1982. Chemistry of delignification, 1. A general concept. Part 1. *Holzforschung*, 36(1):43-51.

Gierer, J. 1985. Chemistry of delignification, 1. General concept and reactions during pulping. *Wood Sci. Technol*. 19(4): 289-312.

Gierer, J. 1997. Formation and involvement of supperoxide (O_2•-/HO_2•) and hydroxyl (OH•) radicals in TCF bleaching processes: a review. *Holzforschung.* 51(1): 34-46.

Gilbert, A. F., E. Pavlovova, and W. H. Rapson. 1973. Mechanism of magnesium retardation of cellulose degradation during oxygen bleaching. *Tappi.* 56(6): 95-99.

Gotzinger G., A. Schrittwieser, and R. Muhlbacher. 2000. Monosulfite splitting – an important part of the secondary recovery system of the magnesium base acid bisulfite cooking process. *Lenz. Ber*. 79: 36–38.

Haworth, W. N. 1928. The structure of Carbohydrates. *Helv. Chimie Acta*, 11: 534-548.

Hodgson, M., and D. Thompson. 1985. Uncovering the secrates of soil. *New Scientist*. 44-47

Jambu, M. 1991. In: *Exploratory and multivariate data analysis*, Academic Press (1991),

Karhunen, P., P. Rummakko, J. Sipilä, G. Brunow and I. Kilpeläinen. 1995. Dibenzodioxocins; A Novel Type of Linkage in Softwood Lignins. *Tetrahedron Lett.* 36(1): 167-170.

Kishimoto, T., and F. Nakatsubo. 1998. Non-chlorine bleaching of kraft pulp. IV. Oxidation of methyl 4-O-ethyl-β-D-glucopyranoside with Fenton's reagent: Effects of pH and oxygen. *Holzforschung*. 52(2): 180-184.

Klemm, D., B. Philipp, T. Heinze, U. Heinze, and W. Wagenknecht. 1998. *Comprehensive cellulose chemistry*, Wiley-VCH, Weinheim, vol 1&2

Klemm, D., H. P. Schmauder, and T. Heinze. 2002. Cellulose. In*: Biopolymers: Biology Chemistry*, *Biotechnology, Appications*. E. Vandamme, S. De Baets, A. Steinbuchel, Eds. Wiley-VCH, Weinheim.

Krässig, H. A. 1996. *Cellulose - Structure, Accessibility and Reactivity. Polymer Monographs* Vol. 11. M. B. Huglin. Gordon and Breach science publishers. Amsterdam,

Lachenal D, J. C, Fernandes, and P. Froment. 1994. Behavior of residual lignin in kraft pulp during bleaching. International Pulp Bleaching Conference-Papers Preprints, Tech. Sect., CPPA, Montreal, pp 41

Liden, J., and L. O. Ohman. 1998. On the prevention of Fe- and Mn-catalyzed H2O2 decomposition under bleaching conditions. *J. Pulp Paper Sci.* 24(9): 269-276.

Manouchehri, M., and O. Samuelson. 1973. Influence of catalysts and inhibitors upon the degradation of carbohydrates during oxygen bleaching. *Svensk. Papperstidn*. 76(13): 486-492.

Marton, J. 1971. Reactions in alkaline pulping. In *Lignins Occurance, Formation, Structure and Reactions*; Sarkanen, K. V., Ludwig , C. H., Eds; Wiley: New York; pp 679.

Newman RH. 2004. Homogeneity in cellulose crystallinity between samples of Pinus radiata wood. *Holzforschung* 58(1): 91-96.

Nilsson, S. I. 1995. Current chemical state of Swedish forest soils investigated by principle component (PCA) and regression analysis *Ecol. Bull*. 44: 65-74.

Payen, A. 1842. *Troisième mémoire sur le development végétaux. Extrait des memoires de l'Academie Royale des Sciences: Tomes III des Savants Étrang-ers, Imprimerie Royale, Paris*.

Perng, Y-S., C. W. Oloman, P .A. Watson and B. R. James. 1994. Catalytic oxygen bleaching of wood pulp with metal porphyrin and phythalocyanine complexes. *Tappi. J*. 77(11): 119-125.

Quintana, G. C., G. J. M. Rocha, A. R. Goncalves, and G. C. Velasquez. 2008. Evaluation of heavy metal removal by oxidized lignins in acid media from various sources. *BioResources* 3:4 1092-1102.

Rauret, G., J. F. Lopez-Sanchez, A. Sahuquillo, R. Rubio, C. M. Davidson, A. M. Ure, and Ph. Quevauviller, 1999. Improvement of the BCR three step sequential extraction procedure prior to the certification of new sediment and soil reference materials, Journal Environmental Monitoring, 1, 57–61.

Sarkanen K. V., and H. L. Hergert. 1971. Classification and distribution: In: *Lignins: occurrence, Formaton, Structure and Reaction*, Sarkanen, K. V., and C. H. Ludwig, Eds, Wiley Interscience, New York, 43-49

Schwanninger, M. 2006. Chemistry of oxygen delignification: *In Handbook of pulp,* Sixta Eds vol 2. Wiley-Vch GmbH, Weinheim, Germany.

Scott, S. 2002. Seaweed also plays a role in the formation of sand. "Ocean Watch",Honolulu Star-Bulletin, www.starbulletin.com

Shimizu, K. 2001. Chemistry of hemicelluloses; In: *Wood and Cellulosic Chemistry*. 2nd edition, Eds. D.N.-S. Hon, N. Shiraishi, Marcel Dekker Inc., New York, USA, pp. 177-214.

Sixta, H. 2004. Comperative evaluation of CBC kraft pulping of pine and spruce wood chips. Internal report, R&D Lenzing AG.

Sixta, H. 2006a. Sulfite chemical pulping: *In Handbook of pulp.* Sixta Eds vol 1; Wiley-Vch GmbH, Weinheim, Germany.

Sixta, H. 2006b. Sulfite chemical pulping: *In Handbook of pulp* Sixta Eds vol 1; Wiley-Vch GmbH, Weinheim, Germany.

Sjöström, E. 1993. *Wood Chemistry: Fundamentals and Application*. Academic Press: Orlando. 293 pp

Sjöström, E. Wood pulping, *Wood chemistry. Fundamentals and applications* (2nd ed.), Academic Press Inc, London, UK (1993) pp. 140–164.

Staudinger, H., 1932. In: *Die hochmolekularen organischen Verbindungen–Kautschuk und Cellulose*, Springer Verlag (reprinted 1960).

Süss, H.U. 2000. *Bleaching Ullmann's Encyclopedia of Industrial Chemistry* Wiley-VCH Verlag GmbH & Co.

TAPPI Test Methods ISO 2470-1973, 646 om-86, DIN 53 145.

TAPPI Test Methods Prüfung von Papier Pappe Zellstoff und Holzstoff, Band 1: Chemische und mikrobiologische Verfahren, Springer Verlag 1991; Band 2: Mikroskopische und photometrische Verfahren, Springer Verlag 1993;, TAPPI Press 1996, Atlanta.

Thygesen A, J. Oddershede, H. Lilholt, A. B Thomsen, and K. Stahl. 2005. On the determination of crystallinity and cellulose content in plant fibers. *Cellulose.* 12(6): 563- 576.

Timell, T. E. 1967. Recent progress in the chemistry of wood hemicelluloses. *Wood Sci Technol* 1(1): 45-70.

Timell, T. E. 1986. *Compression wood in gymnosperms*. Springer-Verlag, Berlin, Heidelberg, New York.

Yuzhen Li, H-E Andersen, and R. McGaughey. 2008. A Comparison of Statistical Methods for Estimating Forest Biomass from Light Detection and Ranging Data. *West J. Apil*. 23(4).

Zhang, L., and G. Gellerstedt. 2001. NMR observation of a new lignin structure, a spiro-dienone. *Chem. Commun*. 2744-2745.

Zheng, L., D. G. Watson, B.F. Johnston, R.L. Clark, R. Edrada-Ebel, and W. Elseheri. 2009. A chemometric study of chromatograms of tea extracts by correlation optimization warping in conjunction with PCA, support vector machines and random forest data modeling. *Analytica Chimica Acta.* 642: 257–265

CHAPTER 2: PAPER I

PCA MODELING OF SOIL GEOCHEMICAL PARAMETERS, LABILE METALS AND TREE SPECIES VARIABILITY OF *EUCALYPTUS* FOREST PLANTATION.

Joseph Nyingi Kamau[1], Jane Catherine Ngila[1,3], Andrew Kindness [1], and Tammy Bush[1,2]

[1]University of Kwazulu-Natal, Chemistry department, Private Bag X54001, Westville, Durban 4000, South Africa.

[2]CSIR Natural Resources and the Environment, Forestry and Forest Products Research Centre, P.O Box 17001, Congella 4013, South Africa.

[3]University of Johannesburg, Doornfontein Campus P.O. Box 17011, Doornfontein 2028, South Africa

ABSTRACT

The amount of transition metals and silicon in the *Eucalyptus* wood raw material impacts on the production cost and quality of the final pulp product. If silicon is present in viscose grade pulp the spinning process is impacted due to the clogging of the spinnerets. This work seeks to investigate the pathway of some transition metals and silicon in the *Eucalyptus* forest plantations as well as their role in the forest productivity. Although metals impact on the pulp production they are also essential in the growth of the trees. Principal component analysis was employed to determine the correlation between the observations and the variable of interest. It was established that Fe is a limiting factor in the growth of the *Eucalyptus* trees in the forest under study. The main pathway for the metals and silicon was found to be the exchangeable soil fraction. The *Eucalyptus* trees took in metals from both the ground and bottom soils. The soil geochemistry of the site determined the depth at which the trees took in the metals and silicon.

Key words: Principal component analysis, Metals, *Eucalyptus*, Forest, Pulp.

INTRODUCTION

The pulp and paper production industry in South Africa uses mainly *Eucalyptus* trees as their raw material. Dissolving pulp quality depends both on the chemical constituents of the raw wood material and the pulping process. Transition metals in the *Eucalyptus* wood impacts on the pulping production cost. This is attributed to the transition metal catalytic decomposition of H_2O_2, during the pulp bleaching process. Silicon on the other hand is detrimental to the spinning process as it induces clogging of the spinnerets.

The uptake of metals and nutrients by trees is dependent on the geochemistry and the climatic condition of the locality. Plants have been described as solar driven pumps that can extract and concentrate metals from their environment.[1] Metals exceeding the metabolic needs are transported to the extremities such as the bark, twig tips and leaves.[2] The retention of metals in specific compartments and their distribution to the tissues of the plant is highly species specific and depends on metal resistance mechanisms available to the plant such as chelation of metals, compartmentalization and organic ligand exudation.[3, 4]

Soil porosity and water retention capacity determine the soil drainage efficiency, soils with low porosity and high water retention are prune to water logging during the rains. Anaerobic microorganisms use carbon compounds as substrates and oxidized soil components as electron acceptors in respiration. Oxygen is the first soil component to be reduced followed by nitrate, manganese dioxide and ferric iron hydroxide.[5,6] As a result, flooded soils can have toxic concentrations of plant available nutrients such as iron and manganese compared to well drained soils.[7] Uptake of excess quantities of iron by plants can be potentially toxic because iron promotes the formation of reactive oxygen based radicals that are able to damage cellular membranes. Tree roots may alter the physical and chemical conditions of the soil, changing the ionic equilibria, pH, and redox potential and thus altering the bioavailability of metals in the soil surrounding the roots (the rhizosphere). Uptake is also influenced by interactions among metals, nutritional status, age of the tree, soil microorganisms and there is significant genetic variation between and within tree species for tolerance to metals.[8,9,10]

The objectives of this study were to: (i) investigate the metal and silicon uptake by *Eucalyptus* trees in relation to the soil geochemistry and metal speciation, (ii) Subject the data to Principle Component Analysis and statistically relate the variables to determine their correlations with *Eucalyptus* metal uptake, silicon uptake and growth.

METHODOLOGY

Sampling sites

Soil and *Eucalyptus* tree samples were collected (in the year 2009) from Zululand, Braemar, Sutton and Riverdale located in South Africa (Figure 1). These sites have been categorized into two main zones namely Midlands (Braemar, Suttonand and Riverdale) and Zululand. The zones are unique in their soil geochemical characteristics and climatic conditions. Zululand is mainly composed of sandy soils with very low clay, low water retention capacity and experience subtropical climatic condition. Midlands's sites are mainly composed of clay loam soils and experience temperate climatic conditions. The sites were ranked; site quality 1, 2, 3, and 4 according to the growth rate and quality of *Eucalyptus* trees growing in them. Site quality 1 was the site considered to have the highest *Eucalyptus* tree productivity, the order of productivity decreased with the increase in number ranking. The sampled trees were of the same age group (9 years), categorized according to size classes (small, medium and large) in reference to trunk diameter at breast height.

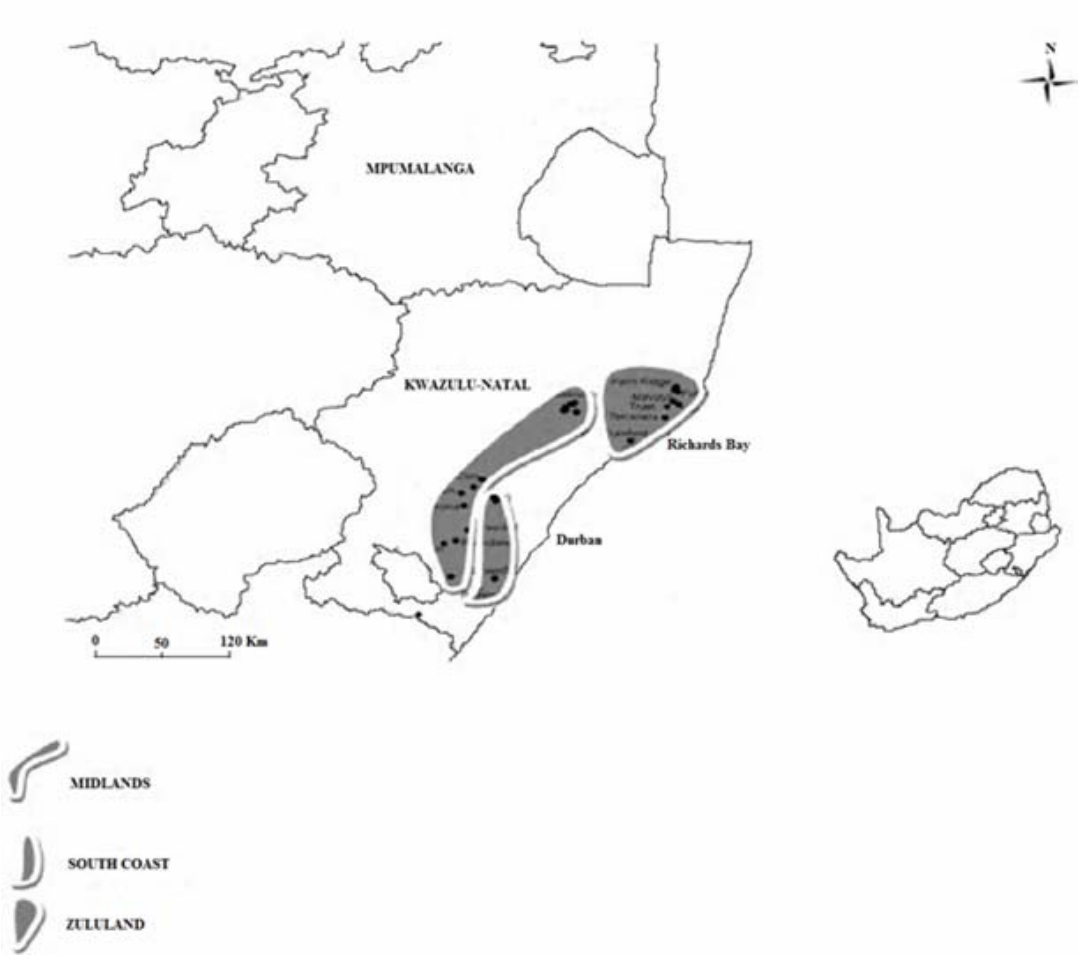

Figure 1. Map of the South African *Eucalyptus* forest sampling zones

Three set of soil samples were collected using a soil auger around the tree at 20 cm below the surface and at 200 cm deep. The samples were labeled and stored in polythene bags for further analysis in the laboratory. The trees were then felled and a disk obtained at the tree's breast height. In the laboratory the disks were dried and ground into sawdust for further analysis. The soil samples collected from the same depth (ether 20 cm or 200 cm) were pooled together and homogeniszed before conducting any analysis.

Analytical protocol

Soil samples

The geochemistry of the sampling site was determined by analyzing soil samples for grain size composition, organic matter, soil pH and exchangeable acidity. Soil metal labile fractions were determined by fractionating the exchangeable and easily reducible metal phases. These are the metal fraction most readily available to the tree depending on the prevailing physicochemical soil parameters. Soil samples were fractionated into different grain sizes by shaking 100 g of soil through vertically arranged sieves of reducing mesh size. The grain size of soil particles and their aggregate structures affect the ability of a soil to transport and retain water, air, and nutrients. Grain size was classified as clay for particle size <0.002 mm, as silt for particle size between 0.002 mm and 0.06 mm, or as sand for particle size between 0.06 mm and 2 mm. Organic matter was determined by weight loss after ashing in the furnace at 450 ^{o}C for six hours. Active acidity was determined as H^{+} ions in soil solution as measured with a pH meter. Active acidity is the quantity of hydrogen ions that are present in the soil water solution. The active pool of hydrogen ions normally is in equilibrium with the exchangeable hydrogen ions that are held on the soil's cation exchange complex. This pool most readily affects plant growth. The second pool, exchangeable acidity, refers to the amount of acid cations, aluminum and hydrogen ions, occupied on the cation exchange capacity (CEC). When the CEC of a soil is high but has a low base saturation, the soil becomes more resistant to pH changes. Exchangeable acidity (exchangeable H^{+} and Al^{3+}) was quantitatively determined by extracting the soil sample with a neutral solution of potassium chloride (1 M KCl;[11]). An aliquot of the extract was then titrated to the phenolphthalein endpoint with standardized base. The equivalent of base added corrected to the volume of the extraction solution was the estimate of total exchangeable acidity.

Labile soil metals were determined by applying the modified BCR stage one and two extraction protocol according to Rauret.[12] 1 g of soil sample was mixed with 40 ml of 0.11M acetic acid (pH 2.85) and placed in a horizontal shaker for 16hours after which the contents were centrifuged at 6000 revolutions per minute and decanted into vials. The fraction of metals extracted after this process includes the exchangeable and carbonate bound metals. Using 20 mL of distilled water, the residue from the first stage extract was washed, centrifuged, and the supernatant discarded. The washed residue from stage one was further extracted by adding 40 mL of 0.1 mol L^{-1} hydroxylammonium chloride (adjusted to pH 2

with 2 mol L^{-1} nitric acid) and the mixture shaken for 16 h, thereafter centrifuged at 6000 revolutions per min. The supernatant was then analysed by ICP-OES (Perkin Elmer Optima 5300DV)

Wood samples

About 0.3 g of dry *Eucalyptus* sawdust sample was accurately weighed in Teflon tubes and 6 ml of HNO_3 (TraceSelect ICP grade >69% supplied by Fluka) added. The tubes were then sealed with a cap fitted with a pressure regulation valve and placed in a microwave oven (Perkin Elmer Paar Physica multiwave). The digested samples were transferred quantitatively into 50 mL volumetric flasks and made to the mark with milli-Q water of resistivity 18.2 Ω cm^{-1}. Silicon was determined by alkaline fusion, about 0.5 g of *Eucalyptus* sawdust samples were weighed in 6 ml nickel crucibles and ashed for 12 hours. The ashed samples were allowed to cool; thereafter 2 g of NaOH and 1 g of Na_2O_2 were added and fused at 470 ^oC for 2 hours. The fusion cake was dissolved in milli-Q water and the contents transferred into 100mL polyethylene volumetric flask. The crucibles were then rinsed with 6 ml of 6 M HCl and the contents transferred into the 100 mL volumetric flask and made to volume with milli-Q water. The fused sample represented the total Si sample content while the acid labile Si was obtained from the microwave acid digest.

Quality check

Interference effects associated with samples arising from co-extracted matrix components in the fraction were investigated by comparing the slopes of the curves obtained by normal calibration standards prepared in Milli-Q water and that of standard addition of a soil acetic acid extract. Precision/reproducibility was determined as relative standard deviation values obtained from eight replicates by using 1.00 g of subsamples. The detection limits of metals were investigated and their % recoveries determined. The calculation of the detection limits were based on three times the standard deviation of the blank intensity divided by the slope of the calibration graph (3s/b, n = 20, where s is the standard deviation of the blank and b is the slope of calibration curve).[13]

For recovery studies, appropriate amounts of standard solutions were added to the soil extracts obtained from the extraction of the same soil sample to increase intrinsic analyte concentrations by ~50 to 100% at the levels intended, the results are represented in %

recovery (Table 2). Extraction efficiency of the BCR stage one was investigated by ashing 125μm grain size soil in a muffle furnace at 550 ºC and washing the ashed soil with distilled water to rinse out salts. The soil was then dried and 0.3 ml of 100 ppm Cu, Si and Pb added to 1 g of the soil and allowed to sand for one hour. Thereafter BCR stage one extraction was performed as above.

Statistical analysis

The data was analysed statistically using Statistica 6.0 program. Variables with values above 10 were log transformed to normalize the data. Principle component analysis was the multivariate method of choice. In principle component analysis (PCA), straight lines are sought that best fit the clouds of points in the vector spaces (of variables and cases), according to the least squares criterion. This in turn yields the principal components (factors) that result into the maximum sums of squares for the orthogonal projections. Consequently, a lower dimensional vector subspace is recovered, that represents the original vector space.[14] Factor coordinates of the variables also referred to as 'factor loadings' are the correlations between the variable and the factor axes. Mathematically speaking, a principal component is a linear combination of the variables that are most correlated with it. The first factor is generally more highly correlated with the variables than the second factor. This is to be expected because, these factors are extracted successively and will account for less and less variance overall.[14]

Mean subtraction ("mean centering") is necessary for performing PCA to ensure that the first principal component describes the direction of maximum variance. If mean subtraction is not performed, the first principal component will instead correspond to the mean of the data. A mean of zero is needed for finding a basis that minimizes the mean square error of the approximation of the data.[14] Assuming zero empirical mean (the empirical mean of the distribution has been subtracted from the data set), the principal component w_1 of a data set x can be defined as:

$$\mathbf{w}_1 = \arg\max_{\|\mathbf{w}\|=1} \operatorname{Var}\{\mathbf{w}^T\mathbf{x}\} = \arg\max_{\|\mathbf{w}\|=1} E\left\{\left(\mathbf{w}^T\mathbf{x}\right)^2\right\}$$

RESULTS AND DISCUSSION

The generated data was both variable and large; the determined variables were selected on their assumed possible influence on metal dynamics. With this information we seek to investigate the pathway of metals and Si in *Eucalyptus* plantations. The interaction between the data was amplified by employing the statistics of principal component analysis (PCA) using Statistica 6.0 statistical program software.

Data quality

The quality of the generated data was tested with standard reference materials related to the specific analytical protocol. Data generated from BCR extraction was qualified using certified reference material CRM BCR-701 (Table 1). The BCR-1 extraction protocol extracts, the exchangeable and carbonate bound metals. The quality check comparative data is presented in Table 1; measured levels were within acceptable limits.

Table 1. CRM BCR-701 stage 1 extraction quality check

	CRM BCR-701 Certified (value in mg Kg^{-1})	CRM BCR-701 Uncertainty	Analysed value in mg Kg^{-1} (± SD; n=2)
Cd	7.34	0.35	7.55 ±0.20
Cr	2.26	0.16	3.56 ±0.09
Cu	49.3	1.7	57.20 ±0.44
Ni	15.4	0.9	15.40 ±0.36
Pb	3.18	0.21	3.27±0.07
Zn	205	6	216.40 ±3.44

SD = Standard deviation

The matrix effect due to acetic acid extraction was investigated by spiking an extracted matrix of a soil sample with a known concentration of metal. The spiked matrix was

analysed for the element of interest and the % recovery calculated (Table 2). The matrix did not significantly affect the solutes concentrations; there was however a slight signal enhancement of about 10% for most of the elements analysed, except Al and Si whose signal was slightly inhibited. The extraction efficiency was determined by spiking a uniform grain sized (125 μm) soil sample with 0.3 ml of 100 ppm Cu, Pb and Si. The spiked soil was allowed to stand for one hour and thereafter extracted according to BCR stage one extraction process. Extracted metals were then analysed by ICP-OES and their extraction efficiency determined (Table 2). The extraction efficiencies for the three elements were about 100%. Detection limits were within single digit ppb levels except for Al, Ca, Mg and Si whose levels were one to two orders of magnitude higher (Table. 2). The extraction process was reproducible %RSD ranged between 3-11%.

Table 2. % Recovery, % extraction efficiency, detection limit and reproducibility expressed in % RSD

Element	% Recovery (n=5)	%Extraction Efficiency (n=5)	Detection limit ($\mu g\ L^{-1}$)	Reproducibility %RSD (n=8)
Al	80	ND	18	3.6
Ca	114	ND	46	9.5
Cu	115	102	1.7	ND
Fe	108	ND	2.4	8.7
Mg	113	ND	18	4.8
Mn	112	ND	1.4	9.4
Pb	114	106	8.9	11.3
Zn	121	ND	2.3	ND

ND = not determined

Calibration slopes obtained from direct calibration using milli-Q water were compared to BCR stage one extracted medium. The percentage change in the slope was determined; it ranged between -0.06 to 1.3 (Table. 3).

Table 3 Matrix effect: Comparison of the slopes obtained from the direct calibration and the standard addition graphs.

Element	Calibration Graph Emission intensities	Standard Addition Emission intensities	Change in Slope, %
Al	66125	65706	0.63
Ca	85419	84908	0.60
Cu	112417	112360	0.05
Fe	108650	108492	0.15
Mg	286189	285191	0.35
Mn	594225	594700	-0.08
Pb	7650	7653	-0.04
Si	42066	41518	1.30
Zn	34572	34520	0.15

The quality of the data obtained from the digested *Eucalyptus* wood samples was tested by analyzing NCS DC 73348 standard reference material. The NCS DC 73348 standard reference material was a homogenized biota sample comprising bush branches and leaves. The analysed data compared well with the certified values as reported in Table 4.

Table 4. Comparing data with standard reference material NCS DC 73348 Bush branches and leaves

	NCS DC 73348 Certified (in mg Kg^{-1})	NCS DC 73348 Uncertainty	Analysed value in mg Kg^{-1}(± SD; n=3)
Ca	2.22	0.13	2.09 ±0.05
Cu	5.2	0.5	5.16 ±0.36
Fe	1020	67	914 ±19
Mg	0.29	0.02	0.26 ±0.002

SD= standard deviation

Interpretation of PCA results

The interpretation of the data by PCA was performed by comparing the score plot with the loading plot. The score plot is a summary of the relationship among the observation while the loading plot is a summary of the variable. Thus by comparing the score and loading plot we can identify the relationships between the samples and the variable of interest. The different *Eucalyptus* forest plantation sites were ranked according to the forest quality and productivity. The ranking was from 1-4 the site with high tree quality and productivity was ranked 1 and the ranking ascended as the tree quality and productivity decreased, with rank 4 having the lowest quality and productivity.

Figure 2 presents a loading plot of the various site qualities and relates them to the observations in the score plot. Site quality 1 related highly with exchangeable acidity of the soil sample obtained from a depth of 2 meters around the *Eucalyptus* trees. There was also observed a high correlation in site quality 1 with the content of Al in the *Eucalyptus* wood sample. The correlations were well related by the first and second principal component that explained 53.6 % and 14.6 % of the data, respectively. The observation implies that the trees in these high site areas obtain their essential mineral nutrients from the bottom and not from the surface soil. Plants have been described as solar driven pumps that can extract and concentrate metals from their environment.[1] Some metals are essential nutrients, these include magnesium, calcium, potassium, iron, manganese, copper, zinc and

molybdenum.[15,16] However some are toxic at higher levels such as Cu, even though it is categorized as a micronutrient.

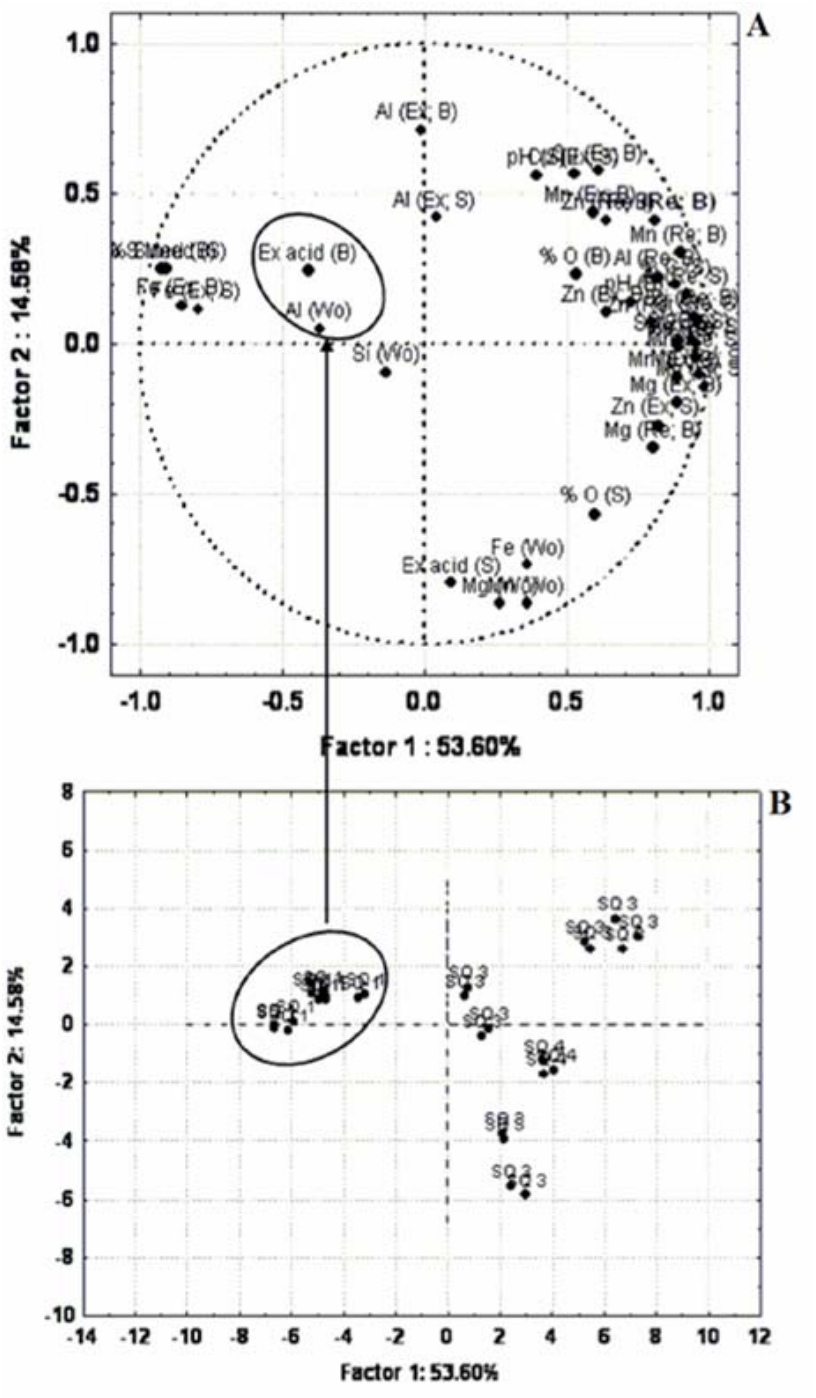

Figure 2. *Eucalyptus* forest data analysed by PCA, presented on the score plot (A) and related to the site quality loading plot (B)

Exchangeable acidity refers to the amount of acid cations, aluminum and hydrogen ions, occupied on the cation exchange capacity (CEC). The acidification of soils results in firstly the dissolution of carbonates and other basic rocks, then the replacement of exchangeable base cations by H^+ and Al, and finally the dissolution of Al and then iron (Fe) bearing minerals.[17] This explains why the high site quality (SQ 1) was related to the Al in the wood sample, since the mobilized Al and metal nutrients were available for uptake by the tree. The active acidity (pH) which is the quantity of hydrogen ions that are present in the soil water solution also played an active role in mobilizing the required metallic nutrients.

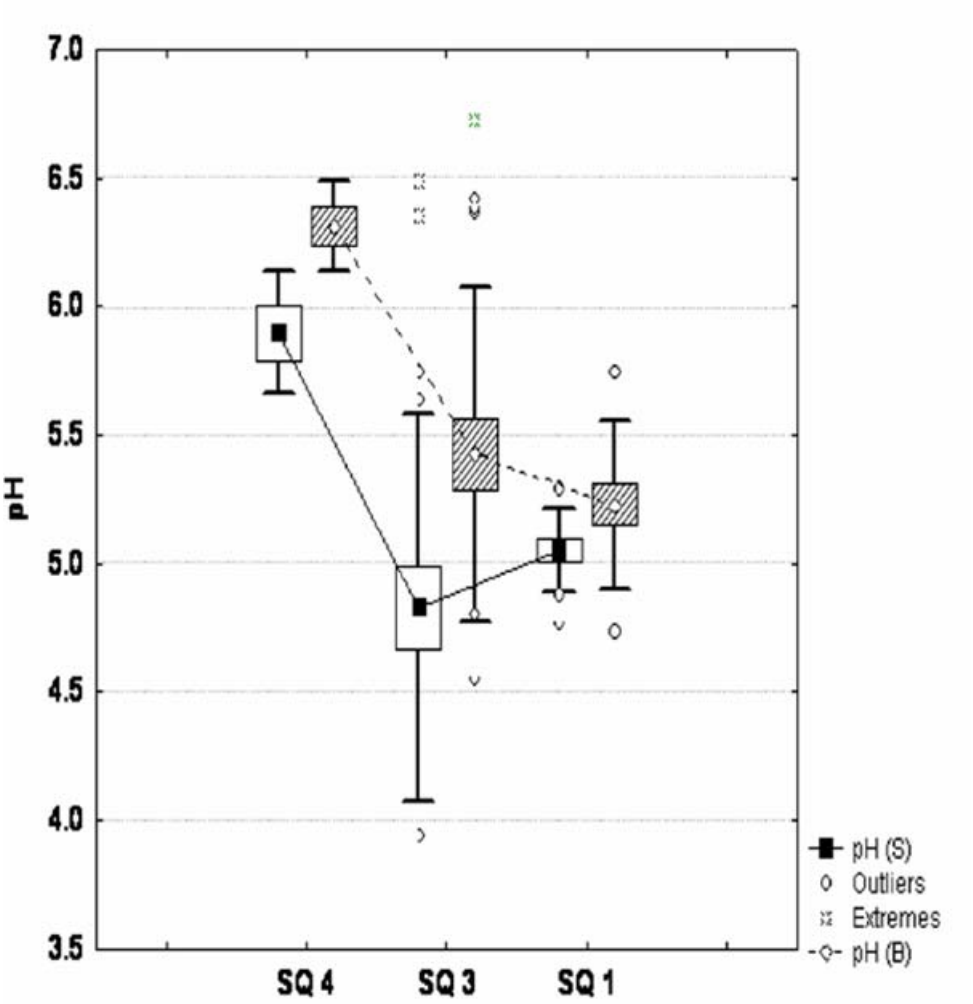

Figure 3. Relationship between soil pH and site quality of the *Eucalyptus* forest under study; pH (S) is soil surface pH and pH (B) is soil bottom pH.

The relationship between the pH and the site quality is presented in Figure 3. The site quality was favored by low pH for both surface and bottom soils. Alhendawi[18] and co-workers reported low Fe levels in plants grown in soils containing high bicarbonate levels. They observed that an increase in the bicarbonate concentration resulted in decreased Fe concentrations in the roots.

Iron is considered as an important micronutrient in plant growth, its influence was investigated by relating the Fe labile fractions with site quality (Figure 4). The reducible Fe fraction did not relate well with site quality. On the other hand the exchangeable fraction did relate to the site quality, high site quality was favored by high exchangeable Fe for both the surface and bottom soils (Figure 4). A number of studies previously have reported a good correlation between extractable metal concentrations and metal content in some biota.[19,20,21] The bioavailability of Fe seemed to be a limiting factor in the *Eucalyptus* forest plantations. The sampled *Eucalyptus* tree species and clones of the same age were categorized into two size groups, small and large. The two tree categories were analysed for their Fe content and the concentration related to the tree size. The observed relationship is presented in Figure 5, the large tree size of each species and clone had a higher mean Fe concentration compared to the small tree size of the same species/clone, though not significantly different. This consistant trend of high Fe concentration levels in biger trees seem to imply that the bioavailability of Fe was essential to the growth of the *Eucalyptus* trees and would imply that Fe is a growth limiting factor in the *Eucalyptus* forests under study.

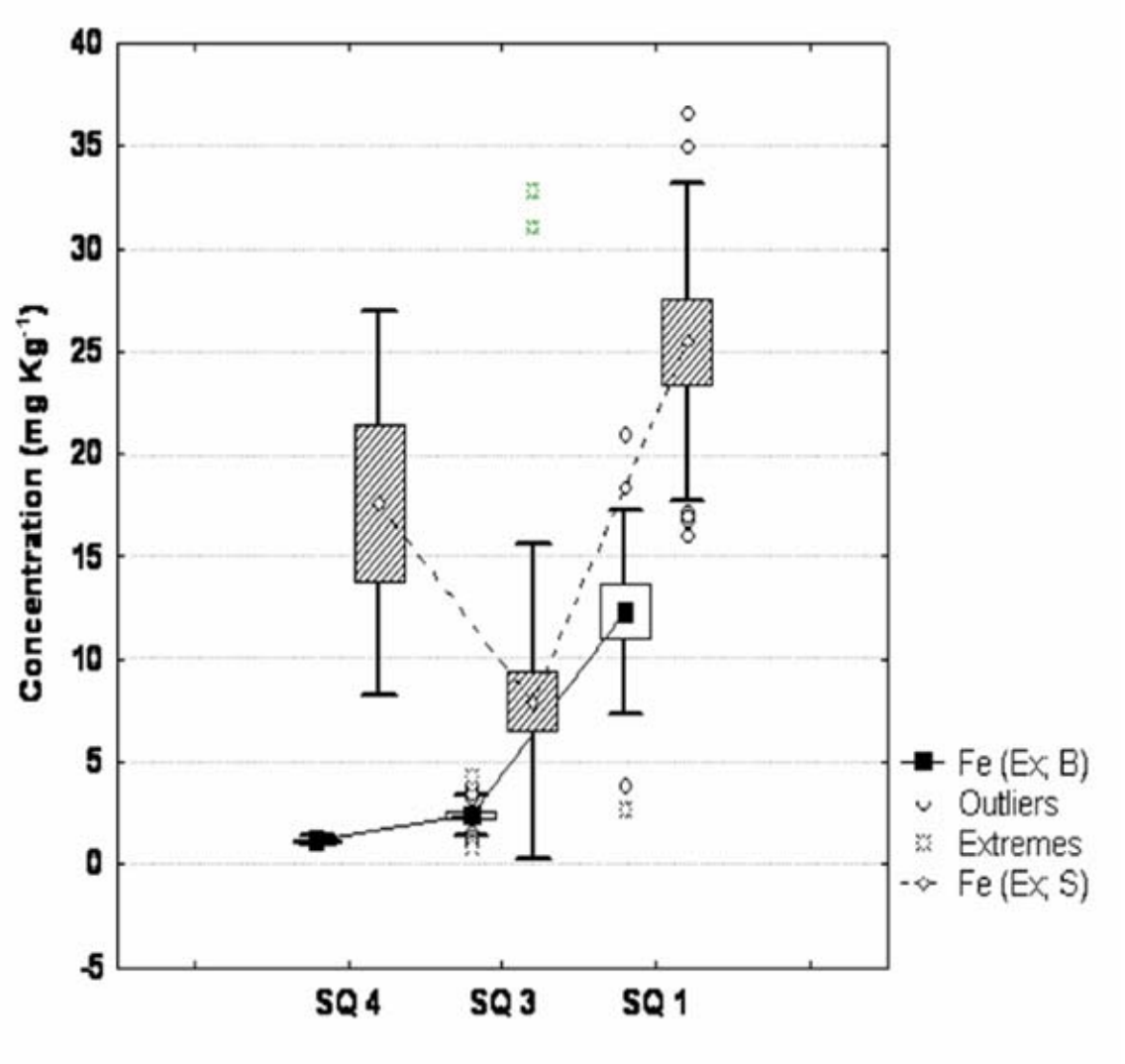

Figure 4. Relationship between surface (Ex; S) and bottom (Ex; B) soil exchangeable Fe fraction and site quality of the *Eucalyptus* forest under study

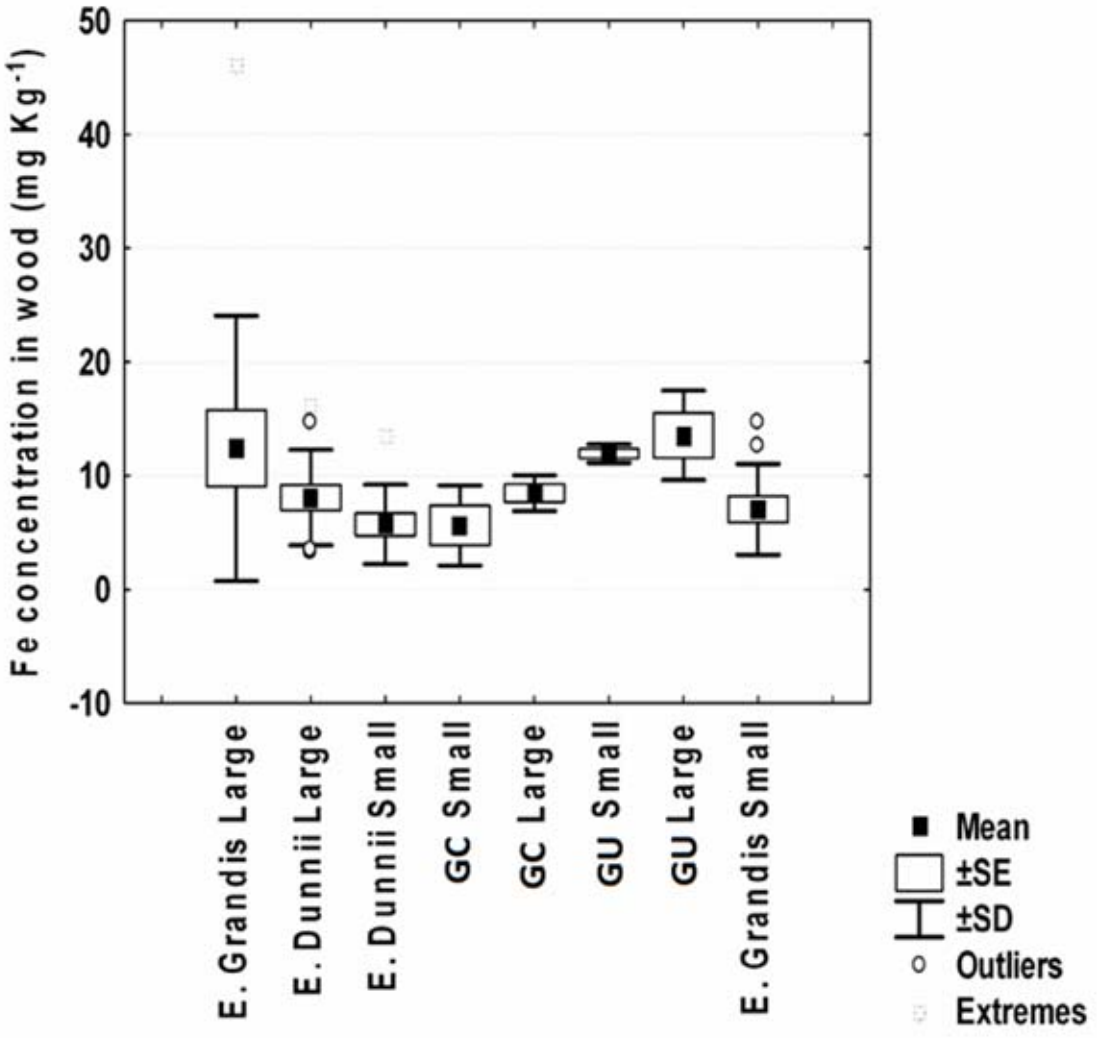

Figure 5. Iron concentrations in *Eucalyptus* wood of different species/clones sampled in two size classes (small and large).

Principal component analysis was employed to investigate the Fe pathway in *Eucalyptus* wood. About 68 % of the generated data was explained by two principal components, the 1st principal component explained 54.5 % of the data while the 2nd principal component explained 13.7 % (Figure 6). The labile Fe species in the soil seemed to follow different pathways into the *Eucalyptus* wood. The variable Fe in the wood was divided into three clusters in the loading plot, which related to different observations in the score plot. Two of these observed clusters were explained well by principle components 1 and 2, while the third cluster was explained by principal component 1 only. One of the clusters on the

loading plot related to exchangeable acidity of the bottom soil and the Al in the *Eucalyptus* wood. Implying that these clusters of *Eucalyptus* trees obtained Fe from the exchangeable fraction and Al was taken up together with Fe when the metal fraction was mobilized. The other two clusters in the loading plot, representing Fe in *Eucalyptus* wood were related to the soil exchangeable acidity and the % organic matter in the surface soil (Figure 6). Although these two clusters related to the same observations one was explained by principal component 1 and 2 while the other was explained by principal component 1 only. The observed correlation implies that the trees in these clusters obtained Fe from the metal exchangeable fraction in the surface soil, while those that correlated with organic matter could have obtained Fe from the degradation of the organic matter.

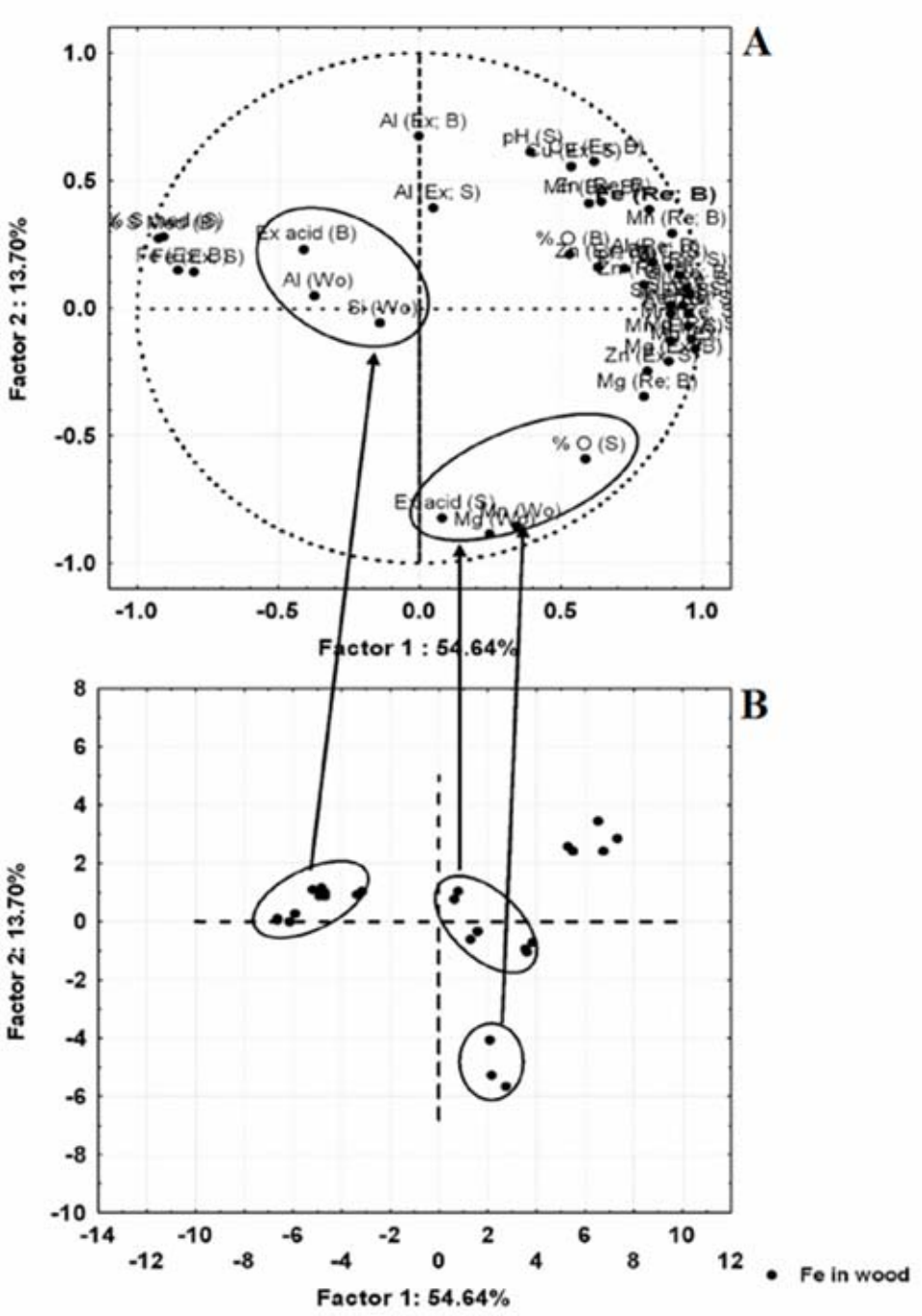

Figure 6. *Eucalyptus* forest data analysed by PCA presented on the score plot (A) and related to the concentration of Fe in the *Eucalyptus* wood loading plot (B).

Polyvalent metals like Fe and Al are hard Lewis acids, capable of strong and specific bonding to hard Lewis base functional groups in organic matter.[22,23] Kalbitz[24] and

coworkers reported that dissolved organic matter can act as a carrier for a variety of components, ranging from nutrients to trace elements. Another possible pathway is due to the soil acidification as a result of released proton during the organic matter oxidation thereby mobilizing Fe from the soil exchangeable fraction. Together, Fe, Al and dissolved organic matter (DOM) play a fundamental role in acidification and pedogenesis in forest soils.[25,26]

The influence of Cu on the site quality was investigated by relating the concentration of Cu in the soil exchangeable fraction to the quality of the site (Figure 7). It was observed that the site quality was favored by low exchangeable Cu concentrations in both the surface and bottom soils (Figure 7). Copper is an essential element for plant growth. However, its presence in the soil in quantities lower or greater than the optimal amount could adversely affect plant growth.[27] Soil pH plays a major role in determining Cu phytotoxicity.[28] The above observation seem to imply that the productivity of the *Eucalyptus* plantation under study is negatively affected by the presence of labile Cu in the soil fraction.

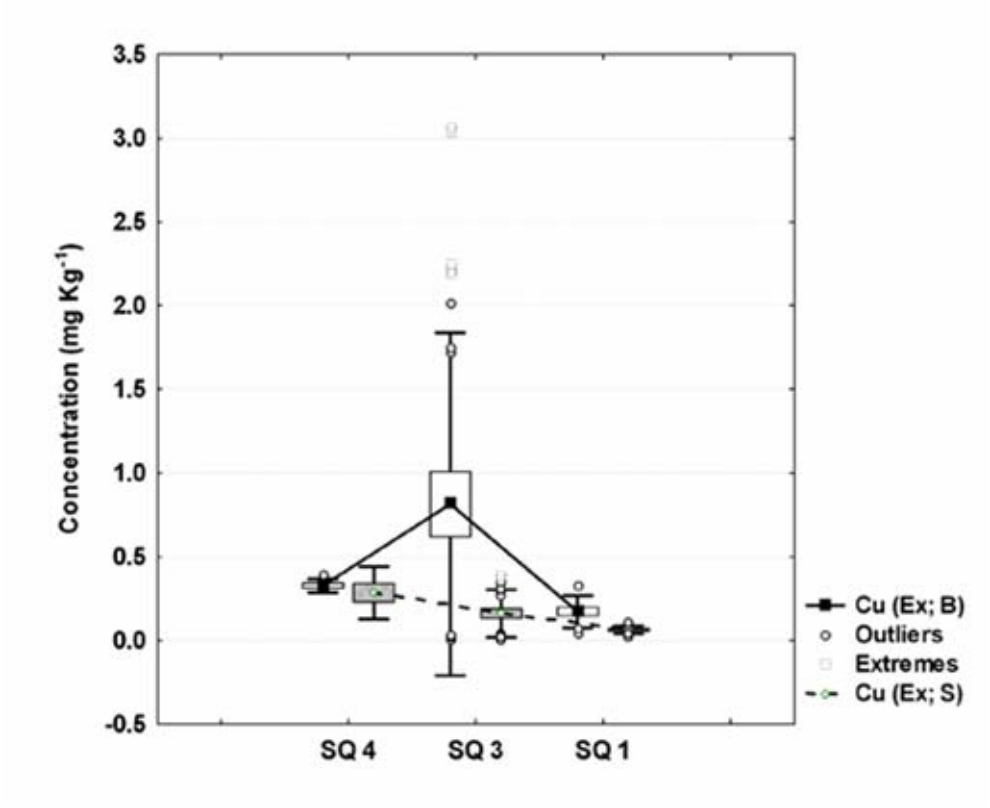

Figure 7. Relationship between surface (Ex; S) and bottom (Ex; B) soil exchangeable Cu fraction and site quality of the *Eucalyptus* forest under study

Most Si is present in the soil as insoluble oxides or silicates, although soluble silicic acid occurs in pore water in the range of 0.1–0.6 mM. Silicon is also one of the most abundant mineral elements in plant tissues and shoot concentrations in excess of 10% dry wt have been reported.[29] Plants growing under natural conditions do not appear to suffer from Si deficiencies. However, Si-containing fertilizers are routinely applied to several crops including rice[30] and sugar cane[31] to increase crop yield and quality. Increased Si supply improves the structural integrity of crops and may also improve plant tolerance to diseases, drought and metal toxicities.[32,33] In this study the Si pathway of the *Eucalyptus* forests under study was investigated by analyzing the generated data statistically using the principal component analysis. The score and loading plot are presented in Figure 8; about 68 % of the generated data was explained by two principal components. The 1st principal component explained 52.8 % of the data while the 2nd principal component explained 15.6 % of the data. The loading plot for the variable, Si concentration in the *Eucalyptus* wood is presented in four clusters. These four clusters in the loading plot were correlated to different observations in the score plot. Two of the clusters were well correlated by both principle component 1 and 2, while the other two clusters were correlated well by principle component 1, which explained 52.8 % of the data (Figure 8). One of the cluster that was explained well by the two principal components, correlated with bottom soil exchangeable acidity and Al in *Eucalyptus* wood, while the other cluster correlated with surface soil exchangeable acidity. This indicates that the *Eucalyptus* trees in one of the cluster obtained Si from the bottom soil exchangeable fraction, while the *Eucalyptus* trees in the other cluster obtained Si from the surface soil exchangeable fraction. One of the other two clusters in the loading plot for the variable Si concentration in wood correlated with surface soil exchangeable acidity, while the other cluster correlated with organic matter and Fe and Mn in *Eucalyptus* wood. These two clusters were explained well by the 1st principle component.

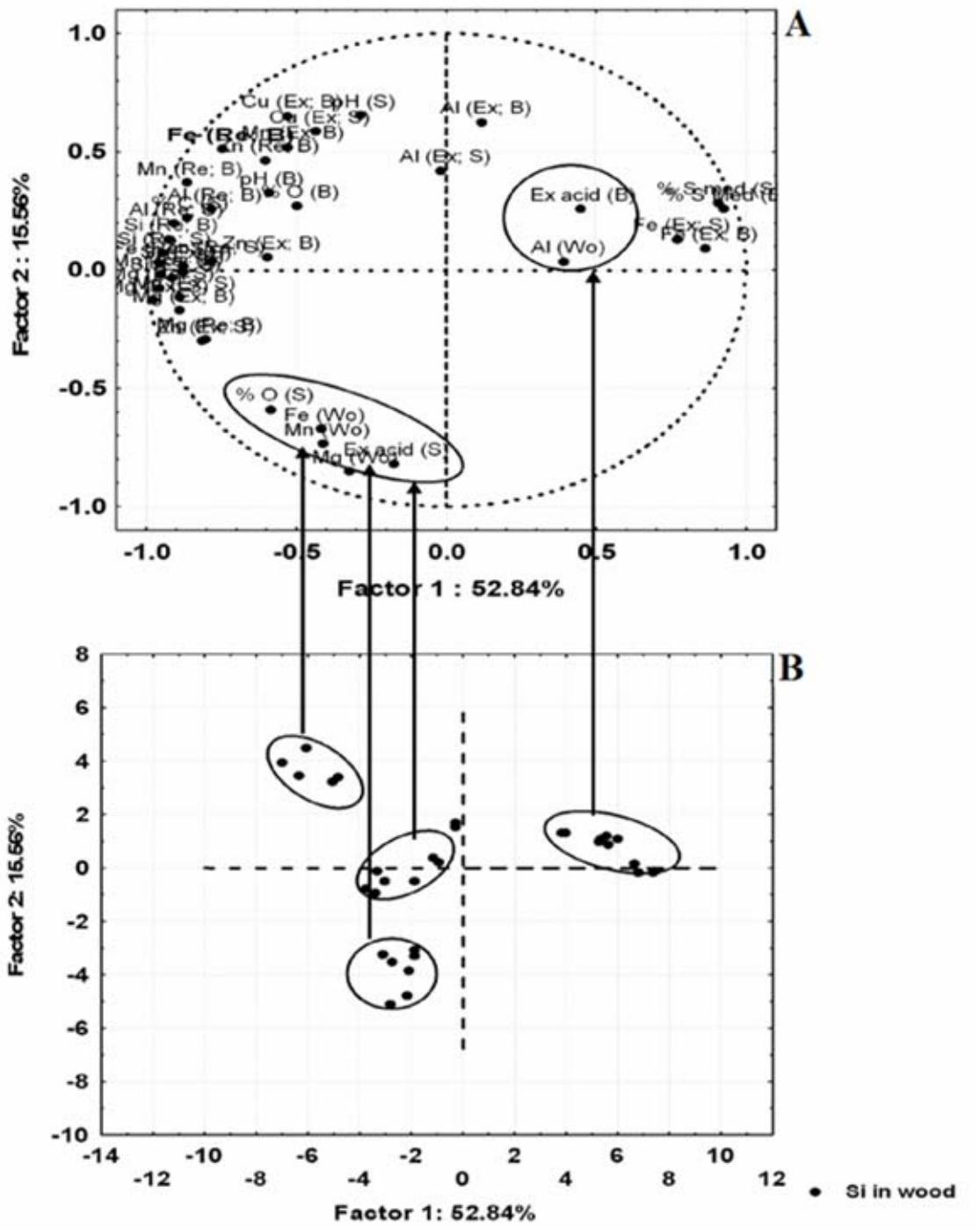

Figure 8. *Eucalyptus* forest data analysed by PCA as presented on the score plot (A) and related to the concentration of Si in the *Eucalyptus* wood loading plot (B).

This observation indicates that some of the *Eucalyptus* trees in the forest under study obtained Si from the surface soil exchangeable fraction. The other cluster of *Eucalyptus* trees obtained Si from the degradation of soil organic matter. The correlation of Si in *Eucalyptus* wood with the concentration of Fe and Mn in *Eucalyptus* wood implies that the Si in the *Eucalyptus* wood was obtained from the same source as the Fe and Mn in the wood. This observed correlation between Si and Mn in *Eucalyptus* wood was further investigated with the aid of scatter plots of bottom and surface soil exchangeable Si and Mn (Figure 9). A direct correlation between Si and Mn was observed with the surface exchangeable fraction ($R^2 = 0.74$), while the bottom soil exchangeable Si and Mn did not correlate ($R^2 = 0.03$). This observation corroborated with the PCA analysis whereby the Si in the *Eucalyptus* wood correlated with surface exchangeable acidity (Figure 8). Above pH 6, oxidation of Mn^{2+} to Mn^{4+} occurs, and Mn $^{2+}$ uptake is reduced.[16] Soil pH and redox potentials control the Mn supply to roots by mass flow and diffusion. Deficiency of Mn usually occurs when soil pH is >6.2, [16] The three major sources of Mn in soils that are primarily responsible for the Mn supply to roots are exchangeable Mn, organically complexed Mn, and Mn oxides.[16]

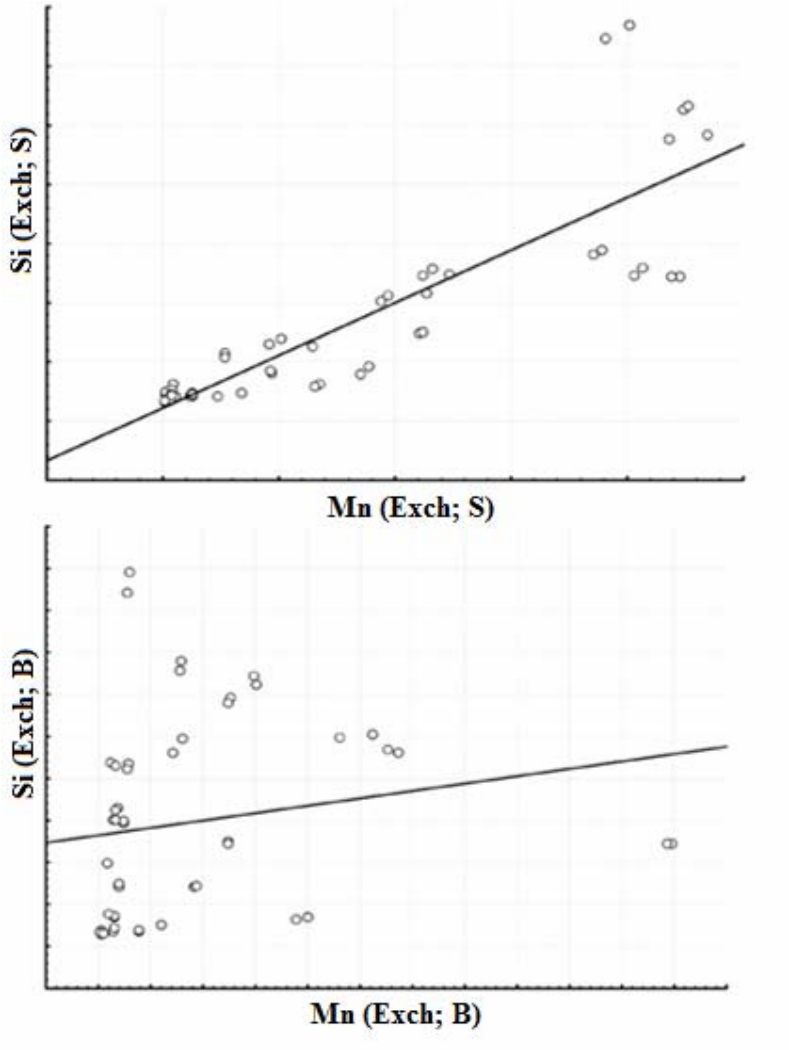

Figure 9. Scatter plots relating surface (Exch; S) and bottom (Exch; B) soil exchangeable fraction of Si and Mn

The proportion of these Mn forms varies with soil type, soil pH, and Organic matter. As the soil pH decreases, the proportion of exchangeable Mn increases dramatically, while the proportions of Mn oxides and Mn bound to Mn and Fe oxides decrease. In soils low in available Fe, root reductase activity is stimulated because of acidification of the rhizosphere and may lead to higher Mn mobility and uptake.[16]

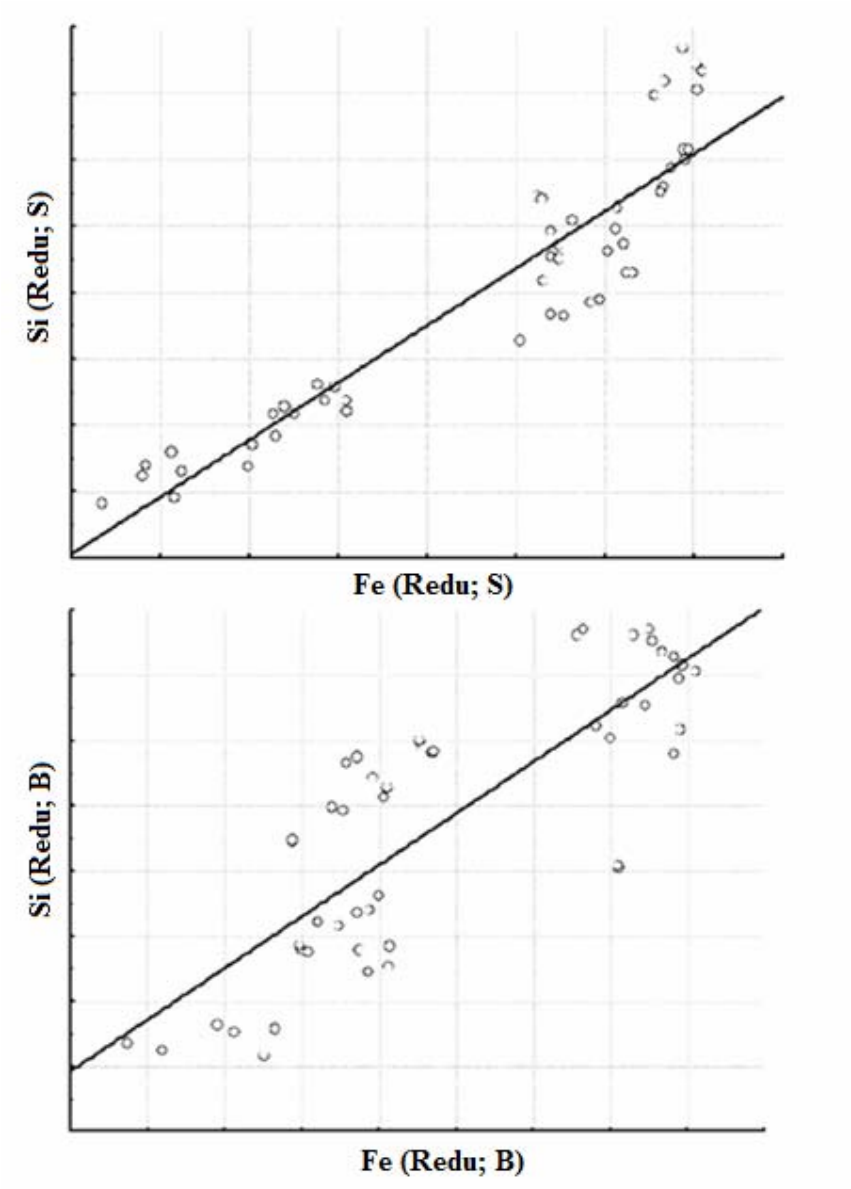

Figure 10. Scatter plots relating surface (Redu; S) and bottom (Redu; B) soil Reducible fraction of Si and Fe

Dissolved Si is present as monosilicic acid (H_4SiO_4) in natural solutions.[34] Apart from clay formation and uptake by biota, monosilicic acid can be withdrawn from soil solution through its sorption onto aluminium and iron oxides.[35,36,37] Their surface OH groups specifically interact with silicic acid by exchanging ligands to form a bi-dendate inner-sphere complex.[38,39,40] The correlation of Si with Fe hydroxides was investigated by plotting scatter plots for Si and Fe in the reducible fraction for both surface and bottom soils (Figure 10). The

plots showed a linear and direct relationship for both surface ($R^2 = 0.87$) and bottom soils ($R^2 = 0.68$).

CONCLUSIONS

The *Eucalyptus* trees under study obtain their nutrients from the surface and bottom soil. The main physicochemical parameter influencing the mobility of metals and Si is the exchangeable acidity. The degradation of organic matter is a major pathway in the mineralization of Fe and Si. The soil exchangeable fraction is the major pathway through which the *Eucalyptus* trees obtain metals and Si from the soil. The labile Si pool of the *Eucalyptus* forest soil is immobilized through its adsorption onto the soil reducible fraction on Fe hydroxides. The bioavailability of soil Fe in a forest site enhanced the site's productivity and *Eucalyptus* tree growth.

REFERENCES

1. Salt, D.E.; Blaylock, M.; Kumar, N.P.B.A.; Dushenkov, V.; Ensley, B.D.; Chet, I.; Raskin, I. Phytoremediation: A novel strategy for the removal of toxic metals from the environment using plants. Biotechnology **1995**, *13(5)*, 468-474.
2. Sailerova, E.; Fedikow, M.A.F. The effects of seasonal changes, sample site drainage and tree morphology on trace element contents of black spruce (Picea mariana) crown twigs and outer bark. Geochemistry: Exploration Environment Analysis **2004**, *4(4)*, 365-379.
3. Rougier, M.; Chaboud, A. Mucilage secreted by roots and their biological function. Israel Journal of Botany **1985**, *34(2-4)*, 129-146.
4. Clemens, S. Molecular mechanisms of plant metal tolerance and homeostasis. Planta **2001**, *212(4)*, 475-486.
5. Faulkner, S.P.; Richardson, C.J. Physical and chemical characteristics of freshwater wetland soils. In *Constructed Wetlands for Wastewater Treatment Municipal, Industrial and Agricultural*; Hammer, D.A., Ed.; Lewis Publishers; New York, **1989**; 41-72.
6. Ponnamperuma, F.N. The chemistry of submerged soils. In: *Advances in Agronomy;* Brady, N.C., Ed.; Academic Press; New York, **1972**; 29-96.
7. Adriano, D.C. *Trace Elements in Terrestrial Environments*; 2nd Ed., Springer-Verlag: New York, **2001**.

8. Punshon, T.; Lepp, N.W. Dickinson, N.M. Resistance to copper toxicity in some British willows. Journal of Geochemistry. Exploration **1994**, *52*, 259-266.
9. Easton, H.S.; Mackay, A.D.; Lee, J. Genetic variation for macro- and micro-nutrient concentration in perennial ryegrass (*Lolium perenne L.*). Australian Journal of Agricultural Research **1997**, *48*, 657-666.
10. Lepp, N.W.; Dickinson, N.M. *Woody Plants: Role in Remediation;* Cunningham and Vangronsveld, Eds.; Springer. **1998**.
11. Thomas, G. W. Soil pH and soil acidity. In *Methods of soil Analysis Part 3 Chemical methods Madison WI: Soil Science Society of America*; Sparks, D. L., ed., American Society of Agronomy **1996**, 475-490.
12. Rauret, G.; Lopez-Sanchez, J.F.; Sahuquillo, A.; Rubio, R.; Davidson, C.M.; Ure, A.M.; Quevauviller, Ph. Improvement of the BCR three step sequential extraction procedure prior to the certification of new sediment and soil reference materials, Journal Environmental Monitoring **1999**, *1*, 57–61.
13. Vandecasteele C.; Block, C.B. *Modern Methods for Trace Element Determination*; John Wiley and Sons: Chichester, UK, **1997**, 68-71.
14. Miranda, A.A.; Le Borgne, Y. A.; Bontempi G. New Routes from Minimal Approximation Error to Principal Components, Neural Processing Letters, Springer, **2008**, *27(3)*.
15. Mills, H.A.; Jones, J.B., Jr. *Plant Analysis Handbook II: A Practical Sampling, Preparation, Analysis and Interpretation Guide*; MicroMacro Publishing Inc: Athens, Georgia, **1996**.
16. Marschner, H. *Mineral Nutrition of Higher Plants*; Harcourt Brace and Company: New York, **1995**.
17. Goulding, K.W.T.; Blake L. Land use, liming and the mobilization of potentially toxic metals Agriculture. Ecosystems and Environment **1998**, *67*,135–144
18. Alhendawi, R.A.; Römheld, V.; Kirkby, E.A.; Marschner, H. Influence of increasing bicarbonate concentrations on plant growth, organic acid accumulation in roots and iron uptake by barley, sorghum, and maize. Jounal of Plant Nutrition **1997**, *20(12)*, 1731-1753
19. Conder, J.M.; Lanno, R.P.; Basta, N.T. Assessment of metal availability in smelter soil using earthworms and chemical extractions. Journal Environmental Quality **2001**, *30*, 1231–1237.

20. Pierzynski, G.M.; Schwab, A.P. Bioavailability of zinc, cadmium, and lead in a metal-contaminated alluvial soil. Journal Environmental Quality **1993**, *22*, 247–254.
21. Weimin, Y.; Batley, G.E.; Ahsanullah, M. Metal bioavailability to the soldker crab Mictyris longicarpus. Science Total Environment **1994**, *141*, 27–44.
22. Martell, A.E.; Motekaitis, R.J.; Smith, R.M. Structure– stability relationships of metal complexes and metal speciation in environmental aqueous solutions. Environmental Toxicology Chemistry 1**988**, *7*, 417– 434.
23. Stevenson, F.J. *Humus Chemistry: Genesis, Composition, Reactions*; Wiley: New York. **1994**, 496
24. Kalbitz, K.; Solinger, S.; Park, J.H.; Michalzik, B.; Matzner, E. Controls on the dynamics of dissolved organic matter in soils: a review. Soil Science **2000**, *165*, 277–304
25. McBride, M.B. *Environmental Chemistry of Soils*; Oxford University Press: Oxford. **1994**.406.
26. Petersen, L. *Podzols and Podzolization*; DSR Forlag: Copenhagen, **1976**.
27. Tucker ,D.P.H.; Alva, A.K.; Jackson, L.K.;.Wheaton. T.A. Nutrition of Florida citrus trees. SP 169. Univ. of Florida, Coop. Ext. Serv., Gainesville. **1995**.
28. Alva, A. K.; Huang B.; Paramasivam, S. Soil pH Affects Copper Fractionation and Phytotoxicity Soil Science Society of America Journal **1998** *64(3)*, 955-962
29. Epstein, E. Silicon. Annual Review of Plant Physiology and Plant Molecular Biology **1999,***50,* 641–664.
30. Pereira, H.S.; Korndorfer, G.H.; Vidal, A.D.; de Camargo MS.;. Silicon sources for rice crop. Scientia Agricola **2004**, *61*: 522–528.
31. Savant, N.K.; Korndorfer G.H.; Datnoff, L.E.; Snyder, G.H.; Silicon nutrition and sugarcane production: a review. Plant Nutrition Journal **1999**, *22*, 1853–1903.
32. Richmond, K.E.; Sussman, M. Got silicon? The non-essential beneficial plant nutrient. Current Opinion in Plant Biology **2003**,.*6*, 268–272.
33. Ma, J.F. Role of silicon in enhancing the resistance of plants to biotic and abiotic stresses. Soil Science and Plant Nutrition **2004**, *50*, 11–18.
34. Lindsay, W.L. *Chemical equilibria in soil*; John Wiley & Sons: New York, **1979**.
35. Beckwith, R.S.; Reeve, R. Studies on soluble silica in soils: I. The sorption of silicic acid by soils and minerals. Australian Journal of Soil Research **1963**, *1*, 157–168.

36. Jones L.H.P.; Handreck, K.A. Effects of iron and aluminium oxides on silica in solution in soils. Nature **1963,** *198*, 852–853.
37. McKeague, J.A.; Cline M. G. Silica in soils. Advances in Agronomy **1963**, *15*, 339–396.
38. Davis, C. C.; Chen, H. W.; Edwards, M. Modeling silica sorption to iron hydroxide. Environmental Science & Technology **2002**, *36*, 582–587.
39. Pokrovski, G.S.; Schott, J.; Farges, F.; Hazemann, J. L. Iron (III)-silica interactions in aqueous solution: insights from X-ray absorption fine structure spectroscopy. Geochimica Cosmochimica Acta **2003**, *67*, 3559–3573.
40. Hiemstra, T.; Barnett, M. O.; van Riemsdijk, W. H. interaction of silicic acid with goethite. Journal of Colloid Interface Science **2007**, *310*, 8–17.

CHAPTER 3: PAPER II

THE DYNAMICS OF METAL EXTRACTION IN A PULP BLEACHING PROCESS

Joseph Nyingi Kamau[1], Jane Catherine Ngila[1,3], Andrew Kindness [1], and Tammy Bush[1,2]

[1]University of Kwazulu-Natal, Chemistry department, Private Bag X54001, Westville, Durban 4000, South Africa.

[2]CSIR Natural Resources and the Environment, Forestry and Forest Products Research Centre, P.O Box 17001, Congella 4013, South Africa.

[3]University of Johannesburg, Doornfontein Campus P.O. Box 17011, Doornfontein 2028, South Africa

ABSTRACT

The mobility of metals in the pulp bleaching stages is influenced by a variety of factors. The environment around the pulp material has a major role in determining the metal dynamics. The pulp environment is constituted by the reactants in solution, these encompass the free metal and reagents that influence the environment's physicochemical parameters. The active sites within the pulp material are also part of the environment. The residual metals in the pulp are influenced by the media pH, the accessibility of the active sites, the affinity of the metal towards the active sites and the degree of delignification and hemicelluloses extraction. There exists equilibrium between the metals in the solid phase (pulp) and those in the aqueous/organic phase. The study observed that the pulp obtained from the *Eucalyptus* clones seemed to be more prone to metal re-adsorption than that obtained from *Eucalyptus* species. This was assumed to imply that the pulp structural composition entailing availability of functional groups was most likely the most influential parameter that determined the extent of metal accumulation other than high pulp porosity.

Key words: Metals, Lignin, Hemicelluloses, Delignification, Pulp bleaching, *Eucalyptus*.

INTRODUCTION

Industrial pulping and bleaching involves the large scale liberation of fibres from lignocellulistic plant material. In acid sulfite pulping, the cooking liquor penetrates through the pits into the porous middle lamella where delignification proceeds from the primary wall (Sixta 2006a). The degradation reaction involving both lignin and carbohydrates thus proceeds from the outer to the inner cell wall layers (Sixta 2006a). The delignification process leads to increased porosity, this has a twofold implication. Inorganic (metals and silicon) and organic wood constituents are expelled during the delignification process. But this also leads to the opening up of the pulp structure availing more active attachment sites. Thus the net inorganic (metals) composition in the pulp after processing is influenced by the process pH, temperature, degree of delignification and the complexing capacities of the ligands in solution. Metal ions in wood are assumed to be bound to carbohydrate groups in hemicelluloses, pectin, lignin and extractives (Liebergott *et al.* 1992).

In oxygen delignification and peroxide bleaching, cellulose degradation is promoted by the presence of even trace amounts of transition elements such as copper, cobalt and iron (Patt *et al.* 1988). The pulp is treated with oxygen in a pressurized vessel at elevated temperature in an alkaline environment. The degree of delignification may vary in the range 40-70% depending on the wood raw material and weather one or two reactors in series are used. Unbleached kraft (sulfate) pulp has a lignin content of 3-5%, which after oxygen delignification can be decreased to about 1.5% or a kappa number of 8-10 (Sixta 2006b).

In the beginning of delignification, the amount of bound water increases, which is a reflection of an increase in the amorphous (cellulose and hemicelluloses) carbohydrate content (Salmén and Berthold 1997). The presence of water converts the ligno-hemicelluloses (located in the pores) to a micro-porous gel, where lignin acts as a cross-linking agent within the wall and hemicelluloses acts as a coupling agent between lignin and cellulose (Scallan and Tigerström 1992). Hemicelluloses promote fibre swelling, and lignin inhibits it (Niskanen 2000). In the later state of delignification, when the hemicelluloses have been removed, the remaining wood polymers are less water-absorbing due to their higher content of crystalline cellulose (Salmén and Berthold 1997). The pore volume also increases at first, due to the cavities developed when lignin is removed (Scallan 1977). However, extensive delignification leads to a collapse of these cavities, lowering the amount of pore water (Salmén and Berthold 1997).

Fibres immersed in water swell until equilibrium is established between the water in the fibres and the water in the surrounding solution, i.e. until the chemical potential of the water is the same on both sides of the equilibrium (Salmén and Berthold 1997). According to Scallan and Tigerström, (1992) swelling results from the osmotic pressure generated within the fibre wall when the counter-ions of the acidic groups are exchanged from hydrogen to sodium form. The degree of swelling depends on the temperature, ionic strength, chemical composition and internal fibrillation of the fibres, as well as on the mechanical restraints to the swelling of the wood fibre material (Salmén and Berthold 1997)**.**

The residual metals in the pulp obtained from oxygen delignification (O-stage) and alkaline bleaching stage (E-stage) were investigated to determine the effect of cellulose degradation, delignification and hemicelluloses extraction. A laboratory scale acid bi-sulfite pulping process was employed to pulp the wood obtained from different *Eucalyptus* species and clones, grown in South Africa.

EXPERIMENTAL

Laboratory scale acid bi-sulfite pulping

The *Eucalyptus* wood samples were dried chopped into chips thereafter pulped in a laboratory scale acid bi-sulfite pulping setup. The pulping setup is a scaled down version of the commercial process and is based on the use of aqueous sulphur dioxide (SO_2) and magnesium oxide (base). The pulping liquor was made by bubbling sulphur dioxide into 7 litres of water and magnesium oxide slurry constituted at 0.75% - 0.85% (w/v). Sulphur dioxide reacts with water to give sulphurous acid.

$$SO_{2(g)} + H_2O_{(l)} \rightleftharpoons H_2SO_{3(aq)} \quad (1)$$

Thereafter the magnesium oxide reacts with sulphurous acid to form sulfite via the following equations:

$$MgO_{(s)} + 2H_2SO_{3(aq)} \rightarrow Mg(HSO_3)_{2(aq)} + H_2O_{(l)} \quad (2)$$

$$Mg(HSO_3)_{2(aq)} + MgO_{(s)} \rightarrow 2MgSO_{3(aq)} + 2H_2O_{(l)} \quad (3)$$

The pH range for the pulping liquor was 1-2. Approximately 1700 g of air-dried wood chips were loaded into a flow-through digester. This reaction vessel was pressurized to 850 KPa,

and the temperature ramped to 140ºC over 5 h 17 minutes. The reaction vessel (8 liter capacity) was held at 140ºC for 43 minutes. The pulp sample was removed from the reaction vessel and washed repeatedly with water to remove solubilised lignin and excess acid. The pulp samples were then screened through a 0.020 inch mesh to remove unreacted wood chips.

Pulp bleaching

The laboratory bleaching sequence was a scaled down version of the commercial process. The results obtained for the viscosity and lignin content (K-number) at the oxygen delignification (O-stage) were used to adjust the bleaching conditions. The aim of adjusting the bleaching was to produce pulp that conformed to the quality control parameters for α-cellulose. Tables 1 present the bleaching conditions utilized in the laboratory to produce a 92α dissolving pulp sample. The concentration of reagents; consistency of pulp samples; temperature and duration at which the bleaching stage was completed were varied during the 4 stage bleaching cycles (Table 1).

Table 1. Pulp bleaching stages and their conditions for the laboratory production of 92α cellulose.

Stage	***Reagent***	***Concentration (%) (m/v)***	***Consistency (%)***	***Temperature (^oC)***	***Pressure (Kpa)***	***Time (min)***
O	NaOH	2	11	100	300	60
D_1	ClO_2	1	11	60	101	60
E	NaOH	1	11	90	101	120
D_2	ClO_2	1	11	70	101	180
Hypo	OCl^-	1.5	11	60	101	150
			-	-		-

Note: Reagents for hypo bleaching stage also included 0.5% NaOH (w/v); % consistency is the percentage of pulp in the reaction mixture.

Determination of hemicelluloses content

Low molecular weight carbohydrates (hemicelluloses and degraded cellulose) can be extracted from pulps with sodium hydroxide. Solubility of a pulp in alkali thus provides information on the degradation of cellulose and on a loss or retention of hemicelluloses during pulping and bleaching processes. The hemicelluloses content is expressed in % alkaline solubility as per equation 5. The hemicelluloses determination was conducted according to TAPPI (2000).

Calculation

$$G = \frac{Weight\ of\ pulp\ x\ (100 - \%Moisture)}{100} \quad \text{.....(4)}$$

$$\%\ \text{Alkali solubility } (S_{10} \text{ or } S_{18}) = \frac{(B - A)\,x\,0.685\%}{G} \quad \text{.....(5)}$$

$$\text{Alpha hemicelluloses Content} = 100 - \frac{(S_{10} + S_{18})}{2} \quad \text{.....(6)}$$

Where:

A = Volume used for the pulp titration, mL

B = Volume used for the blank titration, mL

G = Oven-dried mass of pulp specimen, g

One milliequivalent of $K_2Cr_2O_7$ has been found to correspond to 6.85 mg of cellulose and other dissolved carbohydrates.

Lignin determination by Kappa (K) number

The Kappa number is the volume (in mL) of 0.1 N potassium permanganate solution consumed by one gram of moisture-free pulp under the conditions specified by Tasman and Berzins, (1957)

Calculation

$$K = \frac{p \times f}{w} \quad \text{.....(7)}$$

$$p = \frac{(b-a)N}{0.1} \quad \text{.....(8)}$$

Where:

K= Kappa number

f = factor for correction to a 50% permanganate consumption, dependant on the value of p to correct for different percentages of permanganate used.

w = weight of moisture-free pulp in the specimen, in g

p = amount of 0.1N permanganate actually consumed by the test specimen, mL

b = amount of the thiosulfate consumed in the blank determination, in mL

a = amount of the thiosulfate consumed by the test specimen, in mL

N = normality of the thiosulfate

RESULTS AND DISCUSSION

The dynamics of metals in the pulp bleaching stages is influenced by a variety of factors, the main driving factors being the reactants in solution, the mode of metal attachment onto the pulp, the structural morphology of the pulp and stability of the metal complexes formed. Equilibrium exists between the metals in the solid phase (pulp) and those in the aqueous/organic phase. This is mainly the case for metals adsorbed physically onto the pulp via weak van der Waals forces. The influence of these factors on the resultant metal levels in the pulp after the bleaching process was investigated by observing the effect of

delignification, and hemicelluloses extraction. The data is presented on surface plots, the Z axis represents the organic compound being extracted, and the X axis represents the metal content in the pulp after delignification and hemicelluloses extraction and the Y axis represents the identity of the individual metals being investigated.

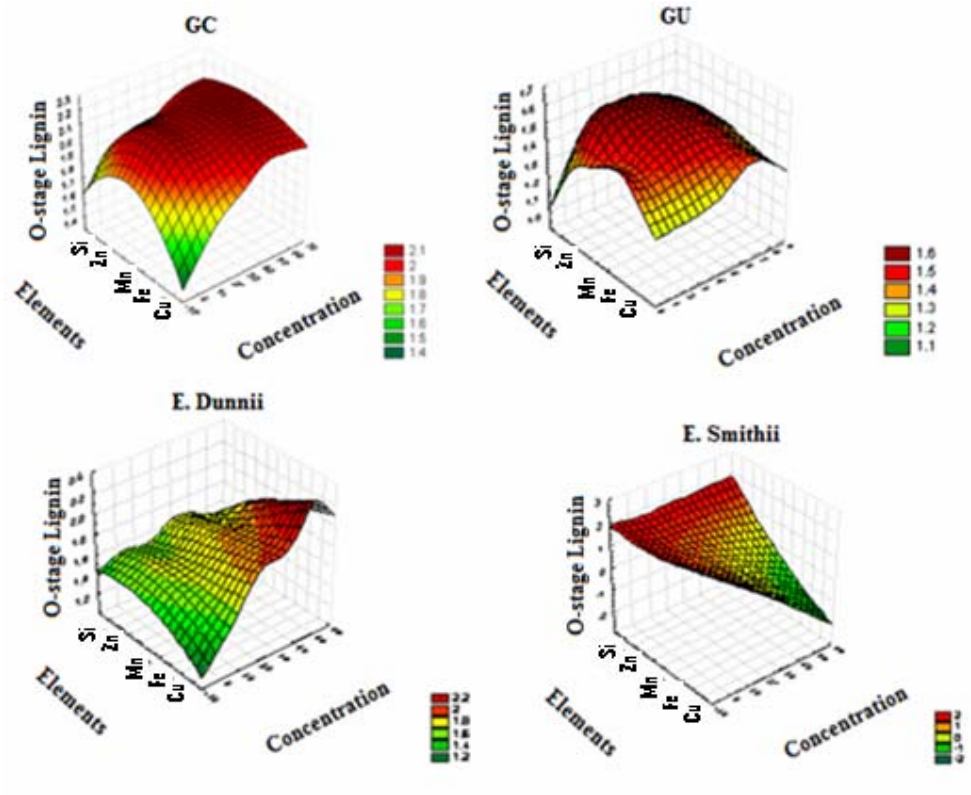

Figure 1. Surface plots of *Eucalyptus* tree species and clones after the O-stage alkaline-oxygen delignification showing the effect of lignin loss on pulp metal composition; GC and GU are *Eucalyptus* clones.

The alkaline-oxygen delignification stage affected the metal compositions in the two clones (GC and GU) in a similar way (Figure 1). It was observed for the two clones under study that both the metal and Si pulp content decreased with decreasing lignin content (Figure 1). These observations suggest that both the metals and Si are attached to lignin and are thus lost during delignification. The metal composition after alkaline-oxygen bleaching stage for

the *Eucalyptus* species (E. *dunnii* and E. *smithii)* were influenced in an opposite manner. High lignin pulp content after oxygen delignification corresponded to high metal content in E. *dunnii* while the opposite was the case for E. *smithii*. This implies that the metals in the E. *dunnii* raw pulp are attached to lignin, thus pulp delignification results in effective metal extraction. While the metals in the E. *smithii* raw pulp are not attached to the lignin, thus delignification does not lead to metal loss. The process of delignification leads to opening up of the cellulose structure, low lignin levels corresponding to high porosity and availing of more metal attachment sites. Whereas this was also the case with E. *dunnii* the metal loss due to delignification overshadowed any metal adsorption due to higher porosity. The highest lignin loss was observed after oxygen delignification with E.*smithii*, where approxmatly.72% of the lignin was extracted (Table 2). Liebergott and co-workers (1992) reported that metal ions in wood are assumed to be bound to carbohydrate groups in hemicelluloses, pectin, lignin and extractives. Oxygen delignification is based on the competitive reactions of oxygen or reactive oxygen species (ROS) within pulp lignin and carbohydrates (Lindholm 1992). Lignin removal under alkali-oxygen conditions is accompanied by a kinetically less favorable oxidation of carbohydrates, whereas the oxidation of the carbohydrates becomes a more favorable process when the kappa number decreases (Lindholm 1992). The reaction of phenolic compounds with oxygen produces ROS, namely the hydroxyl radical (•OH), which can degrade non-phenolic compounds.

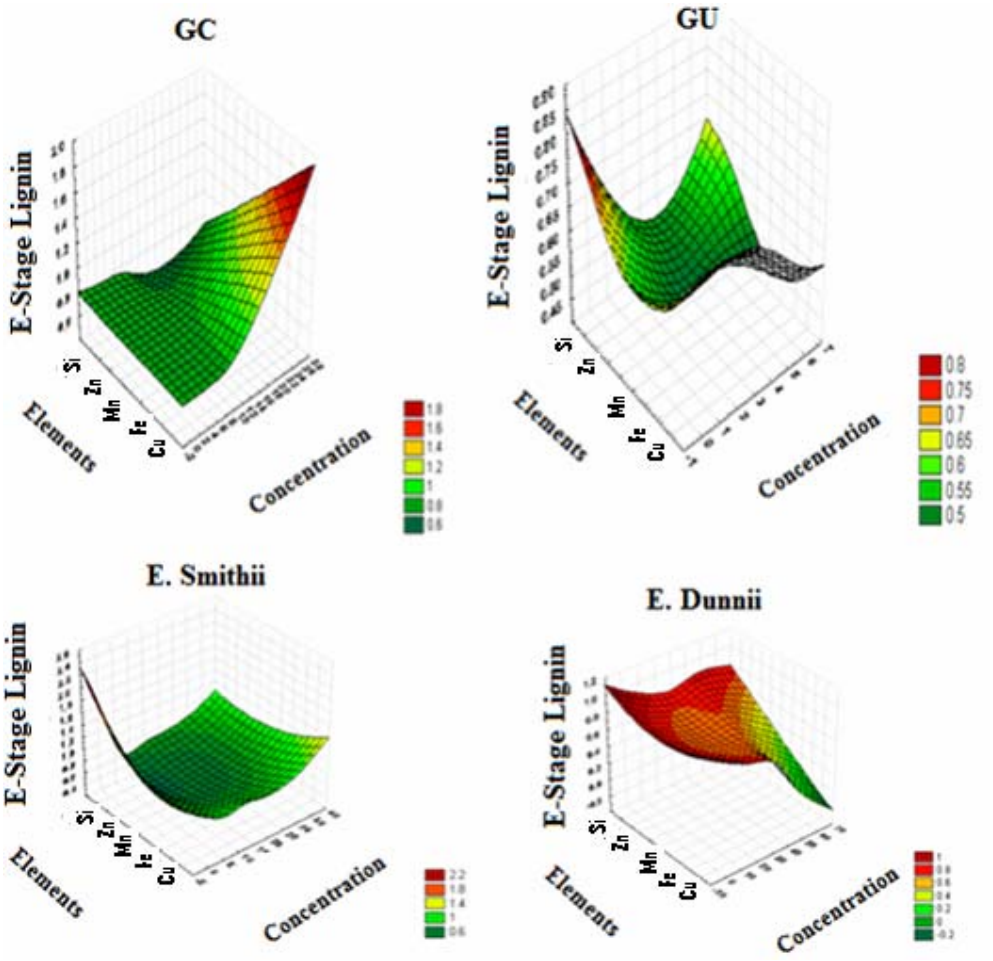

Figure 2 Surface plots of *Eucalyptus* tree species and clones after the alkaline E-stage bleaching process showing the effect of lignin loss on pulp metal composition; GC and GU are *Eucalyptus* clones.

As expected, during the alkaline extraction stage the percentage lignin loss was low for the pulps of all the *Eucalyptus* species/clones, it was however lowest with E. *smithii* about 7 % (Table 2) consequently there was little variance in lignin loss or observable trend with pulp metal composition (Figure 2). High metal levels were observed with E. *dunnii* when the lignin content was low. This can be attributed to higher porosity and consequently greater number of attachment sites. The alkaline extraction bleaching stage leads to the deprotonation of active sites thus availing them for further metal attachment.

Table 2. Percentage lignin and hemicelluloses extraction during the O and E bleaching stage

Stage	***E. dunnii***	***E. smithiii***	***GC G438***	***GU W962***
Lignin O-Stage	63	72	55	43
Lignin E-Stage	33	7	27	37
Hemi O-Stage	13	11	11	18
Hemi E-Stage	14	15	12	12

The amount of metals in the pulp during the alkaline oxygen-delignification stage seemed to be influenced by hemicelluloses content (Figure 3). In the case of the *Eucalyptus* clone GC G438; a high hemicelluloses content correlated with a low pulp metal content (Figure 3). This indicates that the metals in the pulp were not attached to hemicelluloses. The high metal content in the clone GC G438 was favored by low hemicelluloses content. This suggests some form of adsorption of the metal onto the pulp due to increased surface area during hemicelluloses extraction. The metal content in E. *smithiii* pulp from the alkaline oxygen delignification stage was favored by high hemicelluloses content (Figure 3).

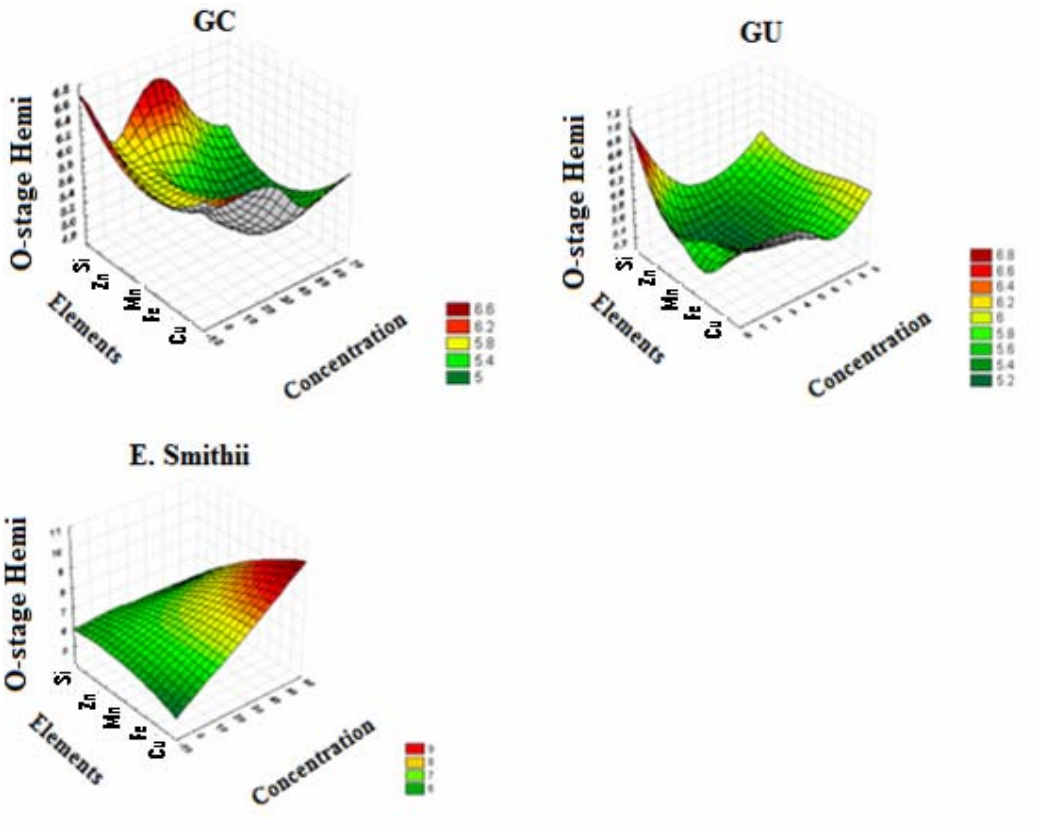

Figure 3 Surface plots of *Eucalyptus* tree species and clones after the alkaline oxygen delignification process (O-stage) showing the effect of hemicelluloses loss on pulp metal composition; GC and GU are *Eucalyptus* clones.

Important pulp properties originate from carboxyl and carbonyl groups, depending on the amount and their distribution along the polysaccharide chains (Sixta 2006b). The carboxyl groups, are mainly derived from uronic acid side chains of hemicelluloses, and aldonic acid groups created by the oxidation of reducing groups, these determine the surface charge (distribution) and hydrophilicity, which in turn exhibits an influence on wetability of the pulp (Sixta 2006b). These properties influence metal adsorption on the pulp as well as the opening up of the pulp structure. Depending on the distribution of these active sites their deprotonation leads to charge repulsion. The open structure has a higher wetability and is more accessible to metals.

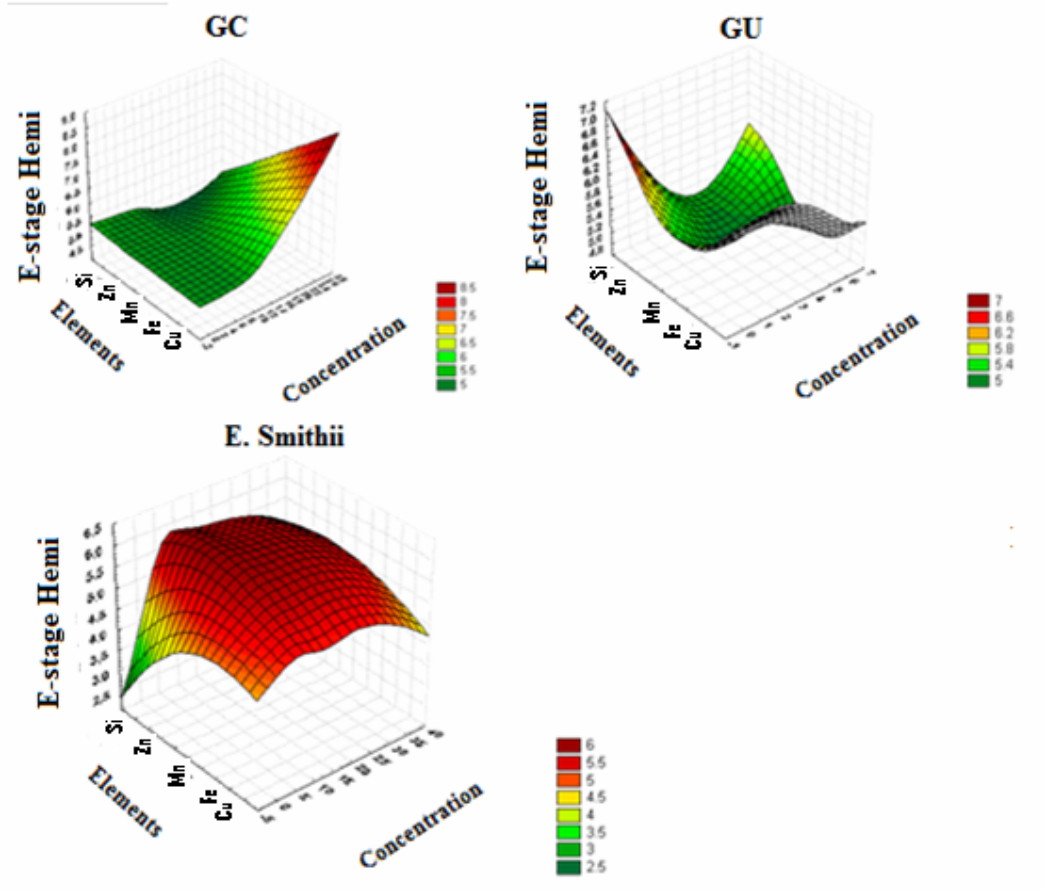

Figure 4 Surface plots of *Eucalyptus* tree species and clones after the alkaline bleaching stage (E-stage) process showing the effect of hemicelluloses loss on pulp metal composition; GC and GU are *Eucalyptus* clones.

Pulp obtained from the alkaline extraction bleaching stage had a higher metal content when the hemicelluloses content was high (Figure 4). This can be attributed to the enhanced availability of the metal attachment sites arising from the formation of acetoxyl anions from the base-catalyzed hydrolysis of hemicelluloses. Sixta, (2006a) reported that hemicelluloses undergoes base-catalyzed hydrolysis of acetoxyl groups to produce acetoxyl anions.

A comparison is made between the residual metals after a bleaching process and the metal content of the *Eucalyptus* wood material. Figure 5 presents box plots (x-axis indicating the elements while y-axis indicates concentrations) that compare the concentration of residual pulp metals (Cu, Fe, Mn, Zn) and Si after the O-stage bleaching with that of the raw wood material. The pulping process was effective in the extraction of Mn and Si (F) (this is the total Si obtained through sample fusion) and to some extent Fe. Copper has been reported to have

a high affinity for organic matter (Sebastia *et al.* 2008; Pérez-Novo *et al.* 2008). This may explain why the residual pulp Cu concentrations were slightly higher than those of the wood raw material, mainly due to the adsorption of the Cu in the bleaching chamber onto the pulp. The extraction of Cu and Fe was similar for *Eucalyptus* species E. *dunnii* and E. *smithiii* but differed from that of E. *nitens* (Figure 5). The Cu and Fe concentration for *Eucalyptus* species E. *nitens* increased after the alkaline oxygen delignification process, as compared to that of the raw wood material. This is an indication that the structural composition of the pulp has an influence on the extractability of metals.

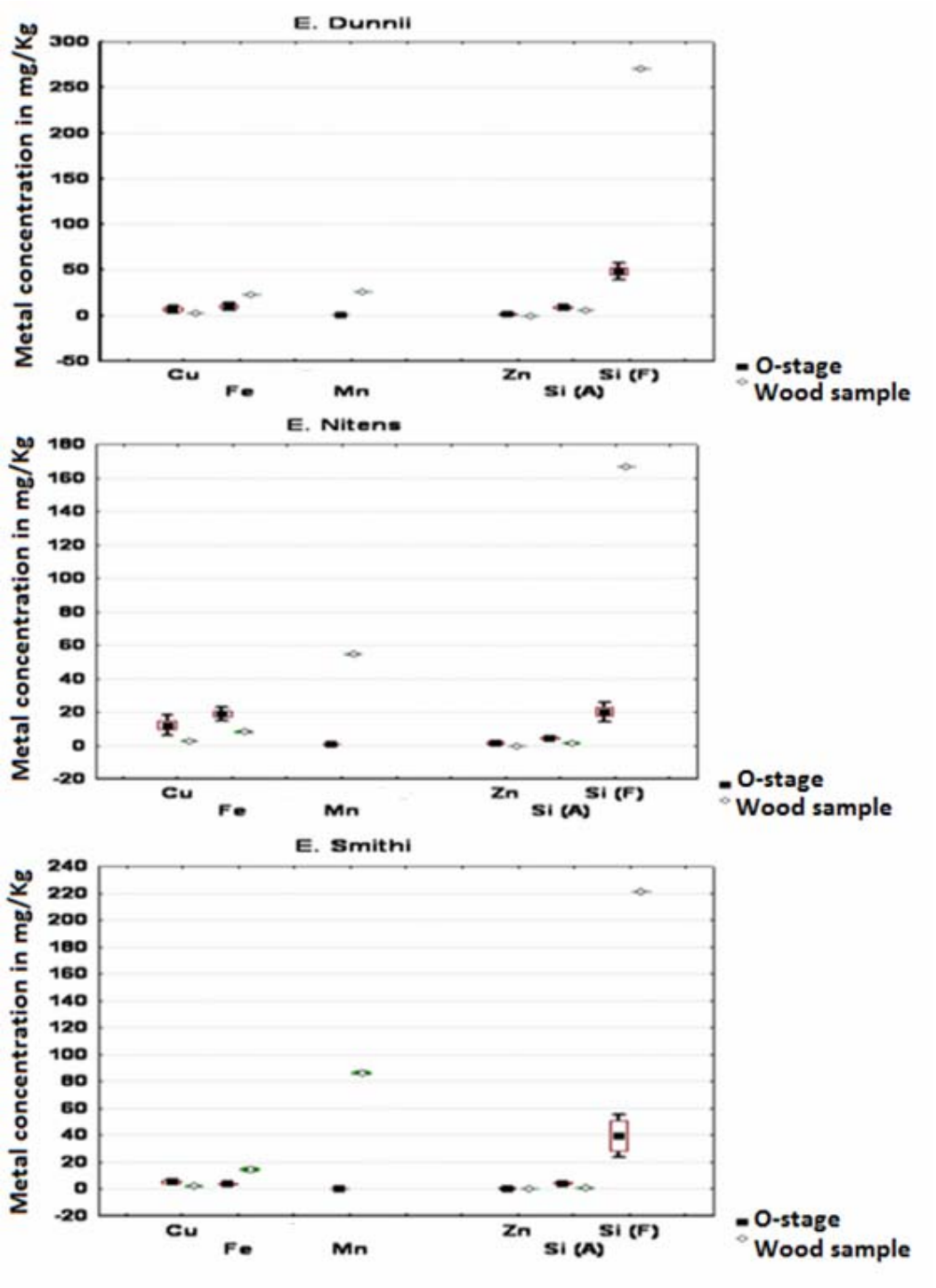

Figure 5. Box plots of *Eucalyptus* species comparing the residual metals after the alkaline oxygen delignification stage (O-stage) with that of the raw wood material; Si (A) is the silicon obtained after acid digestion and Si (F) is the silicon obtained after fussion.

The concentration of metals in the pulp of *Eucalyptus* clones (GU W962) seemed to increase after the O-stage bleaching compared to that in their raw wood material, except for Mn whose concentration was lower than that of the raw wood material. The amount of Si also increased after the alkaline oxygen bleaching stage. These observations are consistent with what was observed on the surface plots of alkaline oxygen stage delignification. It was deduced that metals were adsorbed onto the lignin since the variation in metal levels were proportional to the amount of lignin present in the pulp during the delignification process. The delignification efficiency for *Eucalyptus* clones (GU W962) was lower compared to the other *Eucalyptus* species (Table 2). This also implies that metal extractability is influenced by the organic constituents of the pulp material. Whereby the metal is extracted depending on how and where the metal is attached onto the pulp material. If it is on the lignin or hemicelluloses molecule, the extraction of these molecules will also lead to the extraction of the metal.

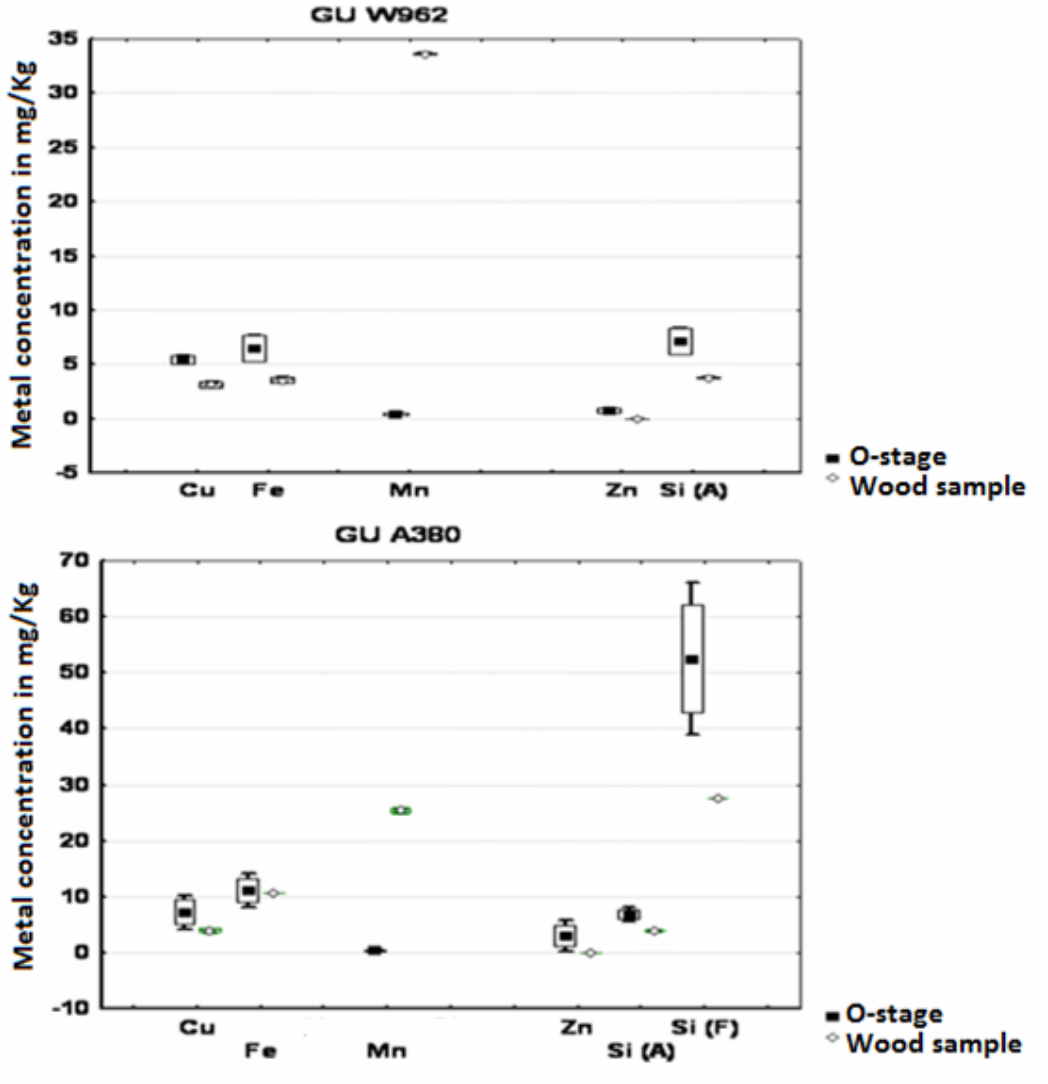

Figure 6. Box plots of *Eucalyptus* clones comparing the residual metals after the alkaline oxygen delignification stage (O-stage) with that of the raw wood material; Si (A) is the silicon obtained after acid digestion and Si (F) is the silicon obtained after fussion.

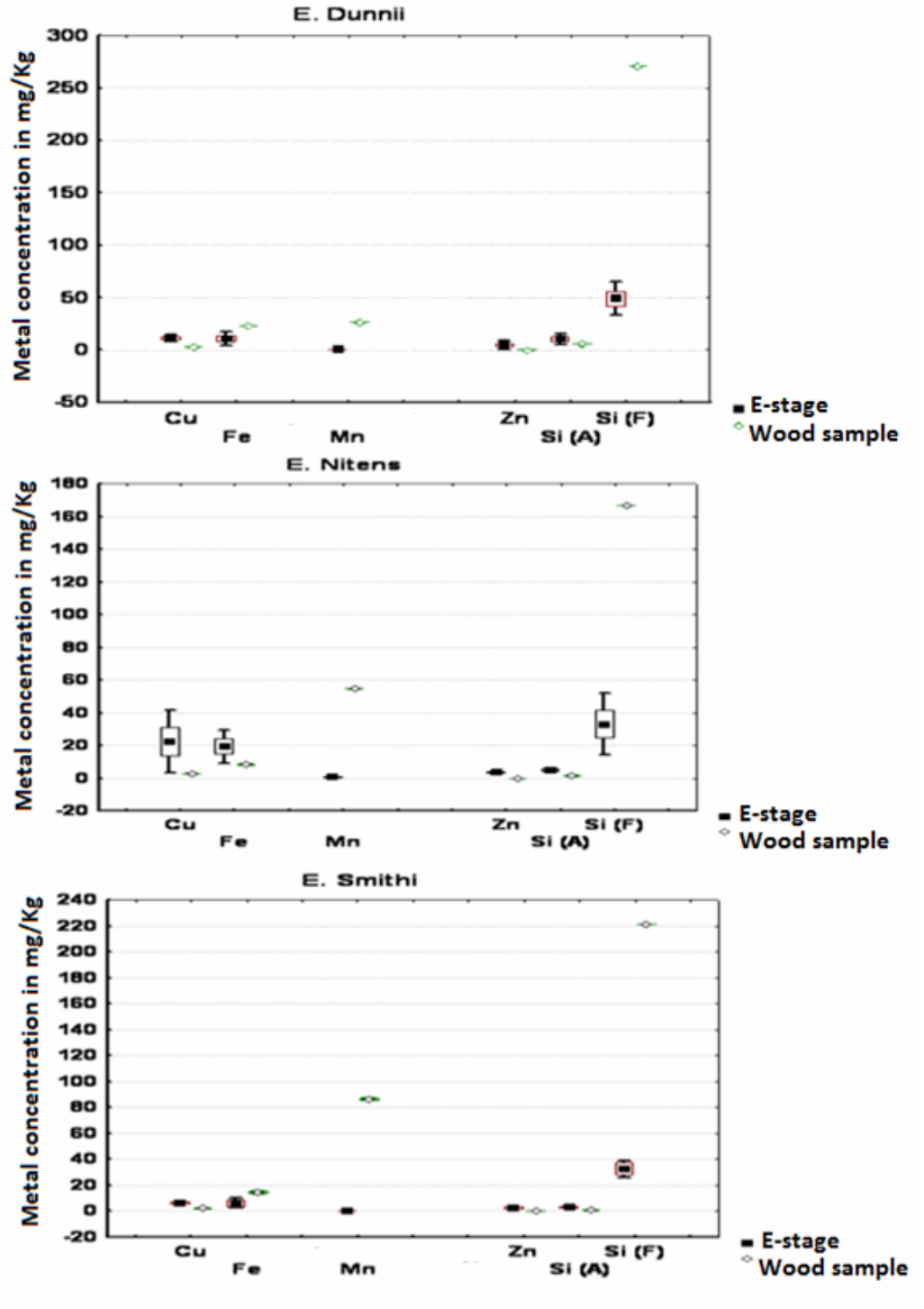

Figure 7. Box plots of *Eucalyptus* species comparing the residual metals after the alkaline bleaching stage (E-stage) with that of the raw wood material; Si (A) is the silicon obtained after acid digestion and Si (F) is the silicon obtained after fussion..

As previously observed in the alkaline oxygen delignification of *Eucalyptus* species E. *nitens* seemed to accumulate metals (Cu and Fe) after the E-stage bleaching. This phenomenon seems therefore to be influence more by the pulp structural composition than the type of bleaching process. The concentration of residual Cu in the pulp of *Eucalyptus* species E. *dunnii* and E. *smithii* seem to be slightly enhanced after the E-stage bleaching compared to the raw wood material. This is likely to be a result of the deprotonation of carboxyl groups in the pulp and the affinity of Cu towards organic matter. This successfully competes with other metals in solution for the available active sites.

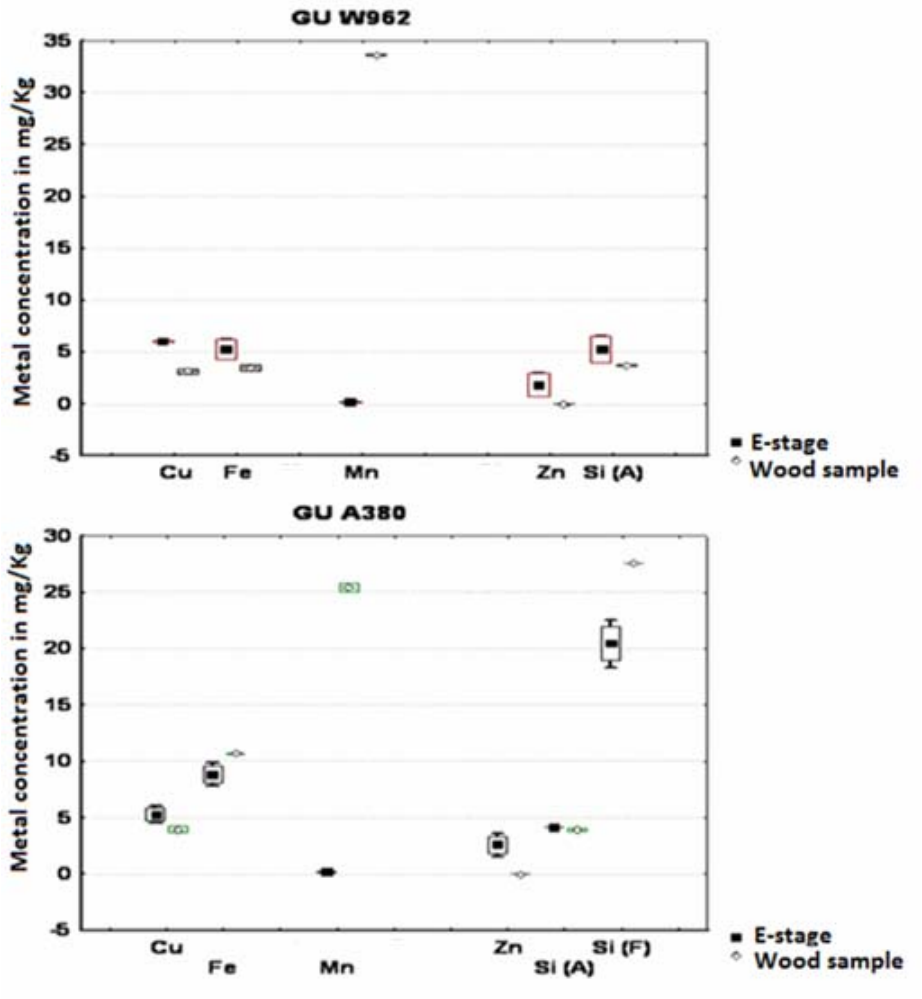

Figure 8. Presents box plots of *Eucalyptus* clones comparing the residual metals after the E-stage bleaching with that of the raw wood material; Si (A) is the silicon obtained after acid digestion and Si (F) is the silicon obtained after fussion..

The concentration of metals (Cu, Fe and Zn) and acid soluble Si in GU W962 alkaline bleached (E-stage) pulp was higher than that of the raw wood material (Figure 8). The Eucalyptus clones seem to be more prone to metal re-adsorption than the Eucalyptus species. The metal accumulation was most likely influenced by the availability of functional groups that easily complex the metals in solution other than high pulp porosity. This is so because the clones lost a lesser amount of lignin and hemicelluloses during the bleaching process as compared to the Eucalyptus species investigated. Manganese was however an exception, its concentration in the clones after the E-stage bleaching was much lower than that of the wood raw material.

CONCLUSIONS

The extractability of metals during pulp delignification and bleaching is influenced by a variety of factors. The affinity of the metals towards organic matter hinders its extractability since it is readily re-attached to the pulp. It can be assumed that the availability of more organic ligands in solution during the alkaline oxygen -stage delignification is a factor that prevents the metals in solution from being re-adsorbed. Therefore the higher metal levels observed after the alkaline extraction stage of bleaching is as much influenced by a lower complexing environment as it is by availability of complexing sites on the pulp.

REFERENCES

Liebergott, N., B. V. Lierop, and A. Skothos, 1992. A survey of the use of ozone in bleaching pulps. Part 2. *Tappi J*. 2: 117-124.

Lindholm, C. A., 1992.Alkaline extraction of ozone-bleached pulp. Part 2. Effect of leachable lignin. *Nordic Pulp paper Res.J.* 2: 95-102.

Niskanen, K. 2000. *Paper Physics, Papermaking Science and Technology*, Book 6A, Fapet Oy, Jyväskylä, 64-72, 211.

Patt, R., O. Kordsachia, D. L-K Wang. 1988. Einsatz von Ozon zur Zellstoffbleiche. Das Papier, 42:(10) 14-23.

Pérez-Novo, C., M. Pateiro-Moure, F. Osorio, J. C. Nóvoa-Muñoz, E. López-Periago and M. Arias-Estévez. 2008. Influence of organic matter removal on competitive and

noncompetitive adsorption of copper and zinc in acid soils. *J. of Colloid and Interface Sci.* 322:(1) 33-40

Salmén L., and Berthold, J. 1997. The swelling ability of pulp fibres, Fundamentals of papermaking materials – 11th fundamental research symposium, Cambrige, 21-26 Sept. 683-701.

Scallan, A.M., A.C. Tigerström. 1992. Swelling and elasticity of the cell walls of pulp fibres, *J.Pulp and Paper Sci*. 18 (5), 188-193.

Scallan, A.M. 1997. The accommodation of water within pulp fibres, BPBIF 6th Fundamental Research Symposium, Oxford, September. 9-27.

Sebastia, J., F. VanOort., and I. Lamy 2008 Buffer capacity and Cu affinity of soil particulate organic matter (POM) size fractions. *Europ. J. Soil Sci.*. 59:(2) 304-314.

Sixta, H., 2006a. Sulfite chemical pulping: *In Handbook of pulp (Eds Sixta)* vol 1. Wiley-Vch GmbH, Weinheim, Germany.

Sixta, H., 2006b. Sulfite chemical pulping: *In Handbook of pulp (Eds Sixta)* vol 2. Wiley-Vch GmbH, Weinheim, Germany.

TAPPI 2000. *Alkali solubility of pulp at 25ºC / 2 T 235 cm-00*

Tasman, J. E., and Berzins, V. 1957. The permanganate consumption of pulp materials. *Tappi.* 40:9 691

CHAPTER 4: PAPER III

INVESTIGATING THE METAL COMPLEXING CAPACITIES OF ORGANIC LIGANDS IN PULP BLEACHING FILTRATE

Joseph Nyingi Kamau[1], Jane Catherine Ngila[1,3], Andrew Kindness [1] and Tamara Bush[1,2]

[1]University of Kwazulu-Natal, School of Chemistry, Westville Durban, South Africa.

[2]CSIR, Natural Resources and the Environment, Forestry and Forest Products Research Centre, Durban, South Africa.

[3]University of Johannesburg, Doornfontein Campus P.O Box 17011, Doornfontein 2028, South Africa

ABSTRACT

The lability of metals in dissolving pulp filtrate, obtained from the beaching stage was investigated by differential pulse adsorptive stripping voltametry. At a pH of 2 the samples obtained from the alkaline oxygen delignification stage were observed to suppress the peak current relatively more than the samples obtained from the alkaline bleaching stage. The filtrate sample of *Eucalyptus* species E. Grandis, obtained from the alkaline oxygen delignification stage caused the highest suppression amounting to 61% relative to the peak of Cu^{2+} ions. The polarogram of a solution of simple cupric ions in a mixture of 0.45 M KNO_3 and 0.05 M HNO_3 supporting electrolyte disappears from the potential region 0.06-0.09 V at a pH of 3.6. The introduction of a filtrate sample into the electrolytic cell containing Cu^{2+} at this pH produced a polarogram whose peak potential varied from +ve 0.02 to -ve 0.1 V depending on the sample filtrate introduced. Filtrate samples obtained from the alkaline oxygen delignification stage showed consistently higher complexing capacities than those obtained from the alkaline bleaching Stage.

Keywords: Pulp, lignin, metals, copper, differential pulse, delignification, bleaching.

INTRODUCTION

The pulp and paper industry uses cellulosic material obtained mainly from soft and hard wood. The main structural wood components comprise of cellulose, hemicelluloses and lignin. Lignin is a phenolic biopolymer its macromolecules consist of phenylpropanoid units that are connected by various types of ether and carbon–carbon linkages.[1,2] The phenolic proton on the lignin molecule is acidic providing metal adsorption sites. Lignin has been used as a biosorbent for the remediation of metal polluted wastewaters.[3,4 Lignin is the main wood component that glues the wood constituents together. The pulping process involves the detachment of cellulose from the wood in the process leading to delignification. The released lignin (in the reagent solution) is believed to participate in metal extraction during the pulping process. This paper seeks to use polarography to investigate metal mobility in the pulp filtrate. A wide variety of techniques can be employed to measure the complexing capacity of a macromolecular ligand.[5,6] However electroanalysis is frequently considered because of its intrinsic capability in distinguishing between the free and the bound metal ions.[7,8,9]

The polarographic method for investigating metal complexes is based on the fact that the half-wave (peak potential) potential of metal ion is shifted cathodically when that ion enters into complex formation. Measuring the shift of the half-wave potential as a function of the complexing ligand concentration provides information concerning the metal complex stability constant. There has been a lot of work done and many efforts put in measuring metal–ligand interactions in model solutions and natural waters.[10,11,12] Voltammetric methods with standard addition of metal ions of interest have shown to be among the most non-destructive and subtle techniques, able to recognize metal–ligand complexation by directly measuring the free and labile fraction of metal and distinguishing free and labile metal from inert metal complexes.[13,14]

When polarography is used the chemical equilibria in the diffusion layer adjacent to the working electrode is strongly influenced (during the reduction reaction of a metal species) by a number of processes such as electron transfer, transport of species to and from the working electrode, association and dissociation of metal complexes, and so on. Some chemical equilibria can be categorized as either rapid then they are called labile metal complexes.[15,16,17]

This paper aims to determine the complexing capacities of filtrates obtained from an alkaline oxygen delignification process and an alkaline bleaching process. As well as make a

comparison of the complexing capacities of filtrates obtained from the bleaching process of different Eucalyptus wood species and clones.

Theory

The potential for the reduction of metallic ions is greatly affected by the presence of ligands that interact with them to form complexes. The half-wave potential ($E_{1/2}$) or peak potential (E_p) for the reduction of a metal complex is generally more negative than that for the corresponding simple metal ion. For small pulse amplitudes, the potential at maximum current (peak potential, Ep) is close to the $E_{1/2}$ polarographic potential.[18] Lingane[19] derived the following relationship between concentrations of ligand (L) and shift in half-wave potential:

$$\left(E_{1/2}\right)_c - E_{1/2} = -\frac{0.0591}{n}\log K_f - \frac{0.0591}{n}\log L \qquad \text{.....(1)}$$

where $(E_{1/2})_c$ and $E_{1/2}$ are the half-wave potentials for the complexed and uncomplexed cations, respectively, K_f is the complex formation constant, p is the molar ratio of complexing agent to cation, and n is the number of electrons transferred for reduction.

The Interaction between organic macromolecules and metal ions consists of weak binding forces such as coordination bonds, hydrogen bonds, charge-transfer interaction, hydrophobic interaction, etc. Because they are plural, these binding forces cooperatively play an important role in polymer metal complexes.[20,21] The deprotonated form of the reactive sites (i.e. carboxylate groups) is primarily responsible for the binding of metal ions onto polymers of a carboxylic nature.[22,23,24] However, the binding of cations with polyacids cannot be reduced to pure ion exchange. Several workers have suggested that the global electric field surrounding the polyacid molecule partially neutralized has a role to play in the resulting metal-polymer complex stability[22,24] (counterion binding is stronger with higher polyionic charge density).

The binding properties of a given macromolecule can be described in terms of saturation of its complexing sites 'A'.[6,25] The complexing capacity of the ligand, C_c, may then be defined as the maximum ability of the molecule to fix a given metal ion. The method commonly used to estimate the value of C_c is the titration (i.e. the progressive saturation) of the ligand with the metal ion of interest at a fixed pH.[6,25] After each addition of the metal ion

in the dilute solution of the studied macromolecule, the current intensity *i* corresponding to the free metal ion concentration, '*m*', is measured. The value of C_c can then be determined from the graphical plot of *i* vs the metal ion total concentration introduced, C_M; C_c corresponds to the value of C_M for which the change in the slope of the curve occurs, which reflects the saturation of all the complexing sites of the ligand by the metal ion. This corresponds to observed C_c value denoted C_{obs}.

From the same experimental data C_c calculated 'C_{cal}' can be derived according to Ruzic.[26] The model assumes that only 1:1 complexes are formed. The conditional stability constant, *K*', of the *MA* complex species formed can then be expressed as follows:

$$K' = \frac{[MA]}{m[A]} = \frac{C_M - m}{m(C_c - (C_M - m))} \quad \text{.....(2)}$$

where *Cc* represents the concentration of the total available complexing sites of the ligand. Equation (2) can be rearranged to produce equation 3.

$$\frac{m}{C_M - m} = \frac{m}{C_c} + \frac{1}{K' \times C_c} \quad \text{.....(3)}$$

A plot of $m/(C_M-m)$ versus *m* gives a straight line, the slope and intercept allow the calculation of C_c and *K'*, respectively. The value of C_c determined in this way will be referred to as "calculated" and denoted C_{cal}.

METHODOLOGY

Background

The study utilized differential pulse adsorptive stripping voltametry (DPAdSV). The combination of accumulation and voltammetric determination is known as adsorptive stripping voltametry (AdSV). Adsorptive stripping voltametry (AdSV) is an efficient method for the trace analysis of elements and can also be used for the determination of surface-active organic molecules with electro-chemically active functional groups. The determination limits

are in the ultra-trace range ~ 10^{-10} mo/L.[27] Adsorptive stripping voltametric methods differ in the complex formation process and in the accumulation mechanism.[27] The analyte M^{n+} can either form the adsorbable complex with the ligand *L* in the solution and then be adsorbed on the surface of the working electrode.[27] Or the complexing agent is adsorbed on the electrode, the complex formation taking place on the electrode surface.[27] The study method considers that if there are ligands that will complex with the metal ion, the complexation equation can be written as follows:

Complex formation in the solution

$$M^{n+} + nL_{(dissolved)} \leftrightarrow ML_n{}^{n+}{}_{(dissolved)} \quad \text{.....(4)}$$

$$ML_n{}^{n+}{}_{(dissolved)} \leftrightarrow ML_n{}^{n+}{}_{(adsorbed)} \quad \text{.....(5)}$$

Complex formation after adsorption of the complexing ligand

$$nL_{(dissolved)} \leftrightarrow nL_{(adsorbed)} \quad \text{.....(6)}$$

$$M^{n+} + nL_{(adsorbed)} \leftrightarrow ML_n{}^{n+}{}_{(adsorbed)} \quad \text{.....(7)}$$

$$K_s = \frac{[ML_q]}{[M^{n+}][L]^q} \quad \text{.....(8)}$$

Hence

$$[M^{n+}] = \frac{[ML_q]}{K_s[L]^q} \quad \text{.....(9)}$$

Where *M* is the metal and *L* is the ligand

Until the electrode surface becomes saturated the peak current increases linearly with accumulation time (t_{acc}) and reaches a maximum according to equation (5). [27]

$$I_{p(max)} = k \,.\, A \,.\, \Phi_{max} \quad \text{.....(10)}$$

Where $I_{p(max)}$ is the maximum peak current, *k* is a constant, *A* is electrode surface area and Φ_{max} is maximum amount of adsorbed compound.

Experimental

Apparatus

Voltammetric measurements were carried out with a Metrohm Model 797 VA Computrace Metrodata in conjunction with a model 797 VA stand. A conventional three-electrode arrangement, consisting of a platinum rod as an auxiliary electrode, a Ag/AgCl/KCl (3 M) double-junction electrode as a reference electrode and a Metrohm multi-mode electrode (MME) used in the glassy carbon rotating disc electrode/solid state electrode mode (RDE/SSE), was employed.

Sample preparation

Electroanalysis was performed on filtrates obtained from the alkaline oxygen delignification stage (O-stage) and alkaline bleaching stage (E-stage). The liquid samples (5 mL) were run through a C-18 column (conditioned with methanol and rinsed with milli-Q water, 18.2 Ω cm^{-1}) at a flow rate of about 3 mL per minute. The organics retained on the C-18 were then eluted with 5 mL methanol and run through 1.5 g of chelex-100 packed in a 6 mL polyethylene column.

Procedure

Voltammetric measurements were carried out in the differential pulse adsorptive stripping voltametry (DPAdSV) mode with a mixture of 0.45 M KNO_3 and 0.05 M HNO_3, as the supporting electrolyte. Metal-ligand solutions were obtained by titrating Cu^{2+} ions into selected amounts of pulp filtrate sample at a fixed pH; this was performed in the Metrohm electrolytic cell. Copper was chosen in the study due to its high affinity for organics and the relatively high stability of its complexes with various organic ligands.

The deposition potential (E_{dep}), was set at -0.75 V vs. Ag/AgCl; at a deposition time of 300 s and allowed to equilibrate for 10 s. A pulse amplitude of 50 mV and voltage step time of 200 ms were used with a scan rate of, 12 mV s^{-1} and pulse duration, 40 ms. A cleaning step of 1.5 V for 60 s was employed to regenerate the electrode surface. High purity nitrogen was used for deaeration of the sample solutions, an initial purge of 5min and 20 s thereafter was employed.

All solutions were prepared in milli-Q water of resistivity 18.2 Ω cm^{-1}; the reagents were of analytical grade, unless otherwise specified. Lignin model solution was prepared from 4-allyl-2,6-dimethoxy phenol (Fulka) in 40% methanol. A blank polarogram was recorded for a 10 mL deaerated supporting electrolyte solution constituting 0.45 M KNO_3 and 0.05 M HNO_3. Next, an appropriate volume of Cu^{2+} ion solution was added that resulted in total Cu metal [MT] of about 50 μM the pH of the solution was adjusted as appropriate with 0.5 M NaOH.

Polarograms were obtained by titrating fixed total Cu^{2+} ion concentration (50 μM) with aliquots of 0.01 μM 4-allyl-2,6-dimethoxy phenol ligand and pulp filtrate samples at a fixed pH of 2.0. Polarograms of the ligand alone in the supporting electrolyte as a function of pH were also recorded in a similar way; the ligand did not show polarographic activity under the experimental conditions employed. The electrode surface was regenerated by polishing with alumina after every series of measurement. The pulp filtrate samples were run through the above polarogaphic process. The experiment was performed at a fixed total ligand (LT) and titrated with Cu^{2+} ions at a pH range of 3.5 -4.

RESULTS AND DISCUSSION

In the absence of complex-forming substances, simple cupric ions aqua complex are reduced directly to the metallic state at a working electrode and the resulting polarogram showed only one wave (Figure 1) Lingane,[19] reported the same observation. The aquo Cu (I) ion is highly unstable and thus reduction proceeds by direct reduction of Cu (II). Hence the polarogram of a solution of simple cupric ions only exhibits the single wave corresponding to the reduction of Cu^{2+} ions.[19]

Owing to the competition between protons and Cu $^{2+}$ ions for the binding sites in the ligand molecule, the pH is a very important parameter. Cukrowski and Adsetts,[28] observed a direct correlation in the peak potential shift vs pH. They also observed regions of different gradients and attributed it to formation of different ligand-metal complexes. This phenomenon was investigated by titrating a fixed total ligand (LT) to total metal (MT) concentration with 0.05 M NaOH, while recording the peak potential. The pH measurements were done using a Hanna pH 211 microprocessor pH meter (pH 0.01).

A fixed Cu metal concentration [MT] of 47 μM and fixed model ligand (4-allyl-2,6-dimethoxy phenol) concentration of 30 μM was titrated with 0.05 M NaOH the results are

reported in Figure 1. Between pH 1.68 and 3.48 the peak was depressed and tended to shift slightly towards the anodic side (0.072 V peak potential). The copper peak disappeared from the 0.072 V potential region when the solution was adjusted to a pH of 3.66. It seemed to have shifted cathodically (-0.225 potential) however with a much depressed current, one order of magnitude lower as seen on the inset (Figure 1). At higher pH the ligand is deprotonated and its attachement sites rendered active. The cathodic shift could therefore be due to the formation of labile ligand-metal species. Reisenhofe and coworkers[29] employed differential pulse polarography (DPP) to study the interaction of copper (II) ions and carboxylic polysaccharides in 0.05 M $NaClO_4$ aqueous solution at 25°C. They observed three main reduction peaks appearing in the range of potentials between +0.10 and −0.23 V *versus* SCE.

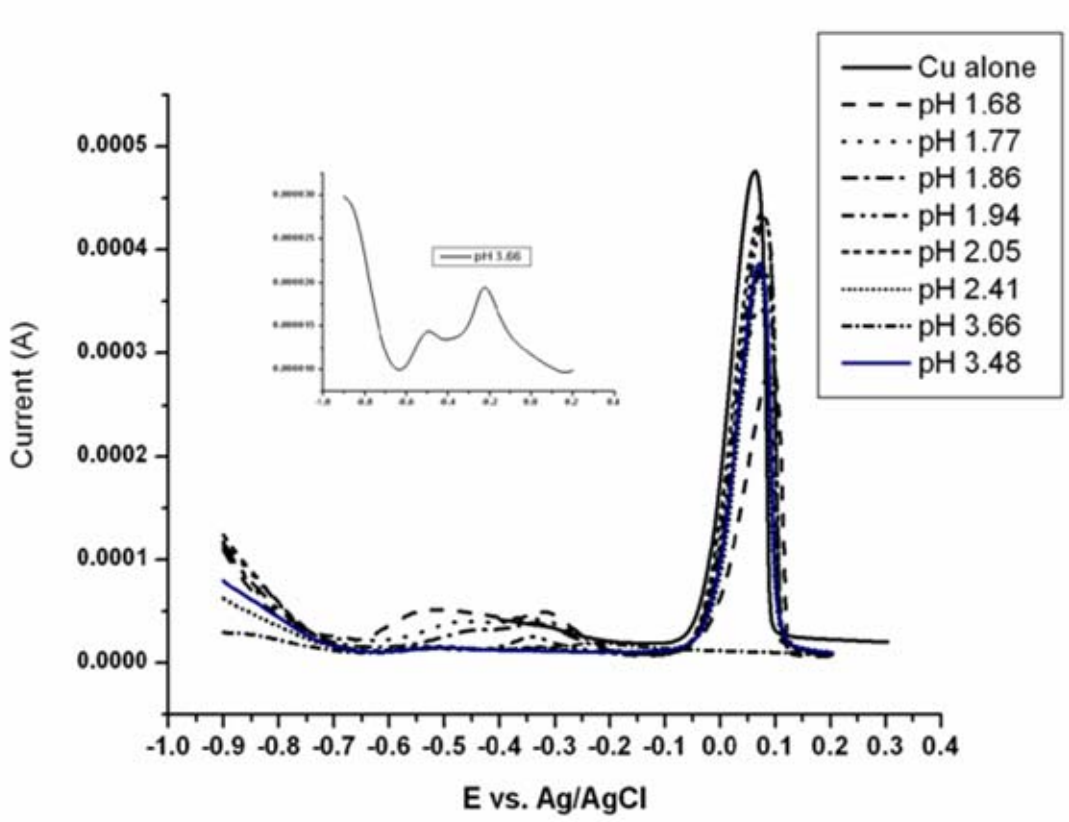

Figure 1. The effect of pH on titrating fixed Cu metal (MT) and fixed model lignin (LT) with 0.5 M NaOH.

Pulp filtrate samples were also spiked into the electrolytc cell containing the supporting electrolyte (pH 2) and 47 μM Cu^{2+} ions, the observed polarograms were similar to that of the model solution (Figure 2). The degree of suppression was however more pronounced than with the model ligand (Table 1) the anodic shift was also slightly more pronounced (Figure 2). Brezonik and coworkers,[30] reported 50-75% shrinkage in Cu peaks using KNO_3 base solutions, to which had been added agar, alginic acid, alkaline phosphatase, polygalacturonic acid or starch. The deviation in shape and size from the model lignin peak would imply the presence of other organic compounds in the filtrate apart from lignin that similarly interact with the metal in solution. On the other hand preliminary investigations by Scarano and Bramanti[31] on the voltammetric determination of copper in the presence of Sep-Pak-extractable marine organic matter showed that this hydrophobic fraction of marine organic matter strongly affects the copper stripping peak. The copper peak appeared to broadened and shifted towards more positive potentials in comparison with the peak shape and position of copper in a ligand-free solution.

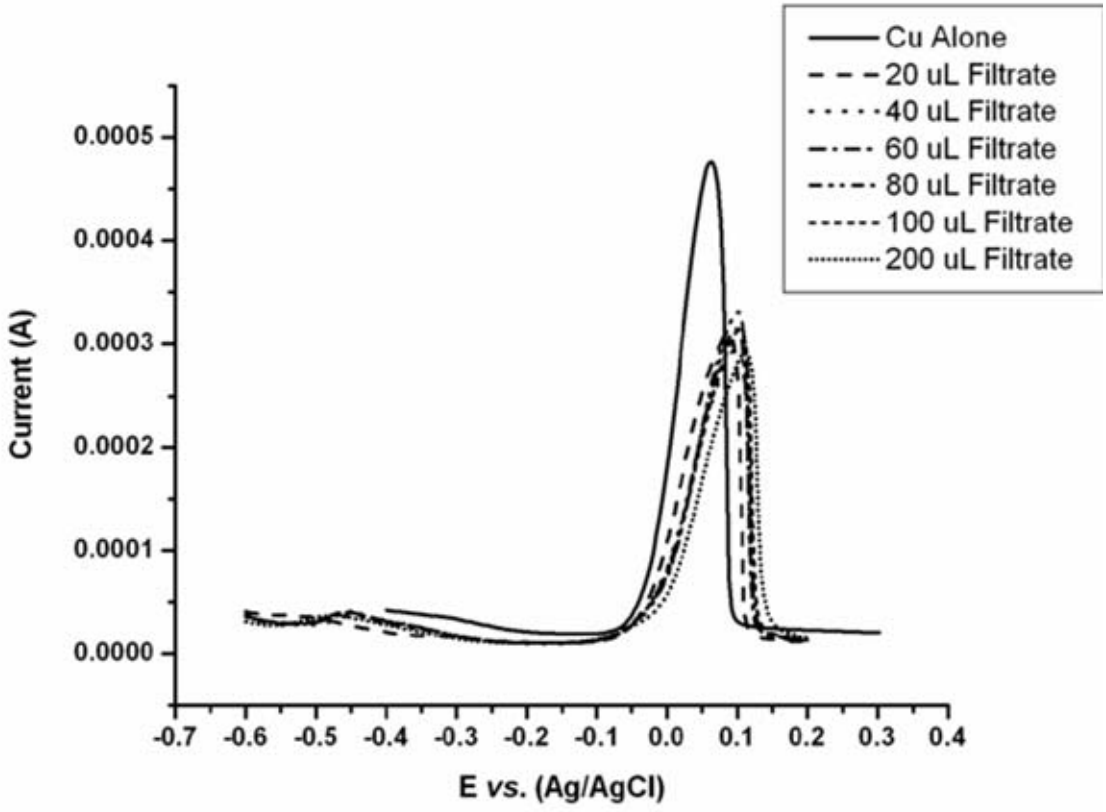

Figure 2 The effect of titrating 47 μM Cu with aliquots of sample filtrate at a fixed pH of 2.

Similarly, it can be concluded that sorption of the organic materials did not yield a coating which served as a barrier to ion diffusion, and so render the metal oxidation process irreversible.[32] However adsorption of surface-active substances on the working electrode may influence the redox properties of metals, affecting peak currents and potentials in anodic stripping voltammetry.[25,33,34] Ugapo and Pickering[35] reported an anomalous behavior of Cu, the stripping peak tending to broaden and split, in the presence of humic acids. They attributed the effect to the reduction (and subsequent oxidation) of Cu-humate species adsorbed on the mercury film.

Table 1. Observed complexing capacity C_{obs} in μM; percentage suppression of Cu peak after sample filtrate and model lignin addition at pH 2; calculated complexing capacity C_{cal} in μM; and the R^2 value for the plots of C_{cal}

Complexing capacity	Model Ligand	E. *grandis* (O)	E. *grandis* (E)	E. *nitens* (O)	E. *nitens* (E)	GC (O)	GC (E)
% peak Suppression	23	61.0	17.4	26.6	21.6	40.1	33.9
C_{obs}	__	31.3	31.3	31.5	15.6	31.3	23.6
C_{cal}	__	123.5	88.5	1.14	__	39.2	__
R^2	__	0.906	0.989	0.949	__	0.984	__

Cukrowski and Luckay[36] were of a different opinion they reported that the formation of a non-labile complex can be predicted from the decrease in the peak height of a labile metal-ligand system provided that no precipitation occurs. Figure 3 shows the effect of the addition of sample filtrate into the electrolyte solution containing 47 μM of Cu^{2+} ions, the Cu peak is depressed, while the peak potential remains more or less fixed (Figure 4). The samples obtained from the oxygen delignification (O-Stage) suppressed the current peak more (Figure 3) than the samples obtained from the alkaline bleaching stage (E-Stage). The degree of peak current suppression by the samples investigated is presented in Table 1. The

filtrate sample obtained from the oxygen delignification stage (O-Stage) of *Eucalyptus* wood, E. Grandis species caused the highest suppression amounting to 61% relative to the peak of Cu^{2+} ions in the absence of the sample filtrate (Table 1).

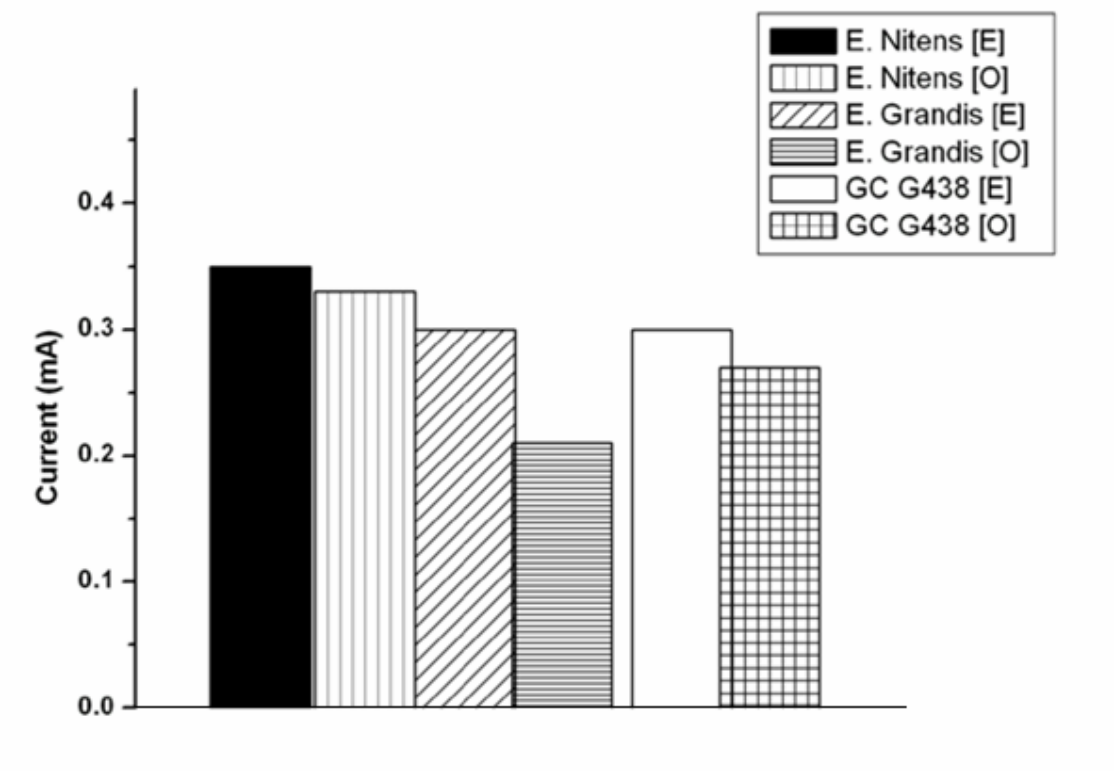

Figure 3. Observed peak currents in the presence of Cu^{2+} ions of O-Stage and E-Stage bleaching filtrates for different Eucalyptus tree species and clone at a fixed pH of 2.

It has been demonstrated that it is possible to estimate the stability constant of a non-labile complex only from the decrease in the peak height representing all labile metal complexes formed in a solution.[37] The high degree of current peak suppression with samples obtained from the oxygen delignification stage (O-Stage) implies the presence of more ligands forming non labile metal-ligand complexes with higher stability constants.

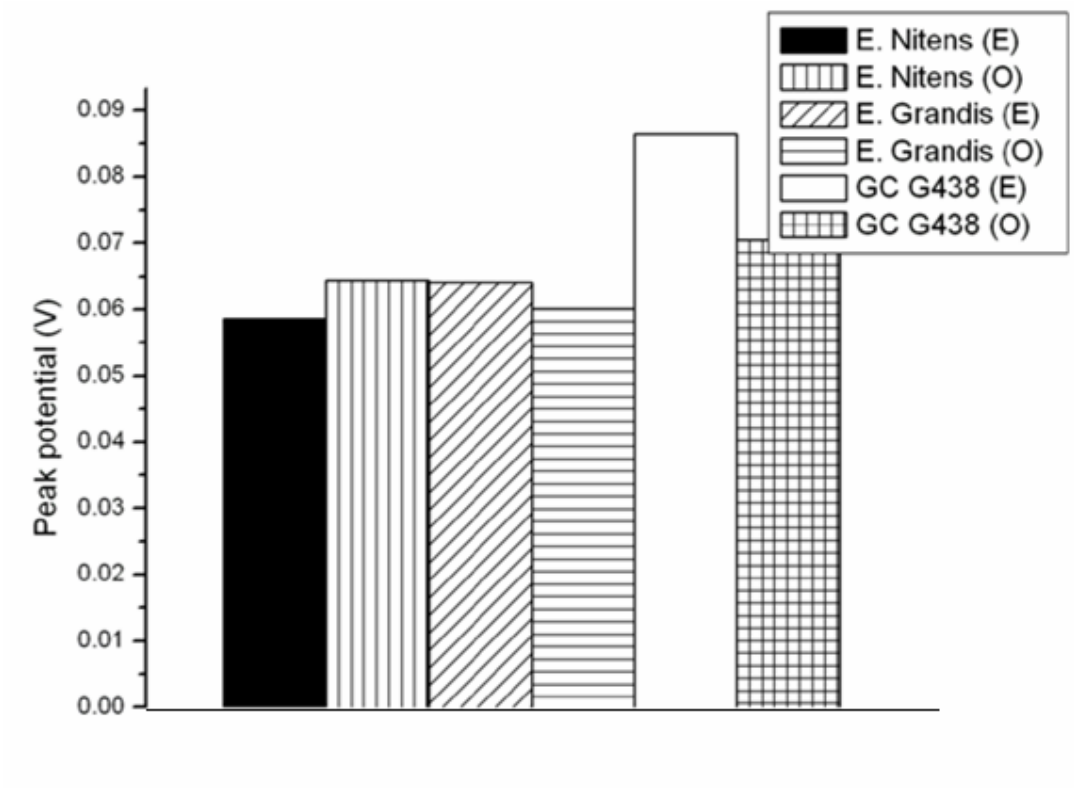

Figure 4. Observed peak potential in the presence of Cu^{2+} ions of O-Stage and E-Stage bleaching filtrates for different Eucalyptus tree species and clone at a fixed pH of 2.

In the oxygen delignification stage the pulp is treated with oxygen in a pressurized vessel at elevated temperature in an alkaline environment. Carbohydrates are attacked during oxygen alkaline delignification, more so than in many other bleaching chemistries.[38] The delignification may vary in the range 40-70% depending on the wood raw material and if one or two reactors in series are used. Unbleached kraft (sulfate) pulp has a lignin content of 3-5%, which after oxygen delignification can be decreased to about 1.5% or of a kappa number of 8-10.[39] Lignin model compound reactions reveal that phenolic and enolic structures are the major reactive sites under O-Stage conditions. The phenolic lignin, diphenylmethane model dimmers are quite reactive to alkali-oxygen solution,[40,41] resulting in the formation of monomeric and oxidative coupling products (Figure 5).

The filtrate obtained from the O-Stage would be expected to contain a variety of organic macromolecules stemming from the different pathways in the alkaline-oxygen delignification process.

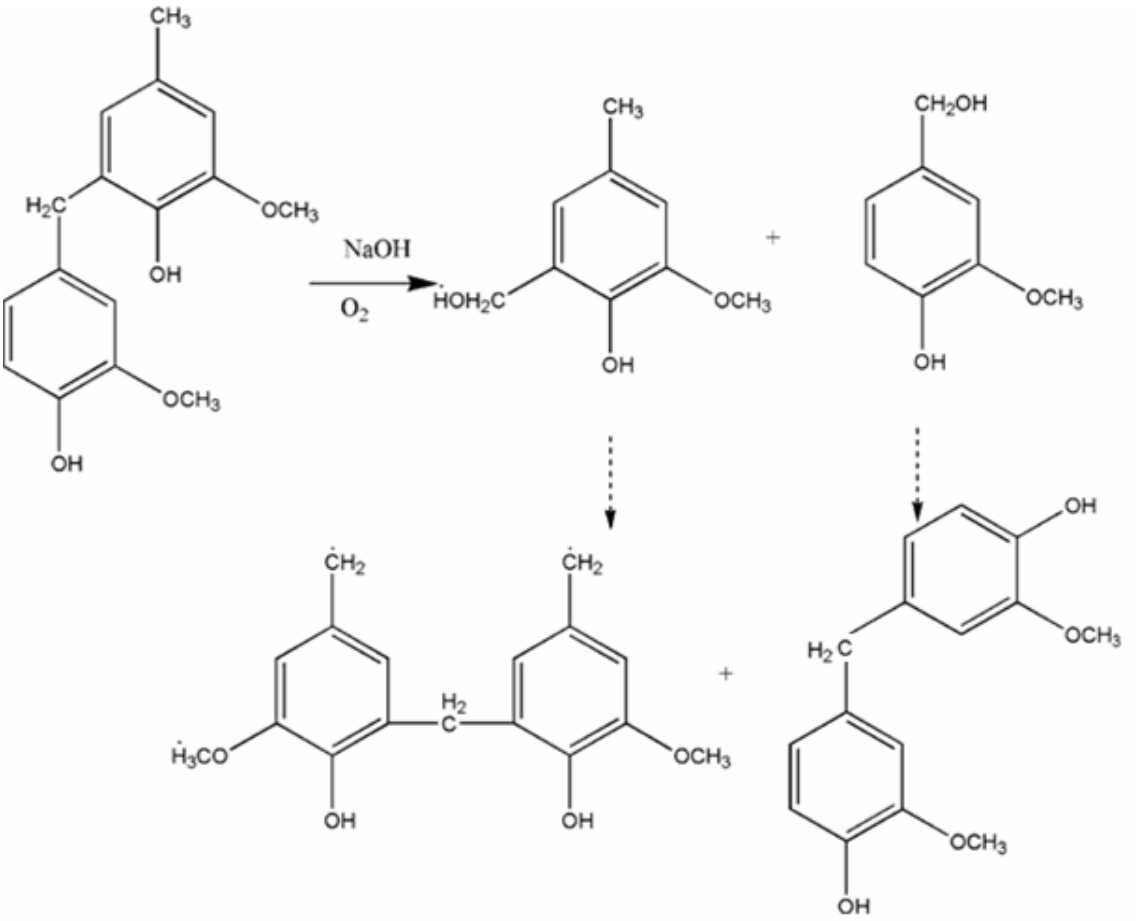

Figure 5. Products of delignification derived from alkali-oxygen treatment of an α-5 lignin diphenylmethane model dimmer.[40]

The polarogram of a solution of simple cupric ions in a 0.45 M KNO_3 and 0.05 M HNO_3 supporting electrolyte disappears from the potential region 0.06-0.09 V at a pH of 3.6. The introduction of a filtrate sample into the electrolytic cell containing Cu at this pH produces a polarogram whose peak potential varies from +ve 0.02 to -ve 0.1 V depending on the sample filtrate introduced (Figure 6); their peak currents are reported in Figure 7.

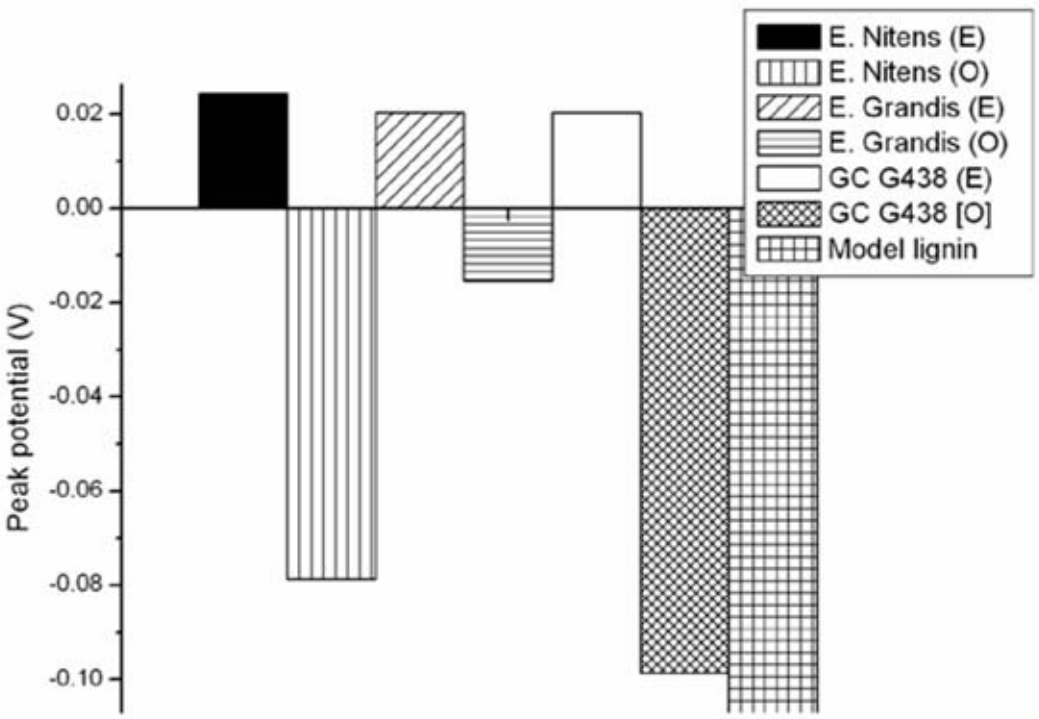

Figure 6. Observed peak potential in the presence of Cu^{2+} ions of O-Stage and E-Stage bleaching filtrates for different *Eucalyptus* species and clone at a pH of 3.6; and fixed Cu concentration (47 μM) and fixed pulp filtrate volume (20 μL).

As observed in the earlier experiment conducted at pH 2, whereby filtrate samples obtained from O-stage produced a higher current peak suppression indicating the presence of stronger none-labile metal ligands. The same implication was observed with sample filtrates obtained from the O-stage (Figure 6); their peak potentials produced higher cathodic peak shifts. It has been reported that the extent to which the peak potential shifts cathodically is indicative of the magnitude of the stability constant.[11,12] This would imply that the samples obtained from the O-Stage comprise of ligands that form strong metal-ligand complexes.

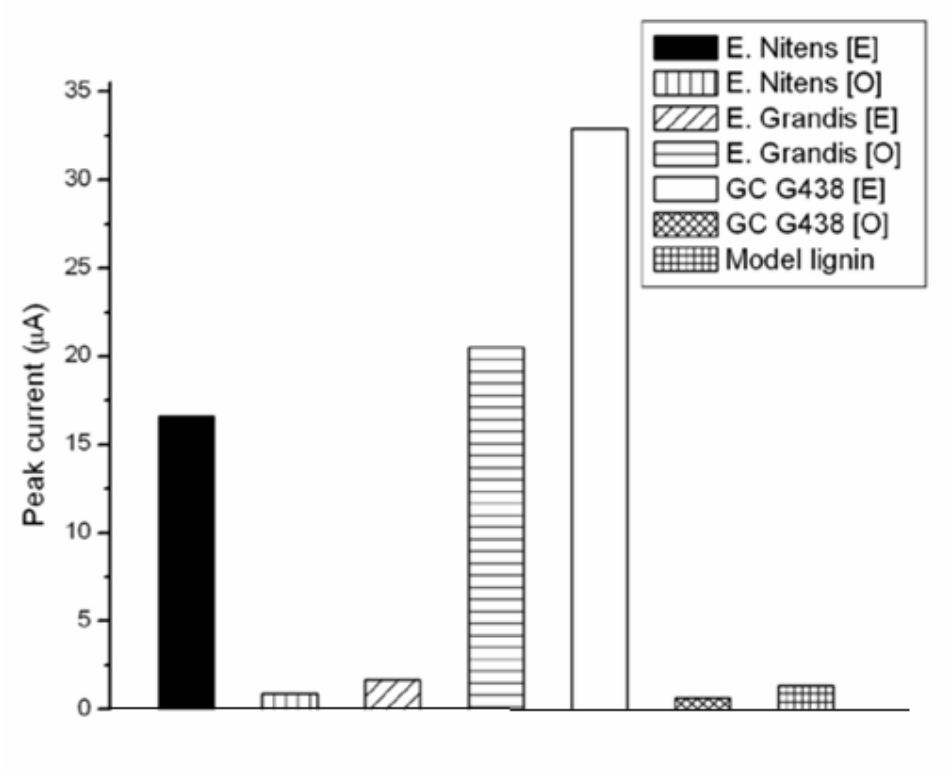

Figure 7. Observed peak currents of O and E-Stage bleaching filtrates for different Eucalyptus tree species and clone at a pH of 3.6; fixed Cu concentration (47 μM) and fixed pulp filtrate volume (20 μL).

Buffle[25] and Batley,[6] described the binding properties of a macromolecule in terms of the saturation of its complexing sites and defined the complexing capacity of the ligand, C_c, as the maximum ability of the molecule to fix a given metal ion. The complexing capacities C_c of the samples investigated were obtained according to Buffle[25] and Batley[6] and the same reported in Table 1. The reported values were obtained from plots of current vs copper concentration (MT) that was introduced into various pulp bleaching filtrate samples of Eucalyptus species, the plots are presented in Figure 8. The observed complexing capacities (C_{obs}) of the filtrate samples corroborated earlier observations relating the assumed ligand complexing capacity to the extent of the cathodic shift in the peak potential.

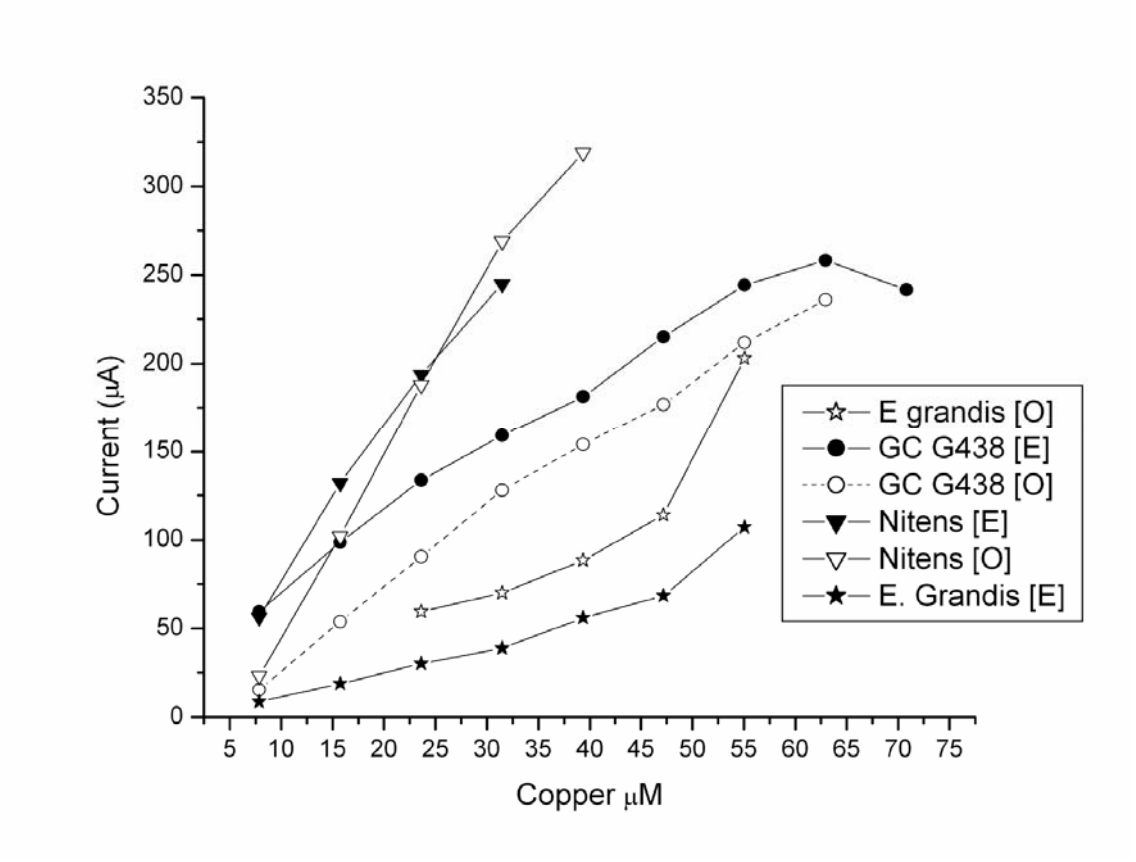

Figure 8. Titrating 70 μL fixed ligand (sourced from the O and E-stage bleaching filtrates of different *Eucalyptus* tree species and clone) with Cu^{2+} ions; titration conducted at a fixed pH (3.6).

Filtrate samples obtained from the O-Stage had consistently higher observed complexing capacities than those obtained from the E-Stage (Table 1). However the calculated complexing capacities (C_{cal}) data was not in agreement with observed complexing capacity (C_{obs}). The model used to obtain the C_{cal} assumes a 1:1 metal to ligand complexation. However this might not be the case with the samples in our study because of the non selectivity of the bleaching process producing a variety of organic ligands. Another reason for the variance is the type of possible interactions between organic macromolecules and metal ions. These consist of weak binding forces such as coordination bonds, hydrogen bonds, charge-transfer interaction, hydrophobic interaction, etc. Because they are many, these binding forces cooperatively play an important role in macromolecule metal complexes.[20,21] Whereas the deprotonated form of the reactive sites (i.e. carboxylate groups) is primarily responsible for the binding of metal ions onto polymers of a carboxylic nature.[22,23,24] It has

been shown that as few as three neutral oxygen atoms suffice a binding site for metal ions if these oxygen atoms are in the correct steric arrangement.[42] If the metal happens to form a complex with the three sterically correct oxygen atoms the C_{cal} will not comply with the model calculation which assumes a 1:1 metal-ligand complexation.

A plot of current vs the concentration of the total metal ion introduced, (C_M) is presented in Figure 8. The experiment was conducted to determine the complexing capacities of the various pulp (*Eucalyptus* species/clones) filtrate samples as well as investigate the levels of ligand metal complex formations. The pulp filtrates (70 μL) were introduced into a 10 mL supporting electrolyte (0.45 M KNO_3 and 0.05 M HNO_3) solution and the solution pH adjusted to 3.6. The electrolyte solution constituting samples of different *Eucalyptus* species obtained from the O and E bleaching stages was then titrated with Cu in increments of 8 mM. The plots showed linearity at varying segments indicating formation of various metal organic complex species. A similarity in the current vs copper plots was observed between the two bleaching stage (O-Stage and E-Stage) for samples processed from the same *Eucalyptus* species/clone. Higher plot gradients were observed as the amount of C_M increased, this could be due to the formation of higher charged complexes.

$$M^{2+} + L^- \longrightarrow ML^+$$

$$ML^+ + L^- \longrightarrow ML$$

$$ML + L^- \longrightarrow ML^-$$

$$ML^- + nL^- \longrightarrow ML^{n-}$$

It is also expected that as the C_M continues to increase the larger size of the formed metal-ligand complex will hinder mobility as is observed with the GC G438 [E] E-Stage bleaching stage (Figure 8).

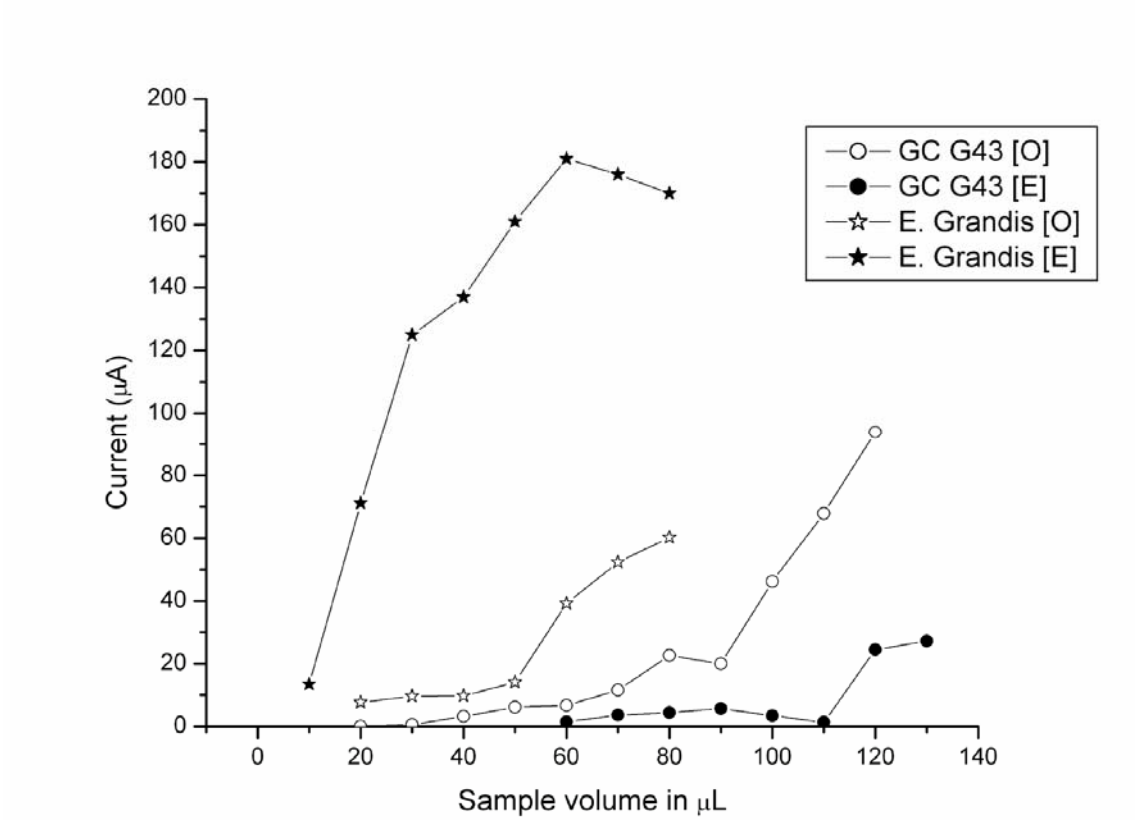

Figure 9. Titrating a fixed Cu^{2+} ions (47 μM) with a ligand sample (sourced from the O and E-stage bleaching filtrates of different Eucalyptus tree species and clone); titration conducted at a fixed pH (3.6).

Data obtained from the addition of sample to the electrolytic cell containing the support electrolyte and 47 μM Cu showed a gradual increase in peak current as the sample volume increased (Figure 9). Similarly as previously observed there was a sharp increase in peak current after the gradual increase, as the sample volume increased. This sharp increase in the peak current at this stage, can be attributed to the formation of higher charge complexes.

CONCLUSIONS

Electroanalytical techniques can be used in the pulp and paper industry to provide an insight on the interaction of the extracted organic macromolecules with the metals in solution. A high percentage of organic extractives are extracted during the alkaline oxygen

delignification stage. Metal-ligand complexes formed during the alkaline oxygen delignification stage are more stable and their complexing capacity are higher than those of the metal complexes formed in the pulp filtrate of the E-stage bleaching. The extracted organic macromolecules in the O-Stage would therefore facilitate increased extraction of metals from the pulp. This is assisted by complexing the metals in the filtrate thereby preventing them from being readsorbed onto the pulp material.

REFERENCES

1. Zhang, L., Gellerstedt, G. NMR observation of a new lignin structure, a spiro-dienone. Chem. Commun. 2001, 2744–2745.
2. Karhunen, P., Rummakko, P., Sipilä, J., Brunow, G., Kilpeläinen, I. Dibenzodioxocins; A Novel Type Of Linkage In Softwood Lignins. Tetrahedron Lett. 1995, 36(1), 169-170.
3. Guo, X., Zhang, S., Shan,.X-q. Adsorption of metal ions on lignin. J. Haz. Mat. 2008, 151(1), 134-142.
4. Wu, Y., Zhang, S., Guo, X., Huang, H. Adsorption of chromium (III) on lignin. Bioresource Technology. 2008. 99(16), 7709-7715.
5. Varney, M. S., Turner, D. R., Whitfield, M., Mantoura, R. F. C. The use of electrochemical techniques to monitor complexation capacity titrations in natural waters. In *Complexation of Trace Metals in Natural Waters*, Kramer, C. J. M., Duinker, J. C. Eds., Nijhoff M. and Junk W. Publishers, The Hague, 1984; 33-46.
6. Batley G.E. *Trace Element Speciation*, In Analytical Methods and Problems. CRC Press, Boca Raton, FL, 1989.
7. Laxen D. P. H., Harrison, R. M. The physicochemical speciation of Cd, Pb, Cu, Fe and Mn in the final effluent of a sewage treatment works and its impact on speciation in the receiving river Water Res. 1981, 15(9), 1053-1065.
8. Florence T. M. Electrochemical approaches to trace element speciation in waters, a review. Analyst. 1986, 111, 489-505.
9. Reisenhofer, E., Cesaro, A., Delben, F., Manzini, G., Paoletti, S. Copper (II) binding by natural ionic polysaccharides. Part II: Polarographic data. Bioelectrochem. Bioenerg. 1984, 12, 455-465.
10. Gustafsson, J.P., Pechov´a, P., Berggren, D. Modeling metal binding to soils: The role of natural organic matter. Environ. Sci. Technol. 2003, 37, 2767–2774

11. Koukal, B., Gu´eguen, C., Pardos, M., Dominik, J. Influence of humic substances on the toxic effects of cadmium and zinc to the green alga Pseudokirchneriella subcapitata. Chemosphere. 2003, 53(8), 953-961.
12. Lorenzo, J.I. Nieto, O. Beiras, R. Effect of humic acids on speciation and toxicity of copper to Paracentrotus lividus larvae in seawater. Aquat. Toxicol. 2002, 58(1), 27-41.
13. Bard, A.J., Faulkner, L.R. *Electrochemical methods fundamentals and applications*, 2nd ed., Wiley, New York, 2000.
14. Town, R.M., Emons, H., Buffle, J. Speciation Analysis by Electrochemical Methods. In: *Handbook of Elemental Speciation: Techniques and Methodology*: Cornelis, R. et al. Eds.; Wiley, 2003.
15. De Jong, H.G., van Leeuwen, H.P., Holub, K. Voltammetry of metal-complex system with different diffusion-coefficients of the species involved. 1. Analytical approaches to the limiting current for the general-case including association dissociation kinetics. J. Electroanal. Chem. 1987, 234, 1-16.
16. De Jong, H.G., van Leeuwen, H.P. Voltametry of metal-complex system with different diffusion-coefficients of the species involved. 2. Behavior of the limiting current and its dependence on association/dissociation kinetics and lability. J. Electroanal. Chem. 1987, 234, 17-29.
17. Torres, M., Mdíaz-Cruz, J., Ariño, C., Grabaric, B.S., Tauler, R., Esteban, M. Multivariate curve resolution analysis of voltammetric data obtained at different time windows: study of the system Cd2+ -Nitrilotriacetic acid. Anal. Chim. Acta. 1998, 371, 23-37
18. Caykara, T., Inam, R., Ozturk, Z., Guven, O. Determination of the complex formation constants for some water-soluble polymers with trivalent metal ions by differential pulse polarography. Colloid. Polym. Sc.i 2004, 282, 1282–1285.
19. Lingane, J.L. Interpretation of the polarographic waves of complex metal ions. Chem. Rev. 1941, 29, 1–35.
20. Pekel, N, Savas, H, Guven, O. Complex formation and absorption of V3+, Cr3+ and Fe3+ ions with poly(N- vinylimidazole). Colloid. Polym. Sci. 2002, 280, 46–51.
21. Howard AG. *Aquatic environmental chemistry*, Oxford University Press, New York, 1998.

22. Manzini, G., Cesaro, A., Delben, F., Paoletti, S., Reisenhofer, E. 1984. Copper (II) binding by natural ionic polysaccharides. Part I: potentiometric and spectroscopic data. Bioelectrochem. Bioenerg. 12, 443-454.
23. Subramanian, R., Natarajan, P. Complexation of Cu (II) with poly(acrylic acids). A polarographic study. Indian J. Chem. 1985, 24, 432-434.
24. Van den Hoop M. A. G. T., Leus, F. M. R., Van Leeuwen H. P. Stripping voltammetry of zinc/polyacrylate complexes: influence of molar mass.Collect. Czech. Chem. Commun. 1991, 56, 96-103.
25. Buffle, J. *Complexation Reactions in Aquatic Systems. An Analytical Approach*. Ellis Horwood, Chichester. 1988.
26. Ruzic, I. Theoretical aspects of the direct titration of natural waters and its information yield for trace metal speciation. Anal. Chim. Acta. 1982, 140, 99-113.
27. Henze, G. *Introduction to polarography and voltammetry,* Metrohm Switzerland Herisau, 2003.
28. Cukrowski, I., Adsetts, M. Experimental and calculated metal complex formation curves for a labile metal-ligand system. J. Electroanal. Chem. 1997, 429, 129-137.
29. Reisenhofer, E., Cesàro, A., Delben, F., Manzini, G., Paoletti, S. Copper(II) binding by natural ionic polysaccharides: Part II. Polarographic data. Bioelectrochem. Bioenergetics. 1984, 12, 455-465
30. Brezonik, P.L., Brauner, P.A., Stumm, W. Trace metal analysis by anodic stripping voltammetry. Effect of sorption by natural and model organic compounds. Water Res. 1976, 10, 605-612.
31. Scarano, G., Bramanti, E. Voltammetric behaviour of marine hydrophobic copper complexes: effect of adsorption processes at a mercury electrode. Anal. Chim. Acta. 1993, 277, 137-144.
32. Beveridge A., Pickering, W.F. Influence of surfactants on the determination of Cu, Pb and Cd by ASV. Water Res. 1984, 18(9), 1119-1123.
33. Buffle, J., Mota, A.M., GoncaIves, M.L.S. J. Interfacial Electrochemistry. Electroanal. Chem. 1987, 223-235.
34. Lukaszewski, Z., Pawlak, M.K., Ciszewski, A. Determination of the stage of the process deciding of the total effect of the influence of organic substances on the peaks in anodic stripping voltammetry. Electroanal. Chem. 1979, 103, 217-223.

35. Ugapo T., Pickering W.F. Effect of organic colloids on ASV signals of Cd, Pb and Cu Talanta. 1985, 32(2), 131-138.
36. Cukrowski, I., Luckay, R. C. A differential pulse polarographic study of bismuthIII complexes with macrocyclic ligands 1,4,7,10-tetraazacyclododecane and 1,4,7,10-tetrakis (2 hydroxypropyl)-1,4,7,10-tetraazacyclododecane. An out-of-cell determination of stability constants of polarographically active and inactive bismuth complexes at fixed ligand to metal ratio and various pH values. Anal. Chim. Acta. 1998, 372, 323-331.
37. Cukrowski, I., Hancock, R.D., Luckay, R.C. Formation constant calculation for non-labile complexes based on a labile part of the metal-ligand system. A differential pulse polarographic study at fixed ligand to metal ratio and varied pH: application of polarographically inactive complexes.Anal. Chim. Acta. 1996, 319(1-2), 39-48.
38. **G**ullichsen J., Fogelholm C.J. Chemical pulping, Papermaking Science and Technology, Book 6A, Fapet Oy, Jyväskylä, 2000, 138, 635-638.
39. McDonough, T.J. Principles and practice. In *Pulp Bleaching*, Dence, C.W., Reeve, D.W., Eds.; Tappi Press, Atlanta, 1996, 213.
40. Xu, H., Omori S., Lai, Y-Z. The Aakaline stability of oc-5 diphenylmethane dimers. Holzforsch. 1995, 49, 323-324.
41. Xu, H., Lai, Y-Z. Procedings. Tappi Pulping Conference., Nashville, TN, 1996.
42. Tips S.R., Derek, H. *Advances in carbohydrates chemistry and biochemistry*. Academic Press Limited 47. 1989.

CHAPTER 5: PAPER IV

DEVELOPMENT OF A NOVEL ENVIRONMENTALLY FRIENDLY METHOD FOR THE EXTRACTION OF RESIDUAL METALS IN DISSOLVING PULP

Joseph Nyingi Kamau[1], Jane Catherine Ngila[1,3], Andrew Kindness [1], and Tammy Bush[1,2]

[1]University of Kwazulu-Natal, Chemistry department, Private Bag X54001, Westville, Durban 4000, South Africa.
[2]CSIR Natural Resources and the Environment, Forestry and Forest Products Research Centre, P.O Box 17001, Congella 4013, South Africa.
[3]University of Johannesburg, Doornfontein Campus P.O. Box 17011, Doornfontein 2028, South Africa

ABSTRACT

Ethylenediaminetetraacetic acid (EDTA) has been used extensively as a ligand in the pulp and paper industries. Although EDTA is non-toxic to mammals at environmental concentrations, there is some concern about the potential of EDTA to remobilize toxic heavy metals out of sediments. The study investigates the use of acetylacetone as a ligand in the extraction of metals in the pulp and paper industry. Desorption and kinetic models were used to quantify desorption and characterize the desorption mechanism. Metal desorption from pulp was more effective when using acetylacetone as opposed to EDTA. Metal desorption under the influence of acetylacetone at both pH 6 and 8 were best described by Langmuir desorption model, indicating that the adsorbed metals were chemically attached on the pulp. The values of maximum metal desorption capacity ($q_{max;}$ representing the amount of metal that remains as residual on the pulp after extraction) were lower when using acetylacetone as a ligand as opposed to EDTA. The Freundlich model also described Mg, Al and Cu desorption suggesting some fraction of these metals to have been physically adsorbed onto the pulp material

Key words: Acetylacetone, metals desorption, Freundlich, Langmuir, pulp.

INTRODUCTION

There has been growing concern over the environmental impacts of Ethylenediaminetetraacetic acid (EDTA) and other complexing agents (ECB 2004). EDTA is an aminopolycarboxylic acid containing six donor atoms, which acts as a hexadentate ligand (Williams 1998). It forms strong and very stable complexes with many metal cations. EDTA is poorly biodegradable and has been found in many water bodies, leading to restrictions to its use and disposal in many countries. (Chaudary *et al.* 2000; Pietsch *et al.* 1995; Pitter and Sýkora 2001; Bolton *et al.* 1993; Allard *et al.* 1996; Hinck 1997). It is poorly adsorbed on wastewater treatment sludge and is resistant to biological waste water treatment operating under normal conditions making it difficult to remove it from wastewaters (Sykora *et al.* 2001; Bernhard *et al.* 2006) According to the European Union risk assessment report on EDTA less than 30% of EDTA was degraded or removed from wastewater with sludge at wastewater treatment in most studies (ECB 2004). Although EDTA is non-toxic to mammals at environmental concentrations, there is some concern about the potential of EDTA to remobilize toxic heavy metals out of sediments and the difficulties to biodegrade this substance (IPPC 2001; ECB 2004). The pulp and paper industry has been identified as a major contributor of EDTA waste water emissions (Fuerhacker *et al.* 2003). EDTA is extensively used in totally chlorine free (TCF) bleaching sequences, to prevent transition metals ions (Mn(II), Cu(II) and Fe(III)) acting as catalysts in free radical forming reactions, which attacks the cellulose affecting pulp quality (Virtapohja 1998; Takahashi *et al.* 1997; Larisch and Duff. 2000)

This paper reports on a novel method for the extraction of metals adsorbed onto pulp using acetylacetone as a ligand. Unlike EDTA, acetylacetone is biodegradable and is known to degrade hydrolytically via cleavage at the central C—C bond of the β-diketone moiety (Sakai *et al.,* 1986; Kawagoshi and Fujita 1998). Straganz and co-workers (2003) isolated an *Acinetobacter johnsonii* strain that grew on acetylacetone as the sole carbon source. Acetylacetone is relatively soluble and it is stable in water (Schwedt 1979). The versatility of acetylacetone as a coordinating ligand is well-known (Sohn and Lee 2000).

EXPERIMENT

Material and method

Dissolving pulp is used in the manufacture of various cellulose-based products. When in use for the production of sausage skins and pharmaceutical products the metal composition especially those that are considered toxic to human, should be at acceptable limits. To maintain the metal levels at acceptable limits the pulp and paper industry utilizes complexing agents, which have the ability to form stable and water-soluble complexes with many metal ions. In the recent decade several new chelating agents have been proposed, e.g., EGTA (ethylene glycol tetraacetic acid), HEDTA (hydroxyethylethylenediaminetri-acetic acid), (Ager and Marshall 2001), EDDS (N,N'-ethylenediaminedisuccinic acid) (Jones and Williams 2001). However EDTA remains the most preferred choice, but its resistance to biodegradation is of concern to the aquatic environment.

Acetylacetone is proposed as an alternative chelating agent, the study seeks to compare its metal extraction efficiency with that of EDTA. Parameters that influence metal extraction such as pH, temperature and time are first established. Thereafter batch experiments are conducted to determine the desorption capacities, desorption kinetics and thermodynamics.

Reagents

All solutions were prepared in milli-Q water 18.2 Ω cm^{-1} resistivity; reagents were of analytical grade unless specified otherwise. Calibration standards were prepared from Fluka TraceCert 10 ppm multielement stock standard. Nitric acid was TraceSelect ICP grade >69% supplied by Fluka. Supelclean LC-18 cartridges (1 g) were supplied by Supelco, Bellefonte, USA. Pulp material used in the study was obtained from the final pulping stage of 96α pulp grade produced in a laboratory simulated dissolving pulp production process. Acetylacetone was analytical grade obtained from Sigma-Aldrich, Germany. Cotton cellulose (IAEA-V-9) Standard Reference Material was obtained from IAEA and used in the study to determine the analytical sample digestion accuracy. EDTA was analytical reagent grade obtained from Thomas Baker, Mumbai, India.

Influence of pH on metal desorption

The solid-liquid adsorption/desorption process is influenced by parameters such as pH, solubility of solute in the solvent, interaction time and solution temperature (Kumar and Sivanesan 2006). In an environment where desorption is aided by a ligand, the desorption/adsorption process is biased towards desorption. The forward desorption process is favored by the formation of a stable metal ligand complex. The ease of metal ligand complex formation is influenced by pH and stability of the formed product.

Acetylacetone forms stable six membered ring quasi aromatic organometalic compounds wherein both oxygen atoms bind to the metal. Acetylacetone (Hacac) exists in three forms (Pearson and Anderson 1970) in aqueous solution-the tautomeric keto (I) and enol (II) forms and the anionic form (III), which is the common product of dissociation of either protonated tautomer (Figure 1). The mechanism of interconversion in acidic aqueous solution is the dissociation of either protonated form to give the anion, followed by very fast recombination (Fay *et al.* 1971). Nakanishi *et al.* (1977) reported an increase in composition of the keto form in polar solvent as acetonitrile and water. Possibly due to intermolecular hydrogen bonding as opposed to the intramolecular hydrogen in the enol form (Nakanishi *et al.* 1977).

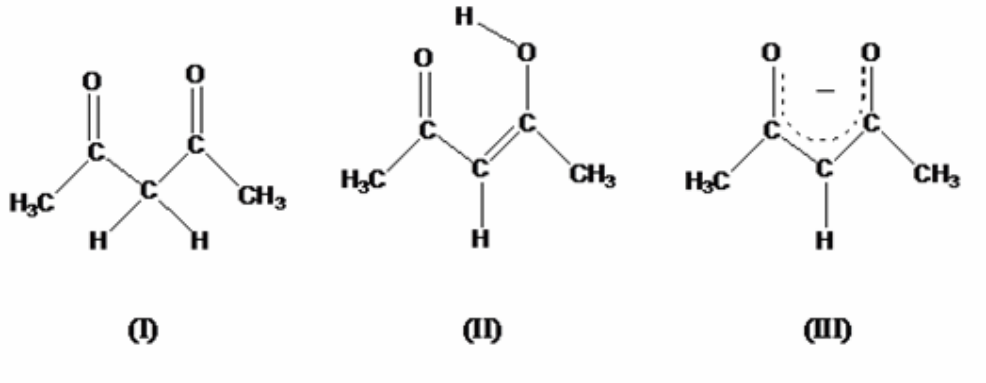

Figure 1. The Keto (I) enol (II) tautomeric structures of acetylacetone and its anion (II)

To determine the optimum pH at which most metals of interest complex with acetylacetone, C-18 solid phase material (SPE) were employed as the stationary material. The C-18 cartridges were factory packed in quantities of 1 g in 6 ml polyethylene tubes. The column were preconditioned according to Kamau and co-workers (2011). A model solution comprising 0.2 ppm of Cd, Cu, Cr, Fe Mn, Pb and Si was prepared in Milli-Q water. Portions

of 30 ml metal solution were dispensed into 100 ml polyethylene sample bottles and 0.4 ml of 1.0 mM acetylacetone was added. The solution was then adjusted to the appropriate pH ranging between 2-10, using various buffer systems. Phosphate buffer solution was prepared by mixing 0.1 M Sodium dihydrogen phosphate (Sigma-Aldrich) solution with an appropriate amount of phosphoric acid to make up pH 2 and adding an appropriate amount of 1 M NaOH solution to obtain pH 7. Acetate buffer solutions were prepared by mixing 0.1 M Sodium acetate solution with an appropriate amount of acetic acid to achieve either pH 4, 5 or 6. Ammonium chloride buffer was prepared by mixing 0.1 M ammonium chloride with an appropriate amount of NH_4OH to obtain pH 8, 9 or 10. A volume of 10 mL of the appropriate pH buffer was passed through the column and thereafter 30 mL of the model metal solution loaded in the column, at a flow rate of approximately 3 mL per minute. The column was then washed with the appropriate buffer and the adsorbed metal eluted with 5ml of 0.5 M HNO_3 at a flow rate of 3 ml per minute.

Batch desorption

Dissolving pulp was obtained from the final pulping stage of 96α pulp grade produced in a laboratory simulated dissolving pulp production process. The pulp was dried and homogenized in a kitchen blender. Samples (0.4 g) of the homogenized pulp were weighed in polypropylene 100 mL bottles. Milli-Q water (40mL) adjusted to either pH 6 or pH 8 was added to the pulp samples in the polypropylene bottles. After which 2 mL of either acetylacetone (1.0 mM) or EDTA (1.0 mM) was added to the sample mixture, depending on whether the set experiment was to determine desorption due to acetylacetone or EDTA. The polypropylene bottles were then tightly screwed and placed in a thermostated water bath shaker with an adjustable speed and temperature. The water bath temperature was adjusted to the desired experiment temperature and the timer set to the duration time of the experiment. After the set extraction time the sample bottles were removed from the water bath filtered and washed under vacuum with three portions of 20 mL milli-Q water. The washed pulp sample was then dried at a temperature of 70 $^{\circ}C$ to a constant weight. Approximately 0.3g of the dried samples was placed in Teflon microwave digestion vessels and 6 mL HNO_3 (TraceSelect ICP grade >69% supplied by Fulka) added to the teflon digestion vessels. The microwave digestion program was set to a maximum digestion temperature and pressure of 300 $^{\circ}C$ and 75 bar, respectively. The digest was made to volume in 50 mL volumetric flask with Milli-Q water and analysed by ICP-OES (Perkin Elmer Optima 5300DV)

Determining the optimum volume of acetylacetone

Varying volumes of 1.0 mM acetylacetone (0.2 - 3 mL) were added to 0.4 g of pulp in 40 mL milli-Q water adjusted to pH 6. The different setups with varying acetylacetone volumes were extracted by batch extraction as stated above. After which the pulp samples were filtered and rinsed with three fractions of 20 mL milli-Q water, then dried and digested as indicated above, followed by analysis using ICP-OES.. The extracted metal concentration was determined by subtracting the metal concentration in the extracted pulp (C_t) from that in the initial (unextracted) pulp (C_o). The concentrations were calculated based on one gram of pulp sample.

The results were presented in percent desorption according to equation1.

$$\%Desorption = \frac{C_o - C_t}{C_o} \times 100 \qquad (1)$$

Determining the optimum desorption temperature and time

Temperature and time have an influence on metal desorption kinetics. The influence of these two parameters were investigated by varying one while maintaining the other constant. The extraction temperature was set at 30, 40, 50 and 60°C and the extraction performed in a thermostated water bath shaker. At each of the stated temperatures the extraction was conducted by a batch process at times 10, 20, 30, 40, 50, and 60 minutes. After the extraction at the specified times and temperatures triplicate pulp samples were filtered digested and analyzed by ICP-OES. The percent desorption was calculated according to equation 1 above and the data presented graphically (Figure 5 & 6).

Desorption isotherm models

Isotherms represent the equilibrium distribution of metal ions between the solid and liquid phases. They help to describe the adsorptive/desorption capacity of a material and further help to evaluate the mechanism of preference of the adsorption/desorption system (Kumar and Sivanesan 2006). The simplest form of adsorption/desorption is the physisorption/physidesorption, due to weak attractive forces, generally Van der Waals forces (Perez *et al.* 2007). The chemisorption/chemidesorption happens when a chemical connection

is formed or broken. In physisorption/physidesorption the adsorbed species conserves its chemical nature, whereas a chemisorbed species undergoes a transformation process, to give a different species. In a physisorption/physidesorption process the adsorbate can be adsorbed forming successive layers, whereas a chemisorptions/chemidesorption process is restricted to a monolayer, since the solid surface is completely covered with the adsorbed substance (Freitas 2008; Perez *et al.* 2007). The chemical transformation of the chemisorbed specie requires a certain activation energy that is not necessary in physisorption/physidesorption (Perez *et al.* 2007). Physisorption/physidesorption depends principally on the superficial area; and the chemosorption/chemidesorption involves other aspects such as: the electronic distribution, the pore size, the active groups and the connection form of the adsorbed molecule. (Barrow 1964).

Langmuir and Freundlich are among the most common isotherms describing these types of systems. Freundlich model represents principally the case of physical adsorption whereas the Langmuir model represents the case of chemical adsorption (*Perez et al.* 2007). Langmuir is based on the assumption that the adsorption is homogeneous, and that each site holds only one adsorbate and there exists no interaction between adsorbed molecules. The Langmuir isotherm can be derived from the Gibbs approach according to Ng and co-workers (2003):

$$q_e = q_{\max} \frac{bC_e}{1 + bC_e} \quad \text{.....(2)}$$

Where q_e is the amount of metal adsorbed on a gram of adsorbent and C_e is the metal concentration of the solution at equilibrium.

The constants $q_{\max}$ and b are the characteristics of the Langmuir equation and can be determined from a linearized form of the above equation, represented by Eq. 3

$$\frac{C_e}{q_e} = \frac{1}{q_{\max}} C_e + \frac{1}{q_{\max} b} \quad \text{.....(3)}$$

A plot of C_e/q_e versus C_e gives a straight line of slope $1/q_{max}$ and intercept $1/ q_{max}b$. $q_{\max}$ is a Langmuir constant of the maximum adsorption/desorption, and b is also a Langmuir constant describing the ratio of the adsorption and desorption rate constant, which is related to the energy of adsorption through the Arrhenius equation (Chong and Volesky, 1995).

Freundlich isotherm (Freundlich 1906) is the most important multi-site adsorption isotherm, widely applied in heterogeneous systems especially of organic compounds and highly interactive species on activated carbon and molecular sieves. However it does not obey Henry's Law at low concentrations (Ng *et al.,* 2003). It is derived by assuming an exponential diminution in the distribution function inserted into Langmuir equation. It describes reversible adsorption and is not restricted to the formation of a monolayer (Freundlich, and Heller, 1939).

$$q_e = K_F C_e^{b_F} \quad \text{.....(4)}$$

The linearized form of eq (4) is obtained by taking logarithms, parameters K_F and b_F can then be obtained from a plot of ln q_e versus ln C_e (eq. 5)

$$\ln q_e = b_F \ln C_e + \ln K_F \quad \text{.....(5)}$$

Where q_e and C_e have the same meaning as in equation (1) above; the numerical value of K_F presents adsorption capacity and b_F indicates the energetic heterogeneity of adsorption sites (Freitas, 2008)

In this study desorption isotherms were obtained through a batch process. Varying weights of dried pulp samples (0.4 – 1.2 g) were placed in 100 mL polyethylene bottles. Milli-Q water (60 mL) adjusted to ether pH 6 or 8 and spiked with either acetylacetone or EDTA was then added. The extraction was performed at the optimized temperature and time previously determined for either acetylacetone or EDTA (Figure 5 & 6).

Desorption kinetics

The kinetic rates were estimated by Lagergren pseudo first order model (1898), and Ho's pseudo second order model (1995), given by Eqs. (6) and (7) respectively.

Pseudo-First-Order Equation. The pseudo-first order equation of Lagergren is generally expressed as follow,

$$dq_t/dt = k_1(q_e - q_t) \quad \text{.....(6)}$$

where k_1 (min^{-1}) is the rate constant of pseudo-first-order adsorption, q_e (μmol·g^{-1} of dry weight) is the amount of metal ion sorbed at equilibrium, and q_t (mmol·g^{-1} of dry weight) is the amount of metal ion on the surface of the sorbent at any time *t* (min). By applying the boundary condition $q_t = 0$ at $t = 0$, eq 6 becomes 7

$$\ln(q_e - q_t) = \ln q_e - k_1 t \quad \text{.....................................(7)}$$

Pseudo-Second-Order Equation. In addition, a pseudo second- order equation may be tested on the experimental data (Ho and McKay, 1998; Wu *et al.,* 2001). The kinetic rate equation is

$$dq_t / dt = k_2 (q_e - q_t)^2 \quad \text{..(8)}$$

where k_2 (g·$mmol^{-1}$·min^{-1}) is the rate constant of pseudo second-order adsorption. Taking into account the initial sorption rate v_0 (mmol·g^{-1}·min^{-1})

$$V_0 = k_2 q_e^2 \quad \text{...(9)}$$

k_2 can be determined from the slope and intercept in a plot of *t*/*q*t against *t*.

Equation 8 can be rearranged to obtain

$$\frac{t}{q_t} = \frac{1}{V_0} + \frac{1}{q_e} t \quad \text{..(10)}$$

The values of v_0 and q_e can be determined experimentally by plotting t/q_t versus *t*.

pseudo-second-order equation, agrees with chemisorption as the rate controlling mechanism (Ho and McKay, 2000; Wu *et al.,* 2001; Wang *et al.,* 2006; Agarwal *et al.,* 2006; Javed *et al.,* 2007; Deng *et al.,* 2007)

Activation energy: Svante Arrhenius (1889) demonstrated that the rate of many chemical reactions vary with temperature in accordance with equation 11.

$$k = A^{-E_a/RT} \quad \text{...(11)}$$

By taking the natural logarithm of both sides of the equation, a linearized equation is obtained. The activation energy E_a can then be obtained by plotting *Ink* against *1/T*

$$Ink = -\frac{E_a}{RT} + InA \quad \text{...(12)}$$

where *A* is the frequency factor for the reaction, *R* is the universal gas constant, *T* is the temperature (in Kelvin), and *k* is the reaction rate coefficient. While this equation suggests that the activation energy is dependent on temperature, in regimes in which the Arrhenius equation is valid this is cancelled by the temperature dependence of *k*. Thus E_a can be evaluated from the reaction rate coefficient at any temperature (within the validity of the Arrhenius equation).

RESULTS AND DISCUSSION

pH influence

Owing to the competition between protons and metal ions for the binding sites in the ligand molecule, the pH is a very important parameter. Acetlylacetone was subjected to a range of pH to determine the optimum pH at which it complexes with the metal of interest. This was done with the aid of a solid phase material, by complexing the metal in solution with acetylacetone and retaining the complex on C-18 solid phase material thereafter eluting it with 5ml of 0.5 M HNO_3 (Figure 1).

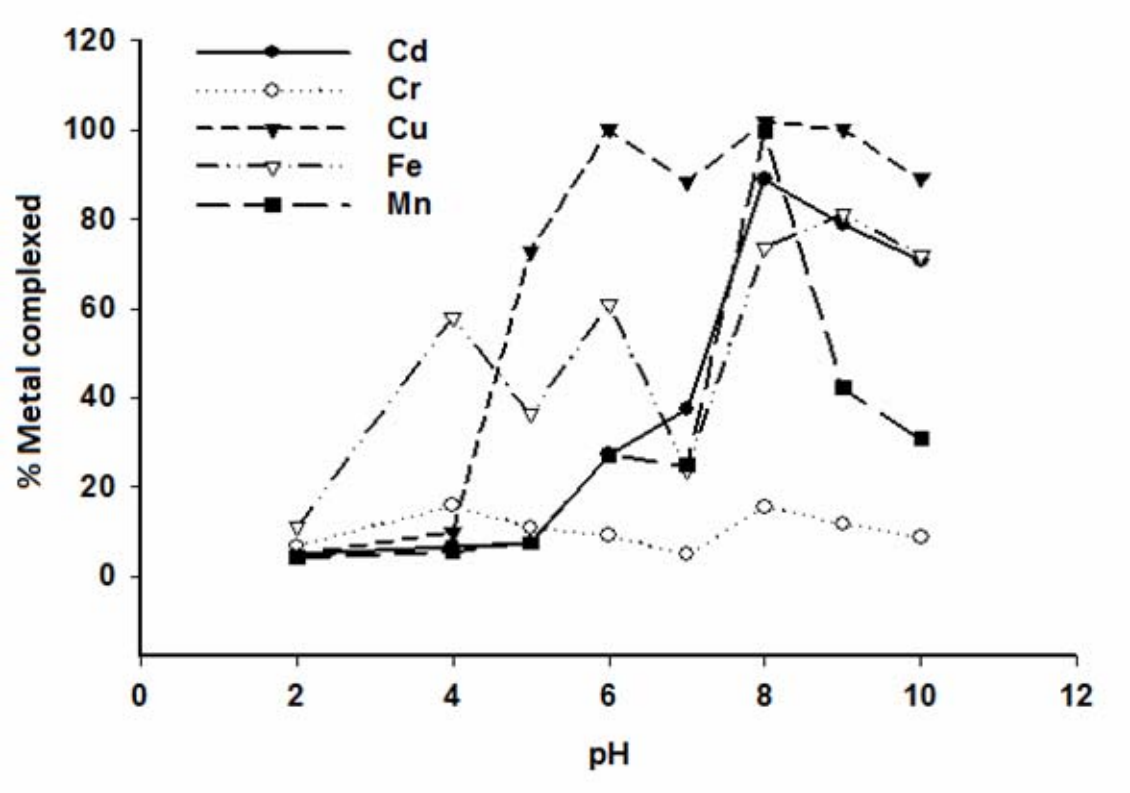

Figure 2. Effect of pH on acetylacetone metal complex formation illustrated by % metal complexed.

Acetylacetone exists in three different forms (Keto, enol and ionized form; (Figure 1); the state that predominates in solution is influenced by pH. Schaefer and Mathisen (1965) assumed metal acetylacetone formation to follow a complexation and ionization reaction as indicated in equation 13, 14 and 15.

$$M^{+n} + Hacac \rightleftharpoons M(acac)^{+n-1} + H^{+} \quad \ldots\ldots\ldots\ldots 13$$

$$M(acac)^{+n-1} + Hacac \rightleftharpoons M(acac)_2^{+n-2} + H^{+} \quad \ldots\ldots\ldots\ldots 14$$

$$Hacac \overset{K_1}{\rightleftharpoons} acac^{-} + H^{+} \quad \ldots\ldots\ldots\ldots\ldots\ldots\ldots\ldots\ldots\ldots 15$$

From the above assumed reaction an alkaline media would favor the forward reaction due to abstraction of the formed protons. This phenomenon was observed with most of the metals

investigated. A high recovery of metals (Cd, Cu, Pb, Fe and Mn) in solution (corresponding to high metal acetylacetone complexation) was observed at pH 8 ranging from 80% to 100% (Figure 2). It has been proposed that the first step in the reaction between copper (I1) and the keto tautomer of acetylacetone in an acidic media involves the formation of a symmetrical precursor complex in which the metal ion is bonded to both keto groups as that shown in (Figure 3) (Pearson and Anderson 1970).

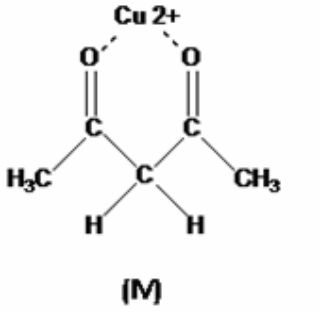

Figure 3. The intermediate complex in the formation of the copper acetonato complex

In this mechanism the cupric ion acts as an electron sink and the rate determining step involves the slow, metal ion catalyzed proton release (Pearson and Anderson, 1970). This rate determining step is influenced by the electronegativity of the metal ion. A higher value enhancing its ability to act as an electron sink. A small difference between the electronegativity of oxygen and the metal (Δ Electronegativity) determines the stability of the transition complex and the ease of metal acetylacetone complex formation. The percentage recovery of metals (at pH 6) in the current study was favored by a low oxygen metal Δ Electronegativity (Table 1). Metals that had high percentage recoveries at pH 6 had low Δ Electronegativity, while those with high Δ Electronegativity were poorly recovered (Table 1). Acetylacetone had two maxima at which most of the metals were recovered (pH 6 and pH 8); the recovery was highest at pH 8.

Table 1. Relating % metal recovery with metal electronegativity and Δ Electronegativity of metal to oxygen atom.

Metal	Electronegativity	% Metal complexed	Δ-Electronegativity (EN)
Cu	1.90	100 ± 0.02	1.54
Fe	1.83	61 ± 12.0	1.61
Pb	2.33	96 ± 0.4	1.11
Mn	1.55	27 ± 0.5	1.89
Cr	1.66	9 ± 1.4	1.78
Cd	1.69	27 ± 0.3	1.75

Δ EN = Oxygen elecronegativity – Metal electronegativity; Electronegativity values quoted from Pauling (1932); *n=3*.

Determining volume of acetylacetone, extraction time and temperature

Extraction of selected metals in a pulp sample (0.4 g) was monitored with increasing volume of 1 mM acetylacetone. The weight of the pulp sample was kept constant while varying the amount of acetylacetone in the extraction mixture. A volume of 2 ml acetylacetone (1 mM) was found to be sufficient for the optimum extraction of most of the metals under study (Figure 4).

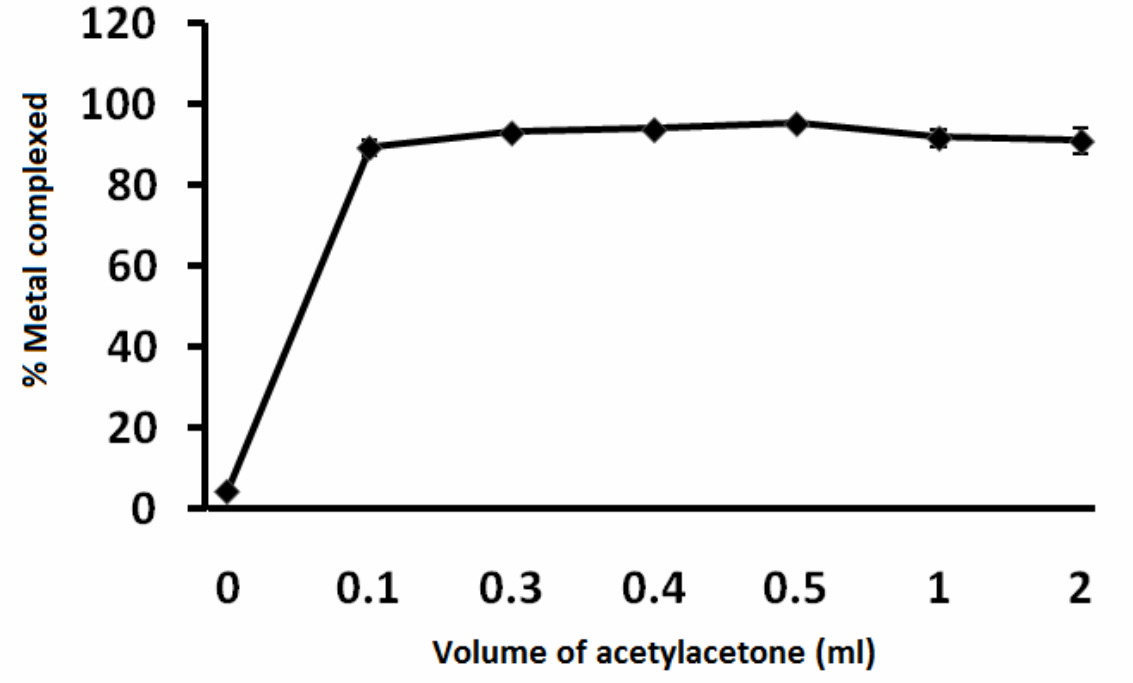

Figure 4. The optimum acetylacetone volume; this corresponds to the volume that enables highest % recovery of the metal (Cu) in solution.

The extraction time and temperature was determined experimentally by varying one parameter while maintaining the other constant. Four sets of experiments (at pH 6 and 8) were conducted at 30, 40 50 and 60 ºC. A batch extraction was setup at varying times (10, 20, 30, 40, 50 and 60 minutes) the extraction was conducted at each of the above mentioned temperatures (30, 40 50 and 60 degrees centigrade). The equilibrium metal extraction time at pH 6 and pH 8 was established graphically (Figure 5 & 6). An equilibrium time was selected that accommodated the metals under study, 30 minutes was selected at pH 6 (Figure 5) and 50 minutes at pH 8 (Figure 6). The optimum extraction temperature was found to be 50 and 30 ºC at pH 6 and 8 respectively. This was determined graphically by plotting % metal desorption against temperature (Figure 7 & 8).

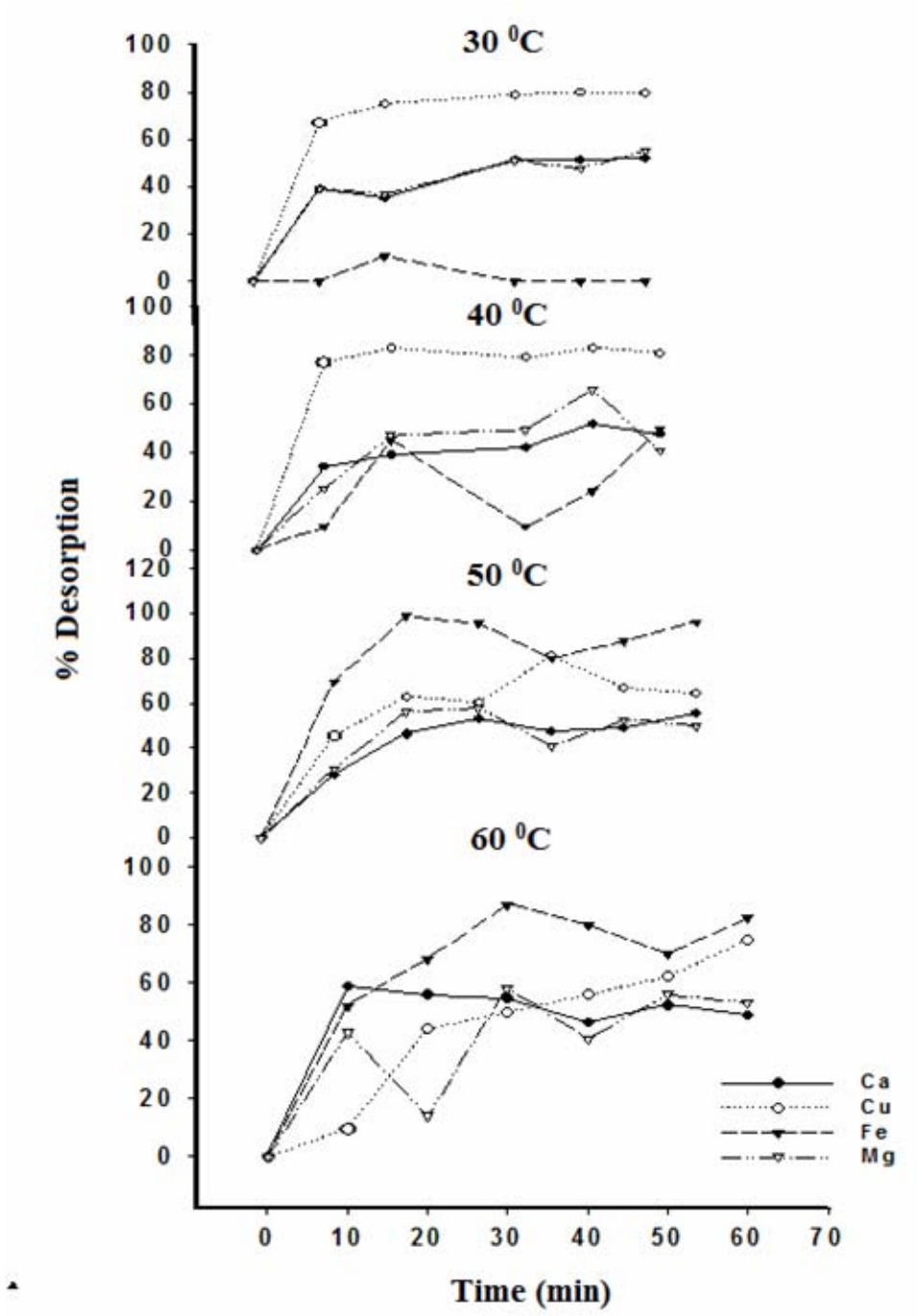

Figure 5. Influence of time and temperature on metal desorption from pulp at pH 6; A, B, C and D = 30, 40, 50 and 60 ºC respectively.

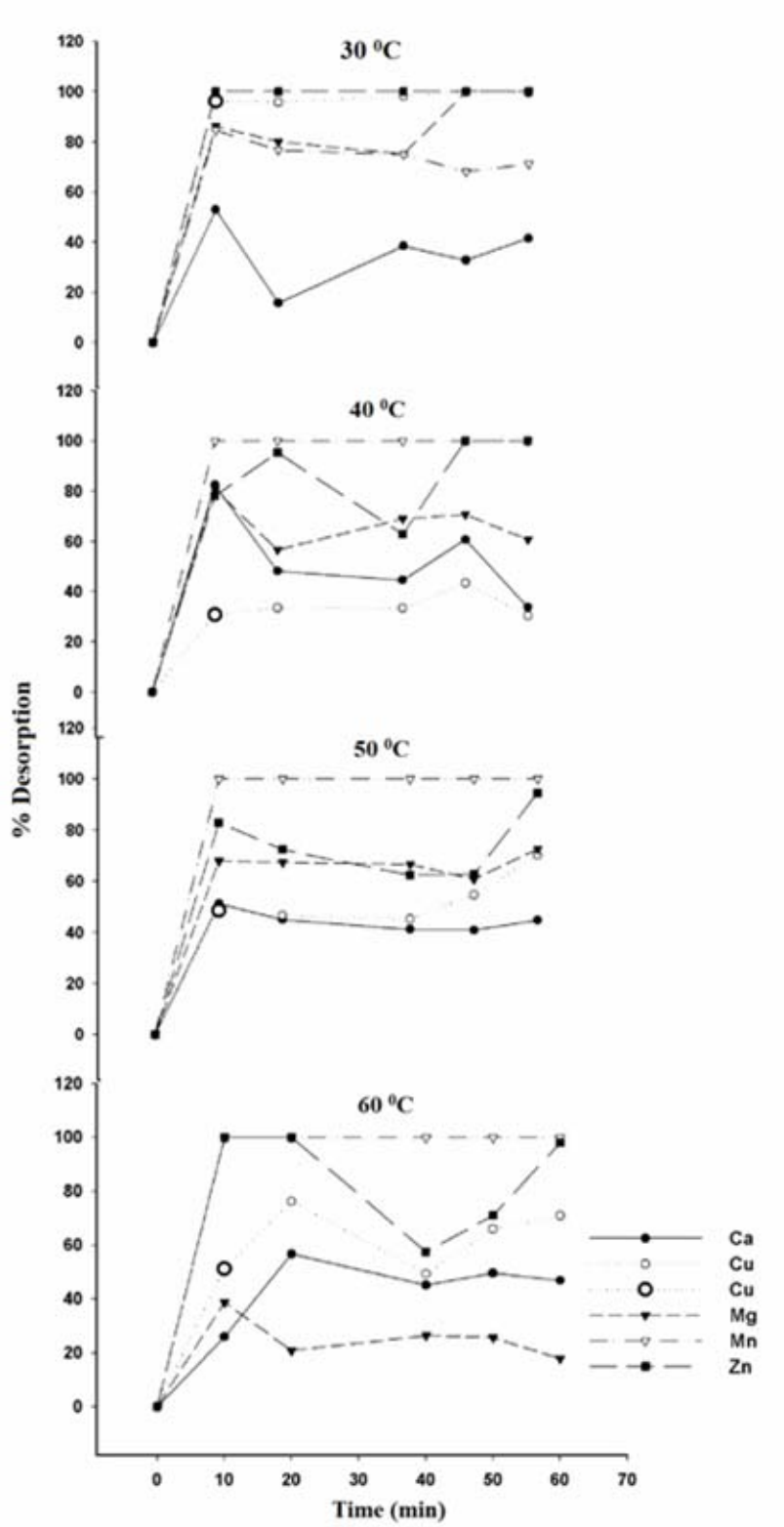

Figure 6. Influence of time and temperature on metal desorption from pulp at pH 8; A, B, C and D = 30, 40, 50 and 60 ºC respectively.

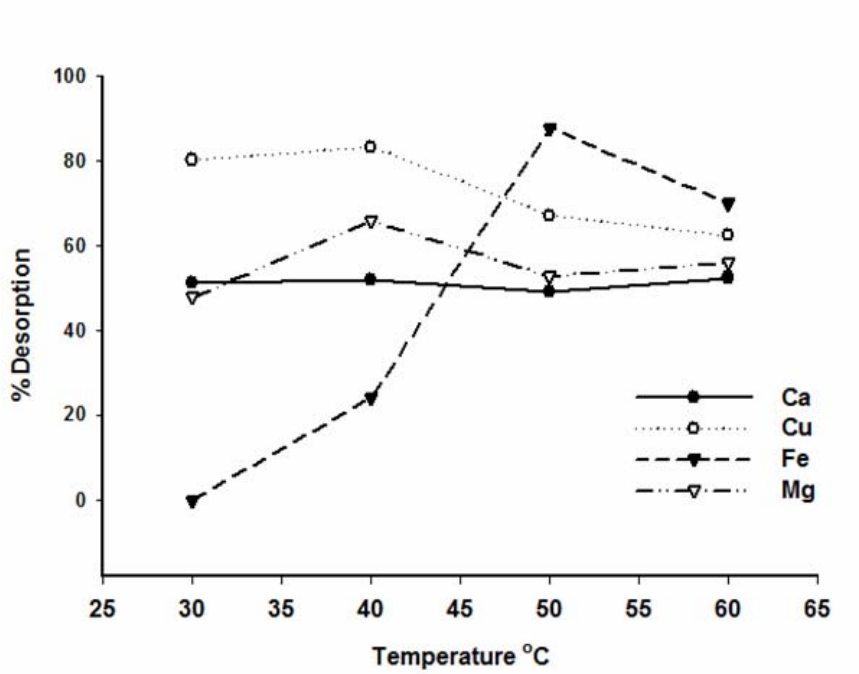

Figure 7. Metal desorption using acetylacetone as the extracting ligand at pH 6 over 30 min under varying temperatures.

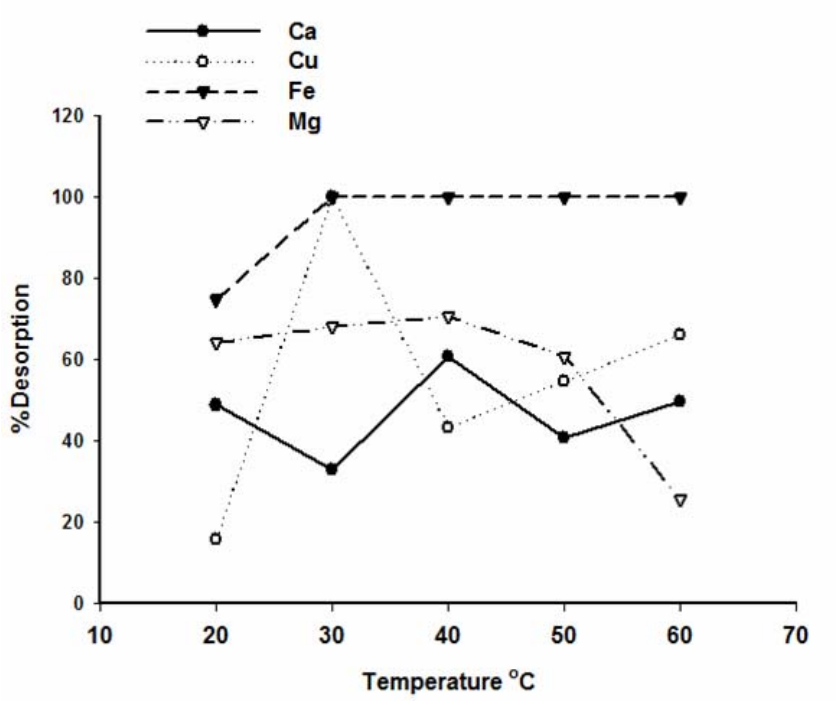

Figure 8. Metal desorption using acetylacetone as the extracting ligand at pH 8 over 30 min under varying temperatures.

Desorption isotherms

The degree of solute desorption from a material depends on the dynamic balance reached between the rate of solute desorption from the surface and the adsorption rate. If the desorption rate is greater than adsorption (due to the influence of a ligand in solution) then desorption takes preference (Kumar and Sivanesan 2006).

Portions (0.4, 0.6, 0.8, 1.0 & 1.2 g) of homogenized pulp were weighed into polyethylene bottles and batch extractions performed. The batch extractions were conducted under the established optimum desorption pH, equilibrium times and temperature. The generated data was fitted onto Langmuir (1918) and Freundlich (1926) equilibrium models. The R^2 values were computed from the linearaized isotherm model equations and the values used to determine the model that best described the desorption process (Table 2, 3, 4 & 5). Metal desorption under the influence of acetylacetone at both pH 6 and 8 were best described by Langmuir desorption model.

Table 2. Langmuir parameters for the desorption of Al, Cu, Fe, Mg, and Ca from pulp at pH 6 by EDTA and acetylacetone

	EDTA at pH 6			**Acetylacetone pH 6**		
n=15	$\mathbf{R^2}$	$\boldsymbol{b}$ $\boldsymbol{L.\mu mol^{-1}}$	$\boldsymbol{q_{max}}$ $\boldsymbol{\mu mol\ g^{-1}}$	$\mathbf{R^2}$	$\boldsymbol{b}$ $\boldsymbol{L.\mu mol^{-1}}$	$\boldsymbol{q_{max}}$ $\boldsymbol{\mu mol\ g^{-1}}$
Al	0.572	1.28	0.12	0.777	2.50	0.09
Cu	0.881	2.73	0.06	0.907	15.00	0.05
Fe	0.998	-1009.67	0.03	0.656	-308.64	0.03
Mg	0.937	1.97	0.27	0.991	-3.39	0.19
Ca	0.985	0.98	0.78	0.807	18.18	0.50

The desorption was performed at a temperature of 50 ºC; for a period of 50 and 30 minutes with EDTA and Acetylacetone respectively

The Langmuir model R^2 for Al (0.777) and Fe (0.656) under the influence of acetylacetone were however low at pH 6, but were still higher than those computed from

Freundlich model, 0.451 and 0.026 for Al and Fe respectively. Pulp metal desorption under the influence of EDTA was also best described by the Langmuir model except for Al (R^2) 0.572 and 0.004, pH 6 and 8 respectively. Langmuir isotherm model mainly describes a homogeneous monolayer chemical desorption/adsorption process (Perez *et al.,* 2007). This implies that most of the metals in the dissolving pulp sample were chemically adsorbed on the surface of the pulp. Aluminum was poorly described by the Langmuir isotherm model (Table 2 & 3). Polyvalent metals like Al are hard Lewis acids, capable of strong and specific bonding to hard Lewis base functional groups on organic molecules (Stevenson, 1994). The most important of such functional groups are carboxylic acid and phenolic OH groups (Pohlman and McColl, 1988; Tam and McColl, 1991).

Table 3. Langmuir parameters for the desorption of Al, Cu, Fe, Mg, and Ca from pulp at pH 8 by EDTA and acetylacetone

	EDTA at pH 8			**Acetylacetone pH 8**		
n=15	$\mathbf{R^2}$	$\boldsymbol{b}$ $\boldsymbol{L.\mu mol^{-1}}$	$\boldsymbol{q_{max}}$ $\boldsymbol{\mu mol\ g^{-1}}$	$\mathbf{R^2}$	$\boldsymbol{b}$ $\boldsymbol{L.\ \mu mol^{-1}}$	$\boldsymbol{q_{max}}$ $\boldsymbol{\mu mol\ g^{-1}}$
Al	0.004	0.05	1.29	0.951	4.33	0.08
Cu	0.914	3.13	0.06	0.938	5.12	0.06
Fe	0.839	7.68	0.04	0.898	-177.63	0.03
Mg	0.920	2.26	0.29	0.973	-5.88	0.17
Ca	0.870	0.55	0.82	0.838	1.99	0.35

The desorption was performed at a temperature of 30 ºC; for a period of 60 and 50 minutes with EDTA and Acetylacetone respectively

Metal desorption from pulp was more effective when using acetylacetone as opposed to EDTA (Table 2 & 3). The minimum amount of metal that remains in the pulp unextracted (q_{max}) was lower when using acetylacetone as a ligand as opposed to EDTA. The pH of the solution affects the surface charge of the pulp, the degree of ionization, and the speciation of the surface functional groups (Reddad *et al.* 2002). At pH 6 acetylacetone will predominantly exist in its tantomeric keto enol forms (Figure 2). At this pH the pulp would

be protonated thus acquire some positive surface charge, which results in electrostatic repulsion between the surface and the ligand (Reddad *et al.* 2002). Acetylacetone would experience less or no repulsion when the keto form approaches the pulp, while EDTA would experience some repulsion when approaching the pulp from the carboxylic end. Sohn and Lee (2000), reported the linking of acetylacetone to an exchangeable metal cation through a water bridge bonding as >C=O----H-O(H)-M^{n+}. The desorption of chemically adsorbed Al was highly affected by pH when using EDTA as the extracting ligand (Table 2 & 3). At pH 8 the data did not fit the Langmuir model (R^2 = 0.004). Al is a polyvalent element and it is strongly held on the pulp (Stevenson 1994), EDTA would need to approach at a close distance to extract Al. At pH 8 EDTA and the pulp are deprotonated and repel each other. It was also observed that the Freundlich model fitted metal desorption better at pH 8 (Table 5). The difference in the Freundlich model fit at pH 6 and 8 was more pronounced when using acetylacetone as the extracting ligand, Mg however was an exception. This is probably due to the presence of the acetylacetone anion at pH 8 (Figure 3) which makes it more receptive to metals. Acetylacetone in an aqueous mixture is polarized by pH. The polarization is a precursor of the formation of the acetonato ion which occurs after the abstraction of a proton by the OH^- ion. It is worthy to note that where metal desorption fitted the Freundlich model EDTA correlated better to the model than acetylacetone. In physical desorption metals are released from the pulp into the bulk solution. EDTA being a better ligand would be more efficient in the immobilization of the metals thus enhancing desorption.

Table 4. Freundlich parameters for the desorption of Al, Cu, Fe, Mg, and Ca from pulp at pH 6 by EDTA and acetylaceton

	EDTA at pH 6			Acetylacetone pH 6		
n=15	R^2	b_F	K_F ($\mu mole\ g^{-1}$)	R^2	b_F	K_F ($\mu mole\ g^{-1}$)
Al	0.342	0.34	0.07	0.451	0.29	0.06
Cu	0.319	-1.66	0.01	0.146	0.11	0.05
Fe	0.039	-0.01	0.03	0.026	-0.09	0.03
Mg	0.624	0.38	0.15	0.682	-0.12	0.24
Ca	0.454	0.15	0.50	0.002	0.02	0.42

The desorption was performed at a temperature of 50 ºC; for a period of 50 and 30 minutes with EDTA and Acetylacetone respectively

Table 5. Freundlich parameters for the desorption of Al, Cu, Fe, Mg, and Ca from pulp at pH 8 by EDTA and acetylaceton

	EDTA at pH 8			Acetylacetone pH 8		
n=15	R^2	b_F	K_F ($\mu mole\ g^{-1}$)	R^2	b_F	K_F ($\mu mole\ g^{-1}$)
Al	0.808	1.00	0.06	0.590	0.20	0.06
Cu	0.884	0.42	0.05	0.663	0.39	0.05
Fe	0.338	0.34	0.04	0.187	-0.13	0.03
Mg	0.119	0.07	0.24	0.082	-0.04	0.20
Ca	0.179	0.15	0.49	0.205	0.16	0.25

The desorption was performed at a temperature of 30 ºC; for a period of 60 and 50 minutes with EDTA and Acetylacetone respectively

The Freundlich model described Mg, Al and Cu desorption suggesting some fraction of these metals to have been physically adsorbed onto the pulp material (Table 4 & 5). It is possible that the metal fraction being physically desorbed was introduced onto the pulp during the pulp production process. Magnesium for instance is added in the pulp cooking process as MgO.

Desorption kinetics

The kinetic rates were estimated by Lagergren pseudo first order model and Ho's pseudo second order model. The data was fitted into the two models and the best fit determined by R^2. The data was found to be best described by the pseudo second order kinetic model. The obtained kinetic parameters (K_2) are presented in Table 6 & 7. The amount of metal desorbed at equilibrium (q_e) from a gram of pulp was determined experimentally (q_e *exp*) as well as calculated (q_e *cal*) from the pseudo second order model. The calculated and experimental q_e values were very close at pH 6 with EDTA and acetylacetone as extracting ligands. There was however some slight variance for Al and Ca (Table 6). The pseudo second order kinetic fit was in agreement with the equilibrium study on the mechanism of metal desorption. Langmuir describes chemical desorption and pseudo second order kinetic model also describes chemical desorption (Wu *et al.,* 2001). The extraction of Al, Cu and Fe at pH 8 with EDTA as the extracting ligand did not fit the pseudo second order kinetic model. The same was observed in the equilibrium desorption study where Al desorption at pH 8 did not fit the Langmuir isotherm model instead fitted the Freundlich desorption model.

Table 6. Pseudo 2nd order Kinetic parameters for the desorption of Al, Cu, Fe, Mg, and Ca from pulp at pH 6 by EDTA and acetylaceton; *K_2 values expressed in g.µmol^{-1} .min^{-1}

	EDTA at pH 6				**Acetylacetone pH 6**			
n=15	**R^2**	**q_e** *exp*	**q_e** *Cal*	***K_2**	**R^2**	**q_e** *exp*	**q_e** *Cal*	***K_2**
Al	0.760	0.073	0.068	2.63	0.958	0.186	0.171	2.42
Cu	0.840	0.034	0.037	3.68	0.921	0.025	0.029	8.46
Fe	1.000	0.033	0.033	-3E+15	0.879	0.064	0.060	80.06
Mg	0.991	0.250	0.246	13.20	0.814	0.054	0.053	2.78
Ca	0764	0.630	0.550	5.91	0.634	0.635	0.836	0.06

The kinetics were performed at a temperature of 50 ºC; over 10, 20, 30, 40, 50 and 60 minutes; *exp = experimental q_e; Cal =calculated q_e*

Table 7. Pseudo 2nd order Kinetic parameters for the desorption of Al, Cu, Fe, Mg, and Ca from pulp at pH 8 by EDTA and acetylacetone; $*K_2$ values expressed in $g.\mu mol^{-1}.min^{-1}$

	EDTA at pH 8				Acetylacetone pH 8			
n=15	**R^2**	***q_e exp***	***q_e Cal***	**$*K_2$**	**R^2**	***q_e exp***	***q_e Cal***	**$*K_2$**
Al	0.527	0.022	0.033	6.15	0.452	0.036	0.048	3.60
Cu	0.408	0.023	0.066	0.13	0.971	0.058	0.056	31.10
Fe	0.448	0.033	0.067	0.26	0.880	0.033	0.035	4.06
Mg	0.963	0.252	0.265	2.19	0.947	0.206	0.197	2.05
Ca	0.880	0.652	0.610	1.23	0.490	0.258	0.303	6.46

The kinetics were performed at a temperature of 30 ºC; over 10, 20, 30, 40, 50 and 60 minutes; *exp = experimental q_e; Cal =calculated q_e*

Activation energy

Rates of metal desorption at different temperatures (30, 40, 50 and 60) were determined from linearized pseudo 2nd order kinetic plots. The obtained rates of reactions were converted to natural logs and plotted against the reciprocal of temperature in Kelvin. And activation energy obtained according to the linerized Arrhenius equation. The Arrhenius parameters are reported in Table 8

Table 8. Arrhenius parameters for the desorption of Al, Cu, Fe, Mg, and Ca from pulp at pH 6 and 8 by acetylaceton

n=15	**Acetylacetone pH 6**		**Acetylacetone pH 8**	
	R^2	**E_a (kJ Moles^{-1})**	**R^2**	**E_a (kJ Moles^{-1})**
Al	0.169	34.0	_____	_____
Cu	0.431	-51.0	0.706	-81.7
Fe	0.669	52	0.713	85.0
Mg	0.418	19.6	0.878	-127.8
Ca	0.950	-32.2	0.409	-69.1

The kinetics were performed at a temperature of 30 ºC; over 10, 20, 30, 40, 50 and 60 minutes; *exp = experimental q_e; Cal =calculated q_e*

Some of the metals under study did not fit the Arrhenius model their R^2 values were < 0.5 (Table 8), however most metals had a better fit at pH 8. The activation energies (E_a) determined from the Arrhenius model were negative except for Al and Fe. Negative values of E_a indicate that lower temperature favour desorption of metals from pulp **(**Ibezim-Ezeani and Anusiem 2010). This was corroborated by Figures 7 and 8 except for Fe an increase in temperature resulted in reduced desorption efficiency. Reactions exhibiting negative activation energies are typically barrierless reactions, in which the reaction proceeding relies on the capture of the molecules in a potential well. Increasing the temperature leads to a reduced probability of the colliding molecules capturing one another. With more glancing collisions not leading to reaction as the higher momentum carries the colliding particles out of the potential well. Chemically adsorbed metals are immobililized in specific sites where the ligand is required to capture them. Depending on the thermodynamics of desorption above the optimum temperature would lead to reduced desorption. Polyvalent metals like Fe and Al are hard Lewis acids, capable of strong and specific bonding to hard Lewis base functional groups on organic molecules (Stevenson, 1994). These metals required positive activation energies in their desorption from pulp probably due to the formation of strong bonds with functional groups in the pulp material.

Quality control

Analytical data quality was verified by digesting cellulose cotton (IAEA-V-9) Standard Reference Material; the results are presented in Table 9. The analysed values were within agreeable limits to those of the standard reference material. The purity of the pulp after extraction was checked for structural modification or traces of acetylacetone and EDTA (Figure 9 & 10). This was done with the aid of Fourier transform Infrared-attenuated total reflectance (FTIR-ATR; Perkin Elmer Spectrum 100) and CP/MAS ^{13}C-NMR spectra recorded (at 290±1°K) on a Bruker Avance III 600 WB instrument. The FTIR and ^{13}C NMR spectra for the treated pulp was superimposed on the blank showing no observable difference between the blank, (which was the pulp material before treatment) and the pulp treated with EDTA or acetylacetone (Figure 9).

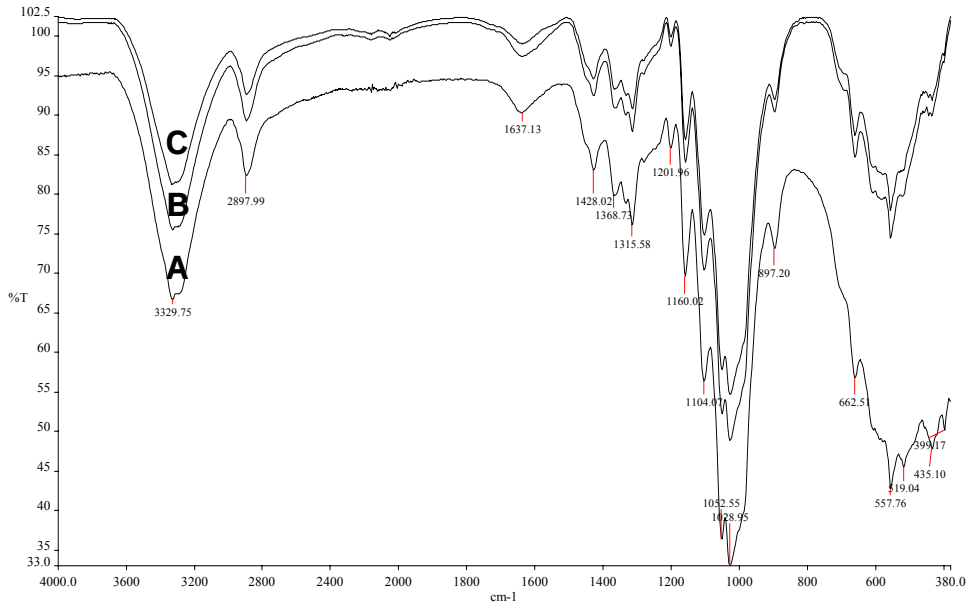

Figure 9. IR spectra of unextracted pulp (A), pulp extracted with acetylacetone (B) and pulp extracted with EDTA (C)

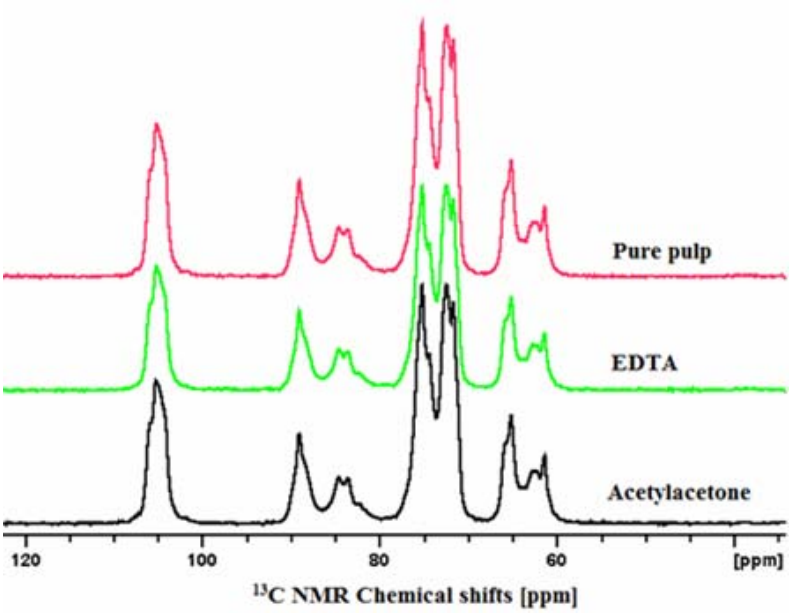

Figure 10. ^{13}C NMR spectra of unextracted pulp (pure pulp), pulp extracted with acetylacetone and pulp extracted with EDTA.

Table 9. Analysed trace elements in IAEA–V-9 cellulose cotton reference material compared to the recommended values.

Eelement	Reference material IAEA-V-9	95% Confidence Interval	Analysis n=3
Al	44	13 - 53	37.8 ± 2.3
Ca	240	220 - 260	222 ± 1.5
Cu	0.59	0.47 – 0.94	1.04 ± 0.05
Fe	11	7 - 15	11.6 ± 0.32
Mg	53	46 - 67	45.5 ± 1.2
Pb	0.25	0.22 – 0.33	0.39 ± 0.1

Note: ± = Standard deviation

CONCLUSIONS

The structural characteristics of acetylacetone endear it to desorption of chemically adsorbed metals from pulp. Acetylacetone performs better than EDTA in desorption of chemically adsorbed metals. The keto enol form participates in the extraction of metals from pulp at low pH, while the resonance stabilized anion participates in the extraction of metals from pulp at high pH. The interaction of the extracting ligand with the surface charge on the pulp influences the metal desorption efficiency depending on the ligand structural characteristic. EDTA is a better ligand for the extraction of physically adsorbed metals. However a large fraction of the residual metals in dissolving pulp is mainly chemically adsorbed on the pulp while a small fraction is physically adsorbed. Desorption of physically adsorbed metals is enhanced by high pH. Polyvalent elements like Al and Fe require higher energy to be desorbed from pulp.

REFERENCES

Agarwal, G. S., H. K. Bhuptawat, and Chaudhari, S. 2006. Biosorption of aqueous chromium(VI) by *Tamarindus indica* seeds, *Bioresource Technology*. 97:949–956.

Ager, P., and W. D. Marshall. . 2001. An approach to complexant recycling in softwood pulping. *Can. J. Anal. Sci. Spectros*. 46: 162-169.

Allard, A., L. Renberg, and A. Neilson. 1996. Absence of $^{14}CO_2$evolution from ^{14}C -labeled EDTA and DTPA and the sediment/water partition ratio. *Chemosphere*. 33: 577-583.

Arrhenius, S. 1889. "On the Reaction Velocity of the Inversion of Cane Sugar by Acids," Zeitschrift für physikalische Chemie. 4: 226.

Barrow G. 1964. Fisicoquimica, *Editorial Reverte* 686-705

Bernhard, M., J. Muller, and T. P. Knepper. 2006. Biodegradation of persistent polarpollutants in wastewater: comparison of an optimised lab-scale membrane bioreactor and activated sludge treatment. *Water Res.* 40: 3419–3428.

Bolton, Jr.H., S. Li, D. Workman, and D. Girvin. 1993. Biodegradation of synthetic chelates in subsurface sediments from the southeast coastal plain. J. *Environ. Qual*. 22: 125-132

Chaudary, A., J. Donaldson, S. Grimes, M. Hassan, and R. Spencer. 2000. Simultaneous recovery of heavy metals and degradation organic species–copper and ethylenediaminetetracetic acid (EDTA). *J. Chem. Technol. Biotechnol*. 75: 353-358.

Chong, K. H., and B. Volesky. 1995. Description of two-metal biosorption equilibria by Langmuir-type models. *Biotechnol. Bioeng*. 47: 451–460.

Chong, K. H., and B. Volesky. 1995. Description of 2-metal biosorption equilibria by Langmuir-type models. *Biotech. and Bioeng*., , 47(4): 451-460.

Deng, L. Su, Y. Su, H. Wang, X. Zhu, X. 2007. Sorption and desorption of lead (II)from wastewater by green algae *Cladophora fascicularis*, *J. Hazard. Mat.* 143: 220–225.

ECB European Chemical Bureau. 2004. European Union Risk Assessment Report 51, Tetrasodium Ethylenediaminetetraacetate. .160.

Fay, D. P., R. Ambrose, Nichols Jr, and K. Sutin. 1971. The Kinetics and Mechanisms of the Reactions of Iron (II1) with p-Diketones. The Formation of Monoacetylacetonatoiron (II1) and the Effect of Copper (II) on the Formation of Mono thenoyl trifluoroacetonatoiron (I1I). *Inorg. Chem.10 (10):* 2096–2101

Freitas, P. A. M., K. Iha, M.C.F.C. Felinto, and M. E. V. Suárez-Iha. 2008. Adsorption of di-2-pyridyl ketone salicyloylhydrazone on Amberlite XAD-2 and XAD-7 resins: Characteristics and isotherms. *J. Colloid Interface Sci*. 323: 1–5

Freundlich , H. 1906. Adsorption in solution. *Phys. Chem. Soc.* 40: 1361–1368.

Freundlich, H., and W. Heller. 1939. On Adsorption in solution. *J. Amer. Chem. Soc*., 61: 2228

Fuerhacker, M., G. Lorbeer, and R. Harberl 2003. Emission factors and sources of diamine tetraacetic acid in waste water- a case study. *Chemosphere*. 52: 253-257.

Green-Ruiz, C., V., Rodriguez-Tirado, and B. Gomez-Gil. 2008. Cadmium and zinc removal from aqueous solutions by *Bacillus jeotgali*: pH, salinity and temperature effects. *Bioresource Tech.* 99: 3864–3870.

Hinck, M., J. Ferguson, and J. Puhaakka. 1997. Resistance of EDTA and DTPA to aerobic biodegradation. *Water Sci.Technol*. 35: 25-31.

Ho Y. S., and G Mckay. 1998. A comparison of Chemisorption Kinetic, Models Applied to Pollutant Removal On various Sorbents. *Trans. Inst. Chem. Eng*. 76b: 332-340.

Ho Y. S., and G. McKay. 2000. The kinetics of sorption of divalent metal ions onto sphagnum moss peat. *Water Res*. 34: 735-742.

Ibezim-Ezeani, M. U., and A. C. I. Anusiem. 2010. Kinetic studies of adsorption of palmitate and laurate soaps onto some metal ores in aqueous media *Int. J. Phys. Sci.* 5 (01): 62-67.

IPPC (Integrated Pollution Prevention and Control). 2001. Removal of chelating agents by modest alkaline biological treatment or by use of kidneys. *Reference Document on Best Available Techniques in the Pulp and Paper Industry.* p117

Javed, M. A. H. N. Bhatti, M. A. Hanif, and R. Nadeem. 2007. Kinetic, Equilibrium modeling of Pb(II) and Co(II) sorption onto rose waste biomass, Separation. *Sci.Technol*. 42:3641–3656.

Jones, P.W., D.R. Williams. 2001. Chemical speciation simulation used to assess [S,S0]-ethylenediaminedisuccinic acid (EDDS) as a readilybiodegradable replacement for EDTA in radiochemical decontamination formulations. *Appl. Radiat. Isotopes* 54: 587–593.

Kamau, J. N., J. C.,Ngila, A. Kindness, and T. Bush. 2011. Equilibrium and Kinetic Studies for Extracting Cu, Mn and Fe from Pulp Wastewater onto a C-18 Column with Acetylacetone Complexing Ligand. *Anal. Lett*. 44:1891–1906.

Kawagoshi, Y., and M. Fujita. 1998. Purification and properties of the polyvinyl alcohol degrading enzyme 2,4-pentanedione hydrolase obtained from *Pseudomonas vescularis* var. *povalyticus* PH. *World J. Microbiol. Biotechnol*. *14*:95-100.

Kumar, K V., and S. Sivanesan. (2006) Equilibrium data, isotherm parameters and process design for partial and complete isotherm of methylene blue onto activated carbon. *J.Hazard. Mat.* 134: 237-244

Larisch, B. and S. Duff. 2000. Effect of DTPA and EDTA on activated sludge reactors treating bleached kraft mill effluent. *Tappi J.* 83: 163-17.

Mutis A., J. Freer, J. Baeza, H. Mansilla, and J. Rodríguez. 1998. Influence of EDTA and DTPA on the activated sludge treatment of a synthetic TCF effluent. In: 7th International conference on Biotechnology in the pulp and paper industry. *Vancouver, Proceedings* C, 235-237.

Nakanishi, H. N., H. Morita, and S. Nagakura. 1977. electronic structures and spectra of the Keto and Enol forms of acetylacetone. *Bull. Chem. Soc. Jap*. 50(9): 2255-2261

Ng, J. C. Y., W. H. Cheung, and G. McKay. 2003. Equilibrium studies for the sorption of lead from effluents using chitosan. *Chemosphere* 52: 1021-1030.

Pauling, L. 1932. "The Nature of the Chemical Bond. IV. The Energy of Single Bonds and the Relative Electronegativity of Atoms". *J. American Chem. Soci*ety 54 (9): 3570–3582.

Pearson, R. G., and O. P. Anderson. 1970. Rates and Mechanism of Formation of Mono(acetylacetonato)copper(II) Ion in Water and Methanol http://pubs.acs.org/

Perez, N., M. Sanchez, G. Rincon, and L. Delgado. 2007. Study of the behavior of metal adsorption in acid solution on lignin using a comparison of different adsorption isotherms. *Latin Ame. App. Res*. 37: 157-162.

Pietsch, J., W. Schmidt, F. Sacher, S. Fichtner, and H. Brauch. 1995. Pesticides and another organic micropollutants in the river Elbe. Fresenius *J. Anal. Chem.* 353: 75-82

Pitter, P., and V. Sýkora. 2001. Biodegradability of ethylene diamine-based complexing agents and related compounds. *Chemosphere*. 44: 823-826.

Pohlman, A. A., J. G. McColl. 1988. Soluble organics from forest litter and their role in metal dissolution. *Soil Sci. Soc. Am. J*. 52: 265–271.

Reddad, Z., C. Ge´rente, Y. Andre`s, and P. Le Cloirec. 2002. Adsorption of Several Metal Ions onto a Low-Cost Biosorbent: Kinetic and Equilibrium Studies *Environ. Sci. Technol*. 36: 2067-2073

Sakai, K., N. Hamada, and Y. Watanabe. 1986. Degradation mechanism of poly(vinyl alcohol) by successive reaction of secondary alcohol oxidase and b-diketone hydrolase from *Pseudomonas* sp. *Agric. Biol. Chem*. 50: 989-996

Schaefer, W. P., and M. E. Mathisen. 1965. Stability Constants of the Acetylacetone-Chromium(l1) Complexes. *Inorg. Chem*. 4(3): 431-433

Schwedt, G. 1979. *Chromatographia.* 12: 289.

Sillanpää, M. 1997. .Environmental fate of EDTA and DTPA. *Rev. Environ. Contam. Toxicol.*152: 85-111.

Sohn, J. R., and S. Lee. 2000. Adsorption Study of Acetylacetone on Cation-Exchanged Montmorillonite by Infrared Spectroscopy. *Langmuir*.16: 5024-5028.

Stevenson, F. J. 1994. *Humus Chemistry: Genesis, Composition, Reactions*. Wiley, New York. 496 pp.

Straganz, G. D., A. Glieder, L. Brecker, D. W. Ribbons. and W. Steiner. 2003. Acetylacetone-cleaving enzyme Dke1: a novel C–C-bond-cleaving enzyme from Acinetobacter johnsonii. *Biochem. J*. 369: 573-581

Sykora, V., P. Pitter, I. Bittnerova, T. Lederer. 2001. Biodegradability of ethylenediamine based complexing agents. *Water Res*. 35(8): 2010–2016.

Takahashi, R., N. Fujimoto, S. Masaharu, and T. Endo. 1997. Biodegradabilities of ethylenediamine-N,N'-disuccinic acid (EDDS) and other chelating agents. Biosci. Biotechnol. *Biochem.*61: 1957-1959.

Tam, S. H., J. G. McColl. 1991. Aluminum-binding ability of soluble organics in Douglas fir litter and soil. *Soil Sci. Soc. Am. J*. 55: 1421–1427.

Vilar, V. J. P., Botelho, C. M. S. Boaventura, R. A. R. 2008. Copper removal by algae *Gelidium,* agar extraction algal waste and granulated algal waste: kinetics and equilibrium, Bioresource Technol. 99: 750–762.

Virtapohja, J. 1998. .Determination of chelating agents (EDTA and DTPA) in bleach liquors. *Pulp Pap. Can*. 99: 330-332.

Wang, X., S. Xia, L. Chen, J. Zhao, J. Chovelon, and J. Nicole. 2006. Biosorption of cadmium(I1) and lead(I1) ions from aqueous solutions onto dried activated sludge, *J.Environ.Sci*. 18: 840–844.

Williams, D. 1998. Storing up trouble? *Chem. Br.* 1: 48-52.

Wu, F.C., R. L. Tseng, and R.S. Juang. 2001. Kinetics modelling of liquid-phase reactive dyes and metal ions on chitosan, *Water Res.* 35,. 613-618

CHAPTER 6: PAPER V

EQULIBRIUM AND KINETIC STUDIES FOR EXTRACTING Cu, Mn AND Fe FROM PULP WASTEWATER ONTO A C-18 COLUMN WITH ACETYLACETONE

Joseph Nyingi Kamau[1], Jane Catherine Ngila[1,3], Andrew Kindness [1] and Tamara Bush[1,2]

[1]University of Kwazulu-Natal, School of Chemistry, Westville Durban, South Africa.

[2]CSIR, Natural Resources and the Environment, Forestry and Forest Products Research Centre, Durban, South Africa.

[3]University of Johannesburg, Doornfontein Campus P.O. Box 17011, Doornfontein 2028, South Africa

ABSTRACT

A preconcentration procedure using solid phase extraction of heavy metals in pulp wastewater is reported. The procedure was optimized by using model solutions of selected heavy metals to investigate the effect of matrix constituents. Equilibrium studies highlighted the bonding and adsorption characteristics. The metal recoveries after spiking pulp waste filtrate with Cu, Ni and Pb each at 0.1 and 0.2 ppm was 120, 91 and 93 %, respectively. The Freundlich adsorption isotherms with correlation coefficients (R^2) 0.612, 0.810 and 0.750, showed a better fit compared to Langmuir isotherm values of 0.277, 0.389 and 0.272 for Cu, Mn and Fe, respectively.

Keywords: Solid Phase Extraction, Acetylacetone, Langmuir and Freundlich Isotherms, Metals, Pulp wastewater.

INTRODUCTION

The direct and accurate determination of trace elements in complex liquid matrices with most instrumental techniques is difficult due to the low concentration of analytes as well as interferences caused by sample matrices. Analysis of trace metal ions in saline matrices using inductively coupled plasma-atomic emission spectrometry (ICP-AES) has several problems because the aspiration of solutions with high salt concentrations into plasma systems leads to nebulizer blockage, considerable background emission, transport and chemical interferences, with a consequent drop in sensitivity and precision (Boumans 1987; Bekjarov *et al*. 1989; Montaser and Golightly 1990; Budic and Hudnik 1994).

In order to solve the problem of matrix interference and trace metal levels, sample clean-up and preconcentration is inevitable. Solid phase extraction is one of the most effective multi-element analyte-matrix separation and preconcentration method because of its simplicity, rapidity and ability to attain a high concentration factor (Dogan *et al*. 1997; Seren *et al*. 2001; Soylak 2001; Killian and Pryznska 2002). The method's ability to eliminate sample matrix makes it attractive for the analysis of liquid samples with complex matrices.

In the present work a novel analytical procedure for the SPE extraction/preconcentration of metals in pulp wastewater matrices and saline environmental water samples prior to their determination by inductively coupled plasma-atomic emission spectrometry (ICP-OES), has been developed. The extraction/preconcentration is based on the chelation of metals with acetylacetone prior to adsorption onto a C-18 column. Though acetylacetone is known to form stable metal complexes (Schaefer and Mathisen 1965) it has not been employed as a complexing agent in solid phase extraction systems.

EXPERIMENT

Reagents

All solutions were prepared in milli-Q water of resistivity 18.2 Ω cm^{-1}; and the reagents were of analytical grade, unless otherwise specified. Calibration standards were prepared from Fluka TraceCert 10 ppm multi-element stock standard. Nitric acid was TraceSelect ICP grade >69% supplied by Fluka. Solid phase extraction (SPE) materials employed in the study were XAD-1180, XAD-2 and Supelclean LC-18 cartridges (1.0 g), all supplied by Supelco, Bellefonte, USA. The SPE material specifications include; C-18 surface area 496 m^2/g (BET Method), average particle size 56.2 μm and average pore diameter of 71 angstroms; XAD-

1180 with surface area 500 m^2/g, mesh size 20-60 μm and average pore diameter 300 angstroms; XAD-2 with surface area of 300 m^2g^{-1}, mesh size 20-60 μm and average pore diameter 90 angstroms. Sea water reference material NASS-5 obtained from the National Research Council of Canada was used to test the method accuracy.

Preconcentration Procedure

The proposed analytical method was tested on 0.2 ppm model solutions comprising either a mixture of metals or just Cu, depending on the parameter being investigated. Five milliliter of appropriate buffer solution (pH 2 to 10) was added to 30-40 mL of model solution containing 6- 36 μg of metal ions. Acetylacetone (0.4 ml of 1.0 mM) was added to the buffered model solution and allowed to stand for ten minutes. The solid phase extraction column was conditioned with 5 mL of methanol flushed with 5 mL milli-Q water. This was followed by washing with 5 mL of 0.5 M HNO_3 in acetone and flushed with 20 mL Milli-Q water, followed by 5 mL of 1 M NaOH, again flushed with 20 mL Milli-Q water and finally conditioned with 10 mL of appropriate buffer. The conditioning process introduces a thin film of water-miscible solvent on the packing which promotes better contact between an aqueous sample matrix and the hydrophobic solid phase. The process also removes possible impurities initially contained in the sorbent or the packaging and removes the air pockets present in the column, filling the void volume with solvent. The model solution was then run through the preconditioned solid phase column under vacuum (in a VacMaster vacuum manifold) at a flow rate of 3 mL min^{-1}. Thereafter the metal ions were eluted with 5 mL of 0.5 M HNO_3 (TraceSelect ICP grade >69% supplied by Fluka) and the retained solutes collected for analysis by ICP-OES. All preconcentrations and extractions were performed in a 'clean room'.

Influences of pH on Sorption

Solid phase materials namely XAD-1180, XAD-7 and C-18 were employed in the experiment to determine the optimum extraction pH. The C-18 cartridges were factory packed in quantities of 1.0 g in 6 mL polyethylene tubes. While XAD 1180 and XAD 7 were packed in the laboratory, the resin material (600 mg) was weighed in a beaker and suspended in methanol for about 10 min. The methanol was decanted and thereafter water added onto the resin and the contents poured into 6 mL polyethylene tubes and allowed to settle. Two frits were inserted one before pouring the resin and the other after the resin had settled. Metal

impurities were removed by flushing through the column with 5 ml of 0.5 M HNO_3 in acetone and then rinsing with 20 mL of milli-Q water, followed by 5 ml of 1 M NaOH. The system was then rinsed with 20 ml of milli-Q water and flushed with the appropriate buffer.

A model solution comprising 0.2 ppm of Cd, Cu, Cr, Fe Mn, Pb and Si was prepared in milli-Q water. Portions of 30 ml metal solution were dispensed into 100 mL polyethylene sample bottles and then 0.4 ml of 1.0 mM acetylacetone was added. The solution was then adjusted to the appropriate pH ranging 2-10, using various buffer systems. Phosphate buffer solution was prepared by mixing 0.1 M sodium dihydrogen phosphate (Sigma-Aldrich) solution with an appropriate amount of phosphoric acid to make up pH 2 and adding an appropriate amount of 1 M NaOH solution to obtain pH 7. Acetate buffer solutions were prepared by mixing 0.1 M sodium acetate solution with an appropriate amount of acetic acid to achieve either pH 4, 5 or 6. Ammonium chloride buffer was prepared by mixing 0.1 M ammonium chloride with an appropriate amount of NH_4OH to obtain pH 8, 9 or 10.

The buffer solution (10 mL of the appropriate pH) was passed through the column and thereafter 30 ml of the model metal solution loaded in the column, at a flow rate of about 3 ml per minute. The column was then washed with the appropriate buffer and the adsorbed metal eluted with 5ml of 0.5 M HNO_3 at a flow rate of about 3 ml per minute. The column was reactivated by washing with 20 ml of milli-Q water and 10 ml of the appropriate buffer solution and was ready for reuse. Care was taken not to allow the solid sorbent to dry in between the conditioning and the sample treatment steps. If this happened, it would induce channeling phenomena due to expansion and contraction of the stationary phase.

Influence of Acetylacetone on Metal Recovery

Acetylacetone (1.0 mM) was added in varying volumes (Figure 1) to 30 mL of 0.2 ppm Cu model solution at pH 6. The mixture was allowed to stand for 10 minutes and thereafter run through a C-18 column at a flow rate of 3 mL min^{-1}. The retained Cu was stripped by passing 5 mL of 0.5 M HNO_3 (TraceSelect ICP grade >69% supplied by Fluka) through the column and eluent collected in 15 mL polyethylene vials for analysis by ICP-OES.

Effect of Sample Volume

Acetylacetone (0.5 mL of 1.0 mM) was added to 30 mL of 0.2 ppm model solution at pH 6. The volumes of the model solutions were varied between 10 mL to 150 mL and run through solid phase extraction column at a rate of 3 mL min^{-1}. The retained Cu^{2+} was stripped by

passing 5 mL of 0.5 M HNO_3 through the column and collected in 15 mL polyethylene vials for analysis by ICP-OES.

Effect of Sample Matrix

The recovery of analyte ions in the presence of selected alkaline and alkaline earth metals was investigated by adding known concentrations of either Ca^{2+}, Mg^{2+} or Na^{+} ions to a model solution containing 0.2 ppm of both Cu^{2+} and Fe^{3+}. The mixture was adjusted to pH 8 with an ammonium buffer and ran through a C-18 solid phase extraction column after the addition of 0.4 mL acetylacetone.

Procedure for Standard Reference Material

Sea water reference material NASS-5 (60 mL), from the National Research Council of Canada was spiked with 0.5 mL of acetylacetone and run through a C-18 SPE column. The spiked sea water reference material was preconcentrated without adjusting their pH. The SPE column was however conditioned with 10 mL of 0.1 M pH 8 ammonium buffer before loading and thereafter cleaned with 5 mL of the ammonium buffer before stripping.

Application of Proposed Method on Pulp Filtrate

The pulp filtrate (2 mL) was made up to 40 mL with milli-Q water and dispensed into a 100 mL polyethelene bottle. The metals in the sample were then extracted / preconcentrated and analysed as discussed under the ‘Preconcentration Procedure’.

Equilibrium Isotherm Models

Background theory

An isotherm describes the relationship between the amount of metal adsorbed and metal ion concentration remaining in solution as the metal concentration in two phases influence the kinetics of metal adsorption. Langmuir and Freundlich are among the most common isotherms describing this type of adsorption system. Langmuir (first studied in 1918) is the most important model for a monolayer adsorption. It is based on the assumption that adsorption can only occur at a fixed number of definite localized sites whereby each site can hold only one adsorbate molecule (monolayer), all sites being equivalent with no interaction

between adsorbed molecules, even on adjacent sites. The Langmuir isotherm can be derived from the Gibbs approach (Yang 1987) according to Ng *et al*. (2003) as shown in Equation 1:

$$q_e = \frac{K_L C_e}{1 + a_L C_e} \tag{1}$$

Where q_e is the amount of metal adsorbed on a gram of adsorbent and C_e is the metal concentration of the solution at equilibrium. The constants K_L and a_L are the characteristics of the Langmuir equation and can be determined from a linearized form of the above equation, represented by Equation 2:

$$\frac{C_e}{q_e} = \frac{a_L}{K_L} C_e + \frac{1}{K_L} \tag{2}$$

A plot of C_e/q_e versus C_e gives a straight line with a slope of a_L/K_L and an intercept of $1/K_L$. The constant K_L is the equilibrium constant and the ratio a_L/K_L gives the theoretical monolayer saturation capacity (Ng *et al*. 2003)

Freundlich isotherm (Freundlich 1906) is the most important multi-site adsorption isotherm, widely applied in heterogeneous systems especially of organic compounds and highly interactive species on activated carbon and molecular sieves. But it does not obey Henry's Law, Equation 3, at low concentrations (Ng *et al*., 2003):

$$q_e = K_F C_e^{bF} \tag{3}$$

The linearized form of Equation 3 is obtained by taking logarithms where the parameters K_F and b_F can then be obtained from a plot of ln q_e versus ln C_e (Equation 4)

$$\ln q_e = b_F \ln C_e + \ln K_F \tag{4}$$

Where q_e and C_e have the same meaning as in Equation 1; K_F and b_F stand for Freundlich isotherm constant, ($dm^3\ g^{-1}$) and Freundlich isotherm exponent constant, respectively.

Procedure for adsorption studies

Dynamic flow adsorption experiments were conducted at 25 $^{\circ}$C on factory packed C-18 solid phase columns (1.0 g). The equilibration was considered to occur at a loading flow rate of 3

mL min^{-1}, determined by monitoring flow rate and the point of maximum adsorption. Model solutions (30 mL) adjusted to pH 8, comprising Cu, Fe and Mn acetylacetone (1.0 mM) complexes of varying concentrations (0.2 ppm to 3.2 ppm), were loaded onto C-18 columns. The adsorbed metal in the acetylacetone complex was stripped from the C-18 column by eluting with 5 mL of 0.5 M HNO_3 and thereafter analysed by ICP-OES.

The amount of the metal adsorbed (mg) per unit mass of adsorbent, q_e, was obtained by using equation 5:

$$q_e = \frac{C_a V}{m} \tag{5}$$

Where C_a in μM is the concentration of the retained metal after acid stripping, m is the dry mass of biosorbent in grams, and V is volume of solution in liters.

RESULTS AND DISCUSSION

pH influence on acetylacetone metal complex formation

In solid phase extraction studies of heavy metal ions based on chelation, the pH of aqueous solutions is one of the main factors influencing the quantitative recoveries of the analytes (Korn *et al.* 2006; Gustavo *et al*. 2004; Gilli *et al*. 1989; Yoon *et al*. 1999; Tateki *et al*. 1999; Xu *et al*. 2004; Pearson and Anderson 1970). Environmental samples comprise of complex matrixes depending on the sample type and sediment biogeochemistry. Physicochemical parameters influence the speciation and mobility of metal ions, a change in solution pH would influence the speciation of a metal ion. For pollution and speciation studies, it is important that the physicochemical parameters are maintained to simulate *in- situ* conditions.

The results obtained in the investigation of the influence of pH on metal preconcentration show Cu to be quantitatively recovered over a wide pH range 6-10 (see Figure 1) as opposed to the other metals under study. The solid phase material is shown to have an influence on the recovery of metal ions; the less polar the solid phase, the more efficient the retention (see Figure 1). Amberlite XAD-7 is a polyacrylic acid ester polymer resin having hydrophilic sites of intermediate polarity (Horwitz et al. 1992; Compano et al. 1994; Lin *et al*. 2007; Tewari and Singh 2000; Korn *et al*. 2004). Amberlite XAD-1180 is a polystyrene divinylbenzene copolymer and is a nonionic polymeric adsorbent (Soylak *et al*. 2003a). The C-18 column used in this work is an octadecyl chain bonded monomerically onto

a silica gel base material, with strong hydrophobicity used to adsorb analytes of even weak hydrophobicity from aqueous solutions.

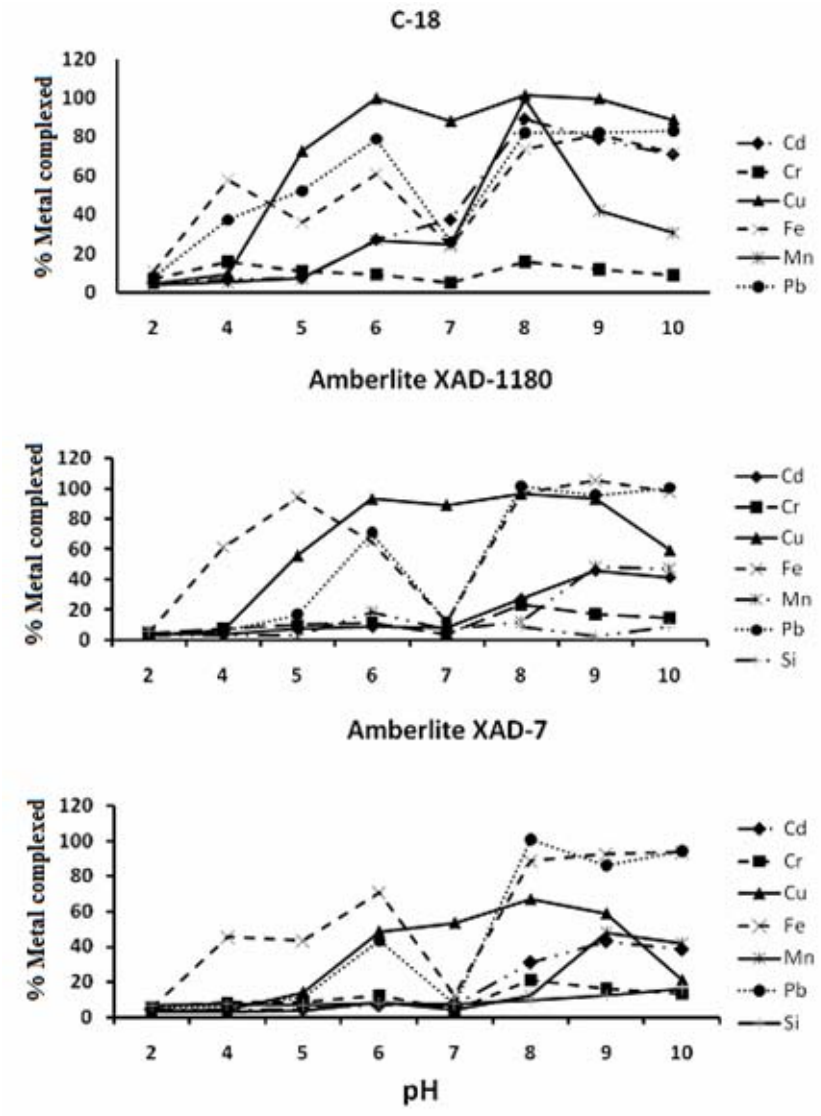

Figure 1**.** Effect of pH on % recovery of metal (Cd, Cr, Cu, Fe, Mn and Pb) as acetylacetone complexes, adsorbed onto different SPE material (C-18, XAD-1180 and XAD-7).

Acetylacetone abbreviated as Hacac, exists in three forms in aqueous solution; the tautomeric keto (I) and enol (II) forms, and the anionic form (III) as shown in Figure 2. The latter scheme is the common product of dissociation of either protonated tautomer (Pearson and Anderson 1970; Fay *et al*. 1971). The enol form is characterized by an internal hydrogen bond which forms a stable six-membered ring and is the predominant species at room

temperature (Fay *et al*. 1971; Pearson and Anderson 1970). Hydrogen bonding in the enol reduces the steric repulsion between the carbonyl groups.

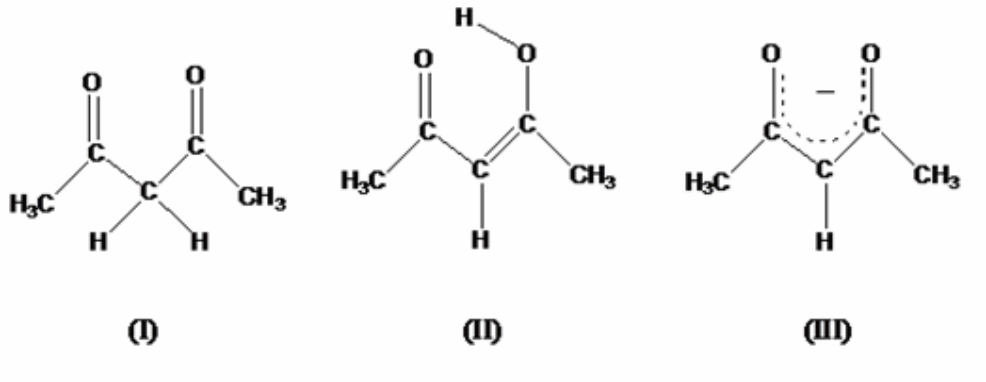

Figure 2. The Keto (I) enol (II) tantomeric structures of acetylacetone and its anion (II)

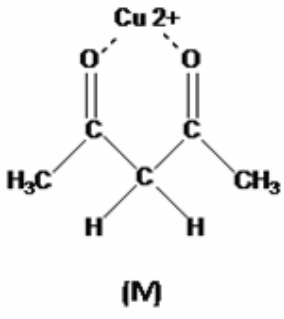

Figure 3. The intermediate complex in the formation of the copper acetonato complex

It has been proposed that the first step in the reaction between copper (II) and the keto tautomer of acetylacetone in an acidic media, involves the formation of a symmetrical precursor complex in which the metal ion is bonded to both keto groups similar to that shown in (IV) (Figure 3). In this mechanism the cupric ion acts as a electron sink and the rate determining step involves a slow, metal ion catalyzed proton release (Pearson and Anderson 1970). This rate determining step is influenced by the electronegativity of the metal ion. A higher value enhances its ability to act as a electron sink. The electronegativities (EN) and

electronegativity differences, ΔEN of the metals under study are listed in Table 1. A higher % analyte recovery corresponded with a low ΔEN of analyte and oxygen. Oxygen donor atoms have a weaker effect on the ligand field stabilization resulting in less electron transfer capability from the ligand to the metal, and a weaker covalent bond as reported by Imura and Suzuki (1985); Sohn and Lee (2000), indicated that cations of higher polarizing power are able to interact more effectively with the oxygen of the carbonyl group in the acetylacetone molecule. Acetylacetone pK_a is 8.95 (Pearson and Dillon 1953) and thus at higher pH the solvent abstracts the acidic proton and the resonance stabilized structure (III) is formed that readily combines with the metals in solution (Figure 2).

Table 1**.** The metal electronegativities (EN), electronegativity difference (ΔEN) of the metal and oxygen and % recovery; recovery performed at pH 6 (slightly acidic).

Metal	Electronegatiovity	% Metal complexed	Δ-Electronegativity (EN)
Cu	1.90	100 ± 0.02	1.54
Fe	1.83	61 ± 12.0	1.61
Pb	2.33	96 ± 0.4	1.11
Mn	1.55	27 ± 0.5	1.89
Cr	1.66	9 ± 1.4	1.78
Cd	1.69	27 ± 0.3	1.75

Δ EN = Oxygen elecronegativity – Metal electronegativity; Electronegativity values quoted from Pauling (1932); *n=3*.

Influence of Acetylacetone on Recovery

The amount of acetylacetone required to optimally extract metal ions in solution was determined by varying the volume of 1.0 mM acetylacetone that was added to 30 mL of 0.2 ppm Cu model solution. The acetylacetone sample mixture was preconcentrated onto a C-18 column and analyzed by ICP-OES. From the results reported in Figure 2, 0.4 mL of 1.0 x 10^{-3} M acetylacetone was chosen as the appropriate volume for a 30 mL model solution. There

was no significant difference (based on ANOVA statistical test, n = 3; p = 0.05) in the extraction efficiency between addition of 0.1 mL and 2 mL acetylacetone.

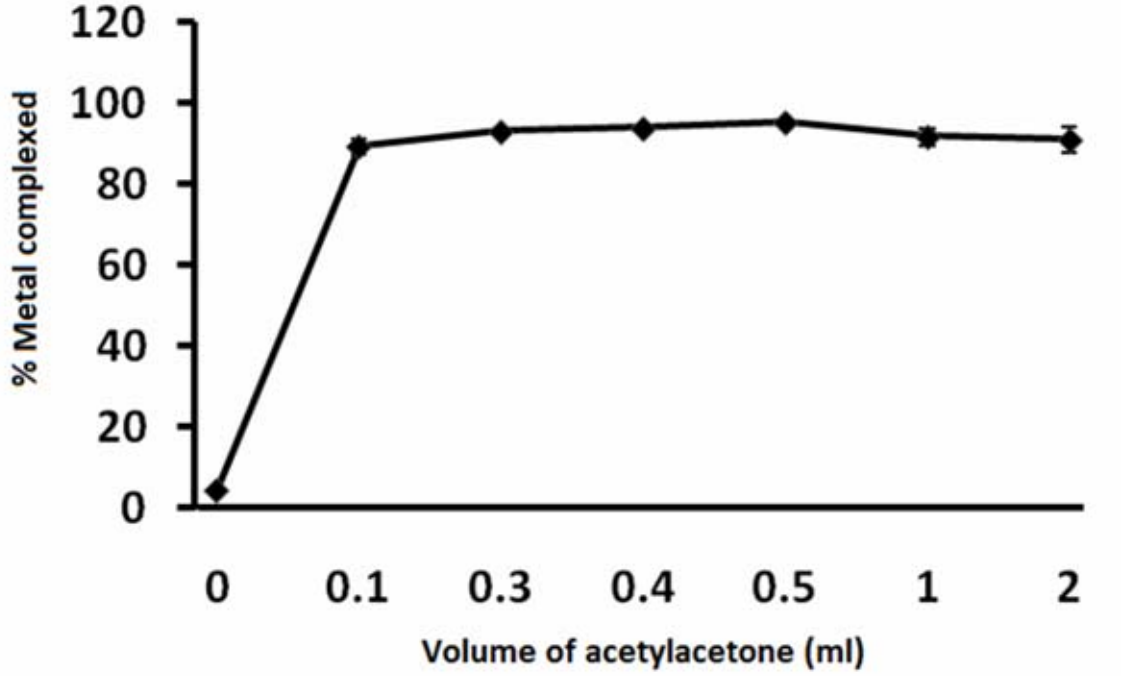

Figure 4. The % complexed of 0.2 ppm Cu model solution (pH 6) adsorbed onto C-18 columns under varying volumes (0 to 2 mL) of 1.0 mM acetylacetone.

Effect of sample volume

The effect of the sample volume on Cu recovery was studied by loading 10–150 ml of 0.2 ppm Cu model solutions adjusted to pH 6, through C-18 SPE column at a flow rate of 3 mL min^{-1}. The results are given in Figure 5, the method is quite sensitive even on sample volumes as low as 10 mL, the extraction efficiency remained consistent over a wide range of sample volumes (10- 150 mL). For samples with low analyte concentration, the detection limit (Table 2) can be improved by increasing the sample volume and still maintain the extraction efficiency.

Table 2. Effect of matrix ions on the recovery of Cu and Fe (pH 8; sample volume: 30ml, n=3)

Ion	[Matrix] in ppm Added	% recovery x± S.D	% recovery x± S.D
Na^+	500	94 ± 2.4	92± 0.5
	1000	94 ± 2.5	80 ± 5.2
	2000	94 ± 4.1	57 ± 1.3
	8000	97 ± 3.2	48 ± 8.7
	10000	88 ± 0.8	28 ± 4.2
	15000	89 ± 3.8	38 ± 9.1
Ca^{2+}	500	87 ± 0.8	87 ± 3.7
	1000	84 ± 1.9	84 ± 1.8
	2000	82 ± 0.9	84 ± 0.5
	4000	85 ± 4.6	85 ± 6.0
	8000		84 ± 4.2
	10000	84 ± 3.1	87 ± 7.6
	15000	80 ± 0.9	71 ± 4.0
Mg^{2+}	500	84 ± 1.0	93 ± 5.9
	1000	83 ± 0.2	
	2000	76 ± 3.0	91 ± 3.0
	4000	86 ± 4.4	94 ± 12.0
	8000	82 ± 0.9	101 ± 0.5
	10000	80 ± 4.7	90 ± 2.5
	15000	85 ± 3.5	96 ± 1.2

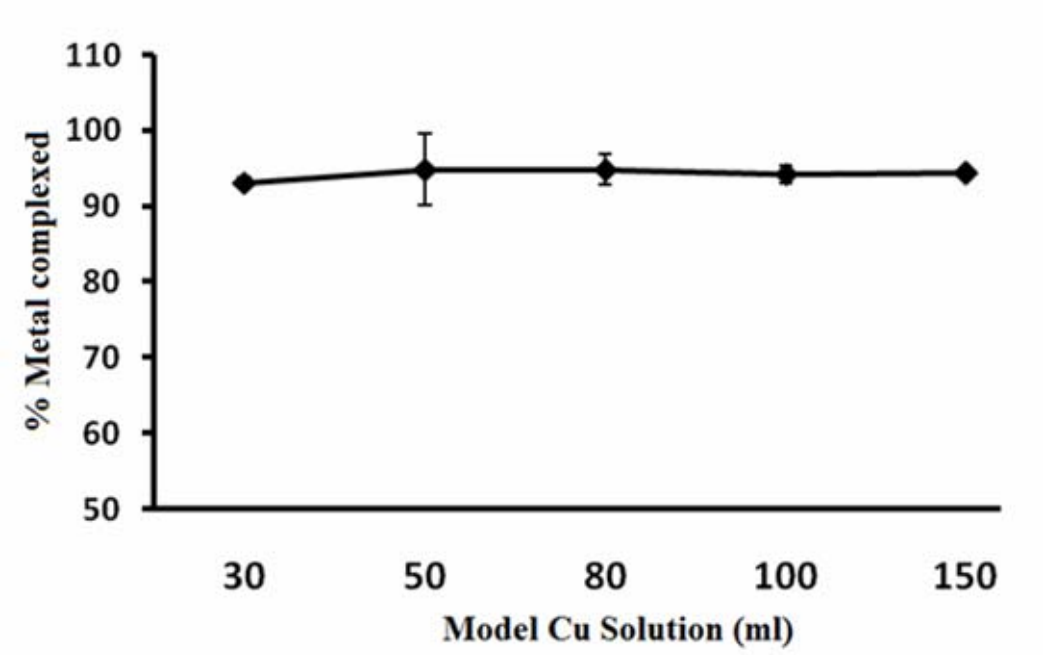

Figure 5. The % Recovery under varying volumes (10 to 150 mL) of 0.2 ppm Cu model solution (pH 6).

Effect of sample matrix

The effect of sample matrix due to alkaline and alkaline earth metals on Cu recovery was investigated by adding the matrix ions into a 30 mL model solution and loading onto a C-18 column. From the results reported in Table 2**,** it was observed that the proposed preconcentration method can be applied on saline samples. The extraction was quantitative in model solutions containing a matrix of up to 8000 ppm Na^+ for Fe.

Detection limit and standard reference material

The detection limits of the analytes based on three times the standard deviations of the blank divided by the slope of the calibration graph (3s/b, n = 20, where *s* is the standard deviation of the blank and *b* is the slope of calibration curve) are reported (Vandecasteele and Block 1997) in Table 3. The proposed method is sensitive to concentrations in ppb levels (Table 4) and compares favorably with other preconcentration methods as reported in the literature (see Table 5 for references). The method was tested on seawater standard reference material

NASS-5 and the results obtained, which gave a pre-concentration factor of 12, was in agreement with those reported for the seawater standard reference material NASS-5.

Table 3**.** Detection limits of metal ions (Cd, Cu, Fe, and Pb) at different sample volumes and the analysis of 60 mL NASS-5 Seawater reference material.

Metal	PF	Detection limit/ ppb	NASS-5 Seawater Reference Material	
			Certified value (ppb)	Our value(ppb)
Cd	4	0.15		
	12	0.05	0.023± 0.003	BDL
	20	0.03		
Cu	4	0.40		
	12	0.14	0.297± 0.046	0.31± 0.12
	20	0.08		
Fe	4	8.4		
	12	2.8	0.207± 0.035	BDL
	20	1.7		
Pb	4	15.7		
	12	5.2	0.008± 0.005	BDL
	20	3.1		

BDL= Below Detection Limit; PF = Preconcentration Factor

Table 4. Heavy metal (Cu, Ni, and Pb) analysis in pulp filtrate after acetylacetone complexation and preconcentration on C-18 SPE

Metal in pulp filtrate	PF	Spike ppm	Concentration ppm ($x \pm s/\sqrt{N}$)	% Recovery
Cu	8	0	0.0061± 0.0004	
Ni	8	0	0.0062± 0.0050	
Pb	8	0	0.0034 ± 0.0008	
Cu	8	0.1	0.1163 ± 0.0150	110
Ni	8	0.1	0.0910 ± 0.0080	84
Pb	8	0.1	0.1084 ± 0.0016	104
Cu	8	0.2	0.2721 ± 0.0060	133
Ni	8	0.2	0.2050 ± 0.0690	99
Pb	8	0.2	0.1662 ± 0.0500	81

PF = preconcentration factor

Table 5**.** Comparative data from literature reports on solid phase extraction.

Analyte	Complexing media	adsorbent	PF	detection limit ppb	Reference
Fe, Pb & Cr	*p*-xylenol	Amberlite XAD-7	6	3.07-18.6	Divrikli et al., 2007
Cu, Fe, Ni & Co	calmagite	Chromosorb-102	10	6-113	Soylak et al., 2003b
Cd & Pb	1-(2-pyridylazo) 2-naphthol (PAN)	Chromosorb-106	250	0.19-0.32	Tuzen et al., 2005
Cd, Cu, Cr Co, Fe, Mn, Pb	alpha-benzoin oxime	Diaion SP-850	50	0.28-0.73	Soylak &Tuzen; 2006
Cu, Cr Co, Fe, Pb	calmagite	cellulose nitrate membrane filter	50	0.06-2.5	Soylak et al., 2002

Application of proposed method on dissolving pulp wastewater

The method was applied on dissolving pulp filtrate obtained from the alkaline bleaching stage. The pulp filtrate matrix comprises mainly of lignin, organic extractives, as well as alkaline and alkaline earth metals. A sample was first analyzed as stated above to obtain its original Cu concentration and there after spiked with Cu solutions to constitute sample concentrations of 0.1 and 0.2 ppm. The metal recovery values after spiking pulp filtrate with a mixture of Cu, Ni and Pb to obtain two model solutions of concentration 0.1 and 0.2 ppm, were 120%, 91% and 93%, respectively (Table 4). This method is highly sensitive for the analysis of Cu, Ni and Pb in complex liquid matrixes and can be applied in the pulp and paper industry to monitor metal levels in wastewater. At elevated levels, Cu is especially toxic to invertebrates which can also lead to growth inhibition and reproduction disturbances in marine invertebrates (Nimmo and Hamaker 1982). The toxicity of Cu is mainly from the

bioavailable fraction and has been shown to be dependent on the concentration of the free copper ion, Cu^{2+} (Sunda and Guillard 1976).

Adsorption isotherms

Sorption and isotherm studies were performed on selected metals (Cu^{2+}, Fe^{2+} and Mn^{2+}) and results are reported in Figures 6 and Table 6. The choice of the three metals was based on their relative abundance to those of the other metals in the pulp.

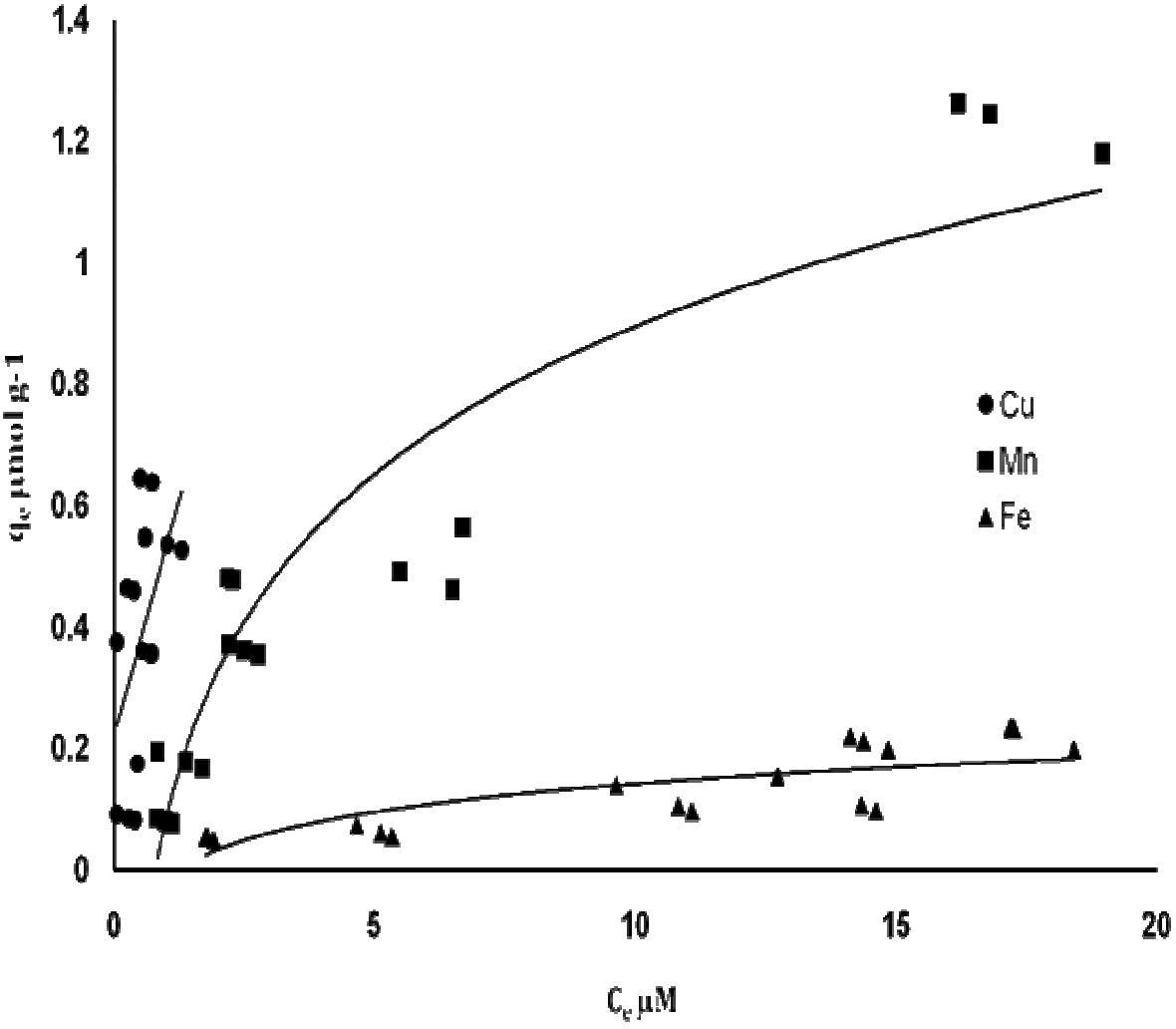

Figure 6. Adsorption isotherm for Cu, Fe and Mn acetylacetone complexes on C-18 SPE column

Table 6**.** Langmuir and Freundlich adsorption isotherm parameters for Cu, Fe and Mn acetylacetone complexes on C-18 SPE. Showing regression line characteristics R^2, a_L/k_L, $1/k_L$, b_F and $\ln K_F$.

	Langmuir isotherm			**Freundlich Isotherm**		
	R^2	a_L/K_L	$1/K_L$	R^2	b_F	$\ln K_F$
Cu	0.277	0.959	1.687	0.612	0.618	-0.963
Mn	0.389	0.407	7.515	0.810	0.779	-1.931
Fe	0.272	2.892	49.66	0.750	0.606	-3.469

The C-18 /acetylacetone dynamic flow system showed a high affinity for Cu and the binding sites were not saturated even after passing 30 mL of 3.2 ppm model solution (Figure 4). The system had a low affinity for Fe with the adsorption capacity $q_e \approx 2.0$ (μmol g^{-1}). Acetylacetone exists in solution in keto and enol forms and at higher pH the ionized form is also present. The existence of acetylacetone in various forms affects the bonding/binding characteristics of Hacac complexed metal species onto the C-18 and therefore it is not a homogeneous solution. Sohn and Lee (2000), reported the linking of acetylacetone to an exchangeable metal cation through a water bridge bonding as >C=O----H-O(H)-M^{n+}. The size of the cation and orientation of water molecules around the cation is controlled by the coordinating power of the cation and the space around it should also be an important factor (Sohn and Lee 2000). The results obtained in this work are in agreement with those reported on non-homogeneous existence of acetylacetone. The experimental adsorption isotherm system did not fit the Langmuir model, which assumes a homogeneous system with no interaction between adsorbed molecules, even on adjacent sites. Thus the linear Langmuir correlation coefficients (R^2) for Cu^{2+}, Mn^{2+} and Fe^{3+} were 0.277, 0.389 and 0.272, respectively (Table. 6). The system however correlated well with the Freundlich adsorption isotherm model which assumes a heterogeneous system especially for organic compounds and highly interactive species on activated carbon (Ng et al. 2003). Linear regression for

Freundlich plots gave correlation coefficients (R^2) for Cu, Mn and Fe of 0.612, 0.810 and 0.750, respectively (Table 6). These values are much better than the coefficients obtained for Langmuir plots. These results (Freundlich) imply that the Hacac ligand provides multiple binding sites for metal ions.

CONCLUSIONS

The proposed analytical method was found to be effective in the analysis of pulp waste and salt matrices for trace metals. It is suitable for the analysis of seawater and wastewater systems with high content of organic matrices. The method is however best suited for the analysis of Cu (up to 0.2 M ~ 12,600 ppm) over a wide pH range (2-10). The advantage of using this method for the analysis of Cu in environmental waters is that there is no need to adjust the sample pH. Analyzing the samples without prior adjustment of the pH is important so as to avoid over- or under- estimation of Cu levels due to precipitation or leaching during sample pH adjustment.

Acetylacetone complexes of Cu, Mn and Fe fitted the Freundlich adsorption model implying that they were retained on the solid phase material via physical adsorption due to weak attractive forces; generally Van der Waals forces (Perez et al. 2007). Freundlich model principally represents a physical adsorption phenomenon whereas the Langmuir model represents a chemical adsorption process (Perez et al. 2007).

ACKNOWLEDGEMENT

Joseph Kamau acknowledges the financial support of CSIR through Forestry and Forest Products Research Centre in Durban, and Kenya Marine & Fisheries Research Institute for study leave.

REFERENCES

Bekjarov, G., V. Kmetov, and L. Futekov. 1989. Trace analysis in highly concentrated salt solutions of sodium chloride and ammonium fluoride using flame atomic absorption spectrometry . *Fresenius Anal. Chem*. *335*: 971-974.

Boumans, W. J. M. 1987. In Inductively Coupled Plasma Emission Spectroscopy. Part 1: Methodology, Instrumentation and Performance, Interscience, New York.

Budic, B., and V. Hudnik. 1994, Matrix effects of potassium chloride and phosphoric acid in argon inductively coupled plasma atomic emission spectrometry. *J. Anal. At. Spectrom*. *9*, 53.

Compano, R., R. Ferrer, J. Guiteras, and M. D. Prat. 1994. Spectrofluorimetric detection of zinc and cadmium with 8-(benzenesulfonamido)-quinoline immobilized on a polymeric matrix. *Analyst* 119: 1225.

Divrikli, U., A. Akdogan, M. Soylak, and L. Elci. 2007. Solid-phase extraction of Fe(III), Pb(II) and Cr(III) in environmental samples on amberlite XAD-7 and their determinations by flame atomic absorption spectrometry *J. Haz. Mat.* 149: 331–337.

Dogan, M., M. Soylak, and L. Elci. 1997. Determination of some trace metals in natural waters, dialysis solution and various salt matrices by atomic adsorption spectrometry after preconcentration onto activated carbon and Amberlite XAD-resins, 4. International Conference of Chemistry and Its Role in Development, Mansoura, Plenary Lecture, Mansoura University 1, 63-69

Fay, D. P., R. Ambrose, Nichols Jr, and K. Sutin 1971. The Kinetics and Mechanisms of the Reactions of Iron (II1) with p-Diketones. The Formation of Monoacetylacetonatoiron (II1) and the Effect of Copper (II) on the Formation of Mono thenoyl trifluoroacetonatoiron **(I1**I). *Inorganic Chemistry10 (10):* 2096–2101

Ferreira, S. L. C. 2006. Separation and preconcentration procedures for the determination of lead using spectrometric techniques: a review. *Talanta* 69: 16–24.

Freundlich, H. M. F. 1906. Over the adsorption in solution. *Z. Physik. Chem.* A 57: 385-471.

Gilli, G., F. Bellucci, V. Ferretti, and V. Bertolasi. 1989. Evidence for resonance-assisted hydrogen bonding from crystal-structure correlations on the enol form of the .beta.-diketone fragment. *J. Am. Chem. Soc.* 111 (3): 1023–1028.

Gustavo Rocha de, C., A. Ilton Luiz de, and R. Paulo dos Santos. 2004. Synthesis, characterization and determination of the metal ions adsorption capacity of cellulose modified with *p*-aminobenzoic groups. *Mater. Res*. 7: 329–334.

Horwitz, E. P., M. L. Dietz, R. Chiarizia, H. Diamond, A. M. Essling, D. Garczyk. 1992. Separation and preconcentration of uranium from acidic media by extraction chromatography. *Anal. Chim. Acta.* 266: 25.

Imura, H., and N. Suzuki. 1985. Solvent effect on the liquid-liquid partition coefficients of copper(II) chelates with some β-diketones. *Talanta* 32(8B): 785–790.

Killian, K., and K. Pryznska. 2002. Application of 5,10,15,20-Tetrakis (4-carboxyphenyl) porphine for cadmium preconcentration in flow-injection system. Analytical Sciences. 18: 571-574

Korn, M. D. A., A. D. Santos, H. V. Jaeger, N. M. S. Silva, and A. C. S. Costa. 2004. Copper, zinc and manganese determination in saline samples employing faas after seperation and preconcentration on amberlite XAD-7 and Dowex 1X-8 loaded with alizarin red S. *J. Brazil Chem. Soc.* 15: 212.

Korn, M., J. Andrade, D. de Jesus, V. Lemos, M. Bandeira, W. dos Santos, M. Bezerra, F. Amorim, A. Souza and S. Ferreira. 2006. Separation and preconcentration procedures for the determination of lead using spectrometric techniques: A review. Talanta 69: 16-24.

Langmuir, I., 1918. The adsorption of gases on plane surfaces of glass, mica and platinum. *J.Am. Chem. Sco.* 40 (9): 1361-1403.

Lin, H., Z. Liya, Z. Huang, Q. Hu, G. Zhang, and G. Yang. 2007. Studies on the solid phase extraction and spectrophotometric determination of palladium with 2-(2-quinolylazo)-5-dimethylaminoaniline as chromogenic reagent. *Asian J. Chem*. 19: 836.

Montaser, A.. and D. W. Golightly. 1990. In Inductively Coupled Plasma in Analytical Atomic Spectrometry, VHC Publishers, New York

Ng, J. C. Y., W. H. Cheung, and G. McKay. 2003. Equilibrium studies for the sorption of lead from effluents using chitosan. *Chemosphere* 52: 1021-1030.

Nimmo, E.R. and T.L. Hamaker. 1982.Mysids in toxicity testing—a review, *Hydrobiologia* **93**: 171–178.

Pauling, L. 1932. The nature of the chemical bond IV the energy of single bonds and the relative electronegativity of atoms. J. Am. Chem. Soc. 54 (9): 3570–3582

Pearson, R. G., and O. P. Anderson. 1970. Rates and Mechanism of Formation of Mono(acetylacetonato)copper(II) Ion in Water and Methanol. *Inorg. Chem*. 9: 39-46.

Pearson, R. G., and R. L.Dillon. 1953. Rates of Ionization of Pseudo Acids.[1] IV. Relation between Rates and Equilibria. *J. Am. Chem. Soc. 75*: 2439-2443.n

Perez, N., Sanchez, M., Rincon, G., and Delgado, L. 2007. Study of the behavior of metal adsorption in acid solution on lignin using a comparison of different adsorption isotherms. *Latin Ame. App. Res.* 37: 157-162.

Perrin, C. L., and J. B. Nielson. 1997. Strong' Hydrogen Bonds in Chemistry and Biology. *Annu. Rev. Phys. Chem. 48*, 511.

Schaefer, W. P. and M. E. Mathisen. 1965. Stability Constants of the Acetylacetone-Chromium(l1) Complexes. *Inorg. Chem*. 4(3): 431-433

Seren, G., Y. Bakircioglu, F. Coban, and S. Akman. 2001. Investigation on the preconcentration of trace elements on activated bentonite. Fresenius. Environ. Bull. 10: 296-299.

Sohn, J. R., and S. Lee. 2000. Adsorption Study of Acetylacetone on Cation-Exchanged Montmorillonite by Infrared Spectroscopy. *Langmuir*,16: 5024-5028.

Soylak, M., 2001. Eser Elementler ve Insan (In Turkish). *Porpular Bilim Dergisi*. 8: 47-48.

Soylak, M., A. U. Karatepe, L. Elci, and M. Dogan. 2003a Column preconcentration/separation and atomic absorption spectrometric determination of some heavy metals in table salt samples using Amberlite XAD-1180, *Turk. J. Chem*. 27: 235–242.

Soylak, M., and M. Tuzen. 2006. Diaion SP-850 resin as a new solid phase extractor for preconcentration-separation of trace metal ions in environmental samples *J. Haz. Mat.* B137:1496–1501.

Soylak, M., S. Saracoglu, and L. Elci. 2003b. Sorbent Extraction of Some Metal Ions on a Gas Chromatographic Stationary Phase Prior to Their Flame Atomic Absorption Determinations. *Bull. Korean Chem. Soc.* 24(5): 555-558.

Soylak, M., U. Divrikli,. L. Elci, M. Dogan. 2002. Preconcentration of Cr(III), Co(II), Cu(II), Fe(III) and Pb(II) as calmagite chelates on cellulose nitrate membrane filter prior to their flame atomic absorption spectrometric determinations. *Talanta* 56: 565–570.

Sunda, W.G., and R. R. L. Guillard. 1976. The relationship between cupric ion activity and the toxicity of copper to phytoplankton, *J. of Mar. Res.* 34: 511–529.

Tateki, I., H. Fumio, and K.Shigeki. 1999. Thermodynamic analysis of the solvent effect on tautomerization of acetylacetone: An *ab initio* approach J. Chem. Phys. 110: 3938..

Tewari, P. K., and A. K. Singh. 2000. Amberlite XAD-7 impregnated with xylenol orange: a chelating collector for preconcentration of Cd (II), Co (II), Cu (II), Ni (II), Zn (II) and Fe (III) ions prior to their determination by flame AAS. *Fresenius J. Anal. Chem*. 367: 562.

Tisanori, A., T. Keiko. and T. Mutsuo. 2009. Fluorescence and metal-ion recognition properties of acetylacetone-based ligands *J. Env. Sci. Supplement* (2009) S84–S87

Tuzen, M., K. Parlar, and M. Soylak. 2005. Enrichment/separation of cadmium(II) and lead(II) in environmental samples by solid phase extraction *J. Haz. Mat.* B121: 79–87.

Vandecasteele, C.,and C. B. Block. 1997. Modern Methods for Trace Element Determination. John Wiley and Sons, Chichester.

Xu, S. J., S. T. Park, J. S. Feenstra, R. Srinivasan, and A. H. Zewail. 2004 Ultrafast Electron Diffraction: Structural Dynamics of the Elimination Reaction of Acetylacetone. *J. Phys. Chem*. *A* 108: 6650-6655.

Yang, R. T., 1987. *Gas separation by adsorption processes*. Butterworths, Boston.

Yoon, M. C., Y. S. Choi, and S. K. Kim. 1999. Photodissociation Dynamics of acetylacetone: the OH product state distribution. *J. Chem. Phys*. 110 (24): 11850-11855.

CHAPTER 7

7.0 GENERAL CONCLUSIONS

The analysis of the data generated to determine the pathway of metals from the soil to the *Eucalyptus* tree, produced a number of findings. The growth of all the *Eucalyptus* tree species/clone investigated in the study was enhanced by increased Fe bioavailability; this was reflected by its accumulation in the wood material. The main pathway of metals and Si was found to be through the exchangeable fraction. The degradation of organic matter was found to be a major pathway in the mineralisation of Fe and Si.

The pathway and fate of metals through the dissolving pulp delignification and bleaching process was investigated. The designed approach was unique in that it related the extraction of lignin and hemicelluloses to metal fluxes from the pulp into the media and vice versa. The extractability of metals during pulp delignification and bleaching was found to be influenced by a variety of factors. Metals with a high affinity towards organic matter hindered their extractability because they were readily re-attached to the pulp during the bleaching process. The genetic composition of the pulp material was a determinant on where the metals were adsorbed in the pulp structure. In some of the pulp species, metals were found to be adsorbed on the lignin while in some they were adsorbed on the hemicelluloses.

This study uniquely demonstrated that electroanalytical techniques can be used in the dissolving pulp industry to provide an insight on the interaction of the extracted organic macromolecules with the metals in solution. Metal-ligand complexes formed during the alkaline oxygen delignification stage were found to be more stable and their complexing capacity higher than those of the metal complexes formed in the pulp filtrate of the alkaline bleaching stage. The extracted organic macromolecules in the alkaline oxygen delignification stage would therefore facilitate increased extraction of metals from the pulp. This is assisted by complexing the metals in the filtrate thereby preventing them from being re-adsorbed onto the pulp material.

A novel extraction technique for metals was developed using acetylacetone as an extracting ligand. The method was applied in the extraction of residual metals from the final dissolving pulp material. Desorption models and kinetic studies were employed to investigate the metal desorption mechanisms thereby determining the mode of metal attachment on the pulp material. It was determined that most of the residual metals in the dissolving pulp

material were chemically adsorbed onto the pulp surface. The extraction of chemically bound metals requires the ligand to approach the pulp material at close proximity. The charge on the pulp material can either be neutral or negative depending on the media pH. In an alkaline media the pulp is negatively charged and EDTA will also be negatively charged hindering its approach to the pulp material. Acetylacetone on the other hand does not experience repulsion as its keto enol form approaches the pulp surface. This structural property is ideal for the desorption of chemically adsorbed metals on pulp. This is why acetylacetone performed better than EDTA in the desorption of chemically adsorbed metals. The developed residual metal extraction technique has shown acetylacetone to be a superior extracting ligand compared to EDTA. Furthermore acetylacetone is readily biodegradable unlike EDTA and therefore reduces the cost of environmental mitigation. This method can be of economical importance to the dissolving pulp production industries, in that it is efficient and environmentally friendly.

A novel analytical method involving the complexation of metals with acetylacetone and thereafter adsorbing the organometalic complex onto C-18 cartridges, was found to be effective for the analysis of trace metals in seawater and wastewater systems with high organic matter. The advantage of using this method for the trace analysis of Cu is that there is no need to adjust the sample pH. Analysing the samples without prior adjustment of the pH is important to prevent over- or under-estimation of metal levels due to precipitation or leaching during sample pH adjustment.

7.1 RECOMMENDATIONS

The *Eucalyptus* clones under study tended to accumulate metals through the dissolving pulp bleaching process. These clones should only be used if the final pulp residual metal content does not affect the end use. Alternatively the residual metals should be extracted by using an appropriate ligand such as acetylacetone during or after the hypochlorite bleaching stage.

The *Eucalyptus* species E. *nitens* behaved in a similar way as did the *Eucalyptus* clones in that it tended to accumulate metals through the pulping process and should therefore be treated in a similar manner as the clones.

The above observed tendency of the *Eucalyptus* clones and E. *nitens* to accumulate metals is an indication of the reactivity of these pulps. They are therefore more suitable for

dissolving pulp production whereby the pulp is further derivatised to different products i.e. viscose, acetate, ether, or microcrystalline cellulose.

The possibility of upscaling the residual metal extraction technique could be explored for commercial application.